AN APPROXIMATE METHOD OF CALCULATING THREE-DIMENSIONAL, COMPRESSIBLE FLOW IN AXIAL TURBOMACHINES

Thesis by

Carl O. Holmquist
Lieutenant Commander
United States Navy

In Partial Fulfillment of the Requirements

for the Degree of

Doctor of Philosophy

California Institute of Technology

Pasadena, California

1953

ACKNOWLEDGEMENT

The author is indebted to Drs. W. D. Rannie, H. S. Tsien and F. E. Marble of the California Institute of Technology for their assistance, guidance and inspiration in the formulation and solution of this problem.

The author also wishes to express his sincere gratitude for the policies of the Bureau of Aeronautics of the Navy Department which have permitted him to complete his graduate studies at the U. S. Naval Postgraduate School and the California Institute of Technology.

Appreciation is also gratefully extended to Mrs. Virginia Boughton, Mrs. Elizabeth Fox, Miss Jeanne Mainwaring, and Mrs. Betty Wood for their excellent work in completing this thesis in its final form.

TABLE OF CONTENTS

PART	TITLE	PAGE
	Abstract	
I	Introduction	1
II	Fundamental Equations	8
	A. Development of Basic Differential Equations	8
	B. Transformation to Non-Dimensional Form	10
	C. Equations for the Direct Problem for an Arbitrary Channel Shape	11
	D. Equations for the Inverse Problem for an Arbitrary Channel Shape	15
	E. Changes in Equations for the Compressor Solution	17
III	Proposed Iteration Procedure	19
	A. Procedure for the Direct Problem	19
	B. Procedure for the Inverse Problem	23
	C. Convergence of Subsonic and Supersonic Solutions	24
	D. Correction for the Displacement of Streamlines	26
IV	Additional Corrections and Simplifications	27
	A. Corrections to the Basic Solution	27
	B. Simplification of Flow Patterns	28
	C. Proposed Optimum Turbine Design Condition	29
V	Results and Conclusions	32
	References	39
Appendix A.	Symbols and Definitions	42
Appendix B.	Development of Equations for the Direct Problem (isentropic)	44

PART	TITLE	PAGE
Appendix C.	Development of Equations for the Direct Problem (polytropic)	49
Appendix D.	Development of Equations for the Inverse Problem (isentropic)	52
Appendix E.	Development of Equations for the Inverse Problem (polytropic)	54
Appendix F.	Iterated Examples	55

ABSTRACT

The two principal existing methods of calculating axially-symmetric compressible flow in turbomachines are: (1) a simplified one-dimensional analysis, and (2) numerical methods using the complete or linearized flow equations. The first is not satisfactory for multi-stage turbines with appreciable wall divergence; the second is very tedious and time consuming. The purpose of this investigation is to extend the approximate methods, successfully used in calculating incompressible flow in compressors with constant blade height, to the analysis of compressible flow in turbomachines with variable blade height. Assuming that the blades can be completely defined by the exit flow angle, and neglecting the influence of downstream blades, the analysis is made considering the flow between successive blade rows only. With these restrictions, subsonic and isentropic supersonic flow patterns can be determined for arbitrary boundary shapes as long as separation does not occur. Average losses can be accounted for by the use of a polytropic law, and the effect of radial variations in stagnation temperature can be included without difficulty. Examples illustrating the flexibility and practical value of the iteration method, and the rapid convergence of successive solutions are given.

I. INTRODUCTION

In the modern aircraft gas turbine, the flow is necessarily in the transonic range for two reasons: (1) to keep the weight and size of the machine at a minimum, and (2) to fit the mass flow and pressure ratio of the compressor. Earlier turbojet engines had single stage transonic turbines, but present engines employ multistage turbines with rapid channel divergence in order to use effectively the increased pressure ratios and keep the axial velocities compatible with the blade speed. In these types of machines, the flow at the mean blade height is mainly axial, and the aspect ratio of the blades is usually above unity for weight saving considerations. As long as the channel wall divergence is not too great so that separation can be avoided, there is no reason for low efficiency, particularly in view of the favorable pressure gradient through the turbine.

Two distinct design problems occur in practice which Marble (Reference 15) has classified as the direct and inverse problems of turbomachine design in analogy with the corresponding classical problems in the theory of finite wings. The direct, or "off-design" problem occurs when the blade speed, blade shape, boundary configuration, and fluid state ahead of all blades is given, and the three-dimensional velocity field, blade loading, and distribution of energy are to be determined. The inverse problem occurs in the original design of turbomachinery, when the blade loading, blade speed, boundary configuration, and fluid state ahead of all blades is prescribed, and the three-dimensional velocity field, blade shape, and distribution of energy in the field are to be determined.

The exact analysis of viscous, compressible flow through an

axial turbomachine will probably never be possible because of the non-linear character of the equations governing the flow. However, the design engineer has a great need for an analysis suitable for engineering purposes, and may have no use for a lengthy, complicated and costly procedure even if it were available. He needs an extremely flexible method of analysis which, while being as simplified as practicable, still produces information accurate enough for effective design work.

The equations governing three-dimensional, compressible channel flow are greatly simplified if terms involving viscosity are neglected. In view of the fact that viscous effects actually are very slight except near the boundaries, and as long as separation is avoided, the assumption of zero viscosity seems justified. Viscosity effects could be accounted for as an added correction to the basic solution. However, with the present day turbines which operate in the high subsonic range, it is obvious that compressibility effects can not be neglected.

One of the principal methods available to the design engineer for the analysis of axially-symmetric, compressible flow in turbomachines is a simplified one-dimensional analysis. This method is used extensively in preliminary design considerations and is simple and straightforward. Since only the exit flow angles from the blade rows at the mean blade height are considered, the radial distributions of velocity and energy are not determined. Although this analysis gives reasonably accurate results for a single stage turbine with a fairly high hub ratio and small channel divergence, the one-dimensional method is inadequate for large channel divergence where the radial

distribution of velocities becomes significant. It is particularly inadequate for the design of multistage turbines with channel wall divergence since it is difficult to get the proper balance of work on the individual stages. This work balance is strongly affected by the radial distribution of the axial and radial velocities. Since the one-dimensional analysis is done at the mean blade height, it gives no information as to the radial distribution of velocities.

The second principal method of analysis of axially-symmetric compressible flow in turbomachines is by numerical methods using the complete or linearized flow equations to solve for the complete velocity and energy field through the machine. Since the determination of the entire flow field involves six unknowns at each point in the flow (the three components of velocity, the pressure, the temperature, and the density), the analysis using these numerical methods is necessarily lengthy and extremely complicated and cannot be considered suitable from the point of view of the design engineer. Monroe (Reference 7) formulated the idealized problem in terms of a stream function for the velocities in the meridional plane, and solved the resulting non-linear differential equation by a simultaneous application of the relaxation technique of Southwell and an iteration process. Wu (Reference 9) has utilized various relaxation methods, matrix systems, and finite difference schemes to solve the complete hydrodynamical equations for the entire flow field in many types of problems. Vavra (Reference 8), Reissner (Reference 10), Goldstein (Reference 11), Wislicenus (Reference 13), and many others have employed various techniques to solve the complete, or nearly complete, equations by some numerical method. Although these numerical methods are not suitable for design purposes,

they are quite general and can be used for centrifugal, mixed flow or axial flow machines with blades of any aspect ratio.

In an effort to simplify the problem of solving for the complete flow field, a linearized analysis has been provided by Marble (References 5 and 15) and Fabri (Reference 6). Marble (Reference 15) proposed a linearized analysis of the problem, satisfactory for high aspect ratio blades, to allow an approximate treatment of the general blade row with prescribed wall geometry. He assumed that the trailing vorticity could be considered to be transported downstream by the mean axial flow and not by the perturbation velocities, that is, disturbances in the radial and axial velocities are small in comparison with the mean axial velocity, and that the blade row is made up of an infinite number of blades of finite chord. The analysis for the inverse problem was carried out in detail and was found to allow a general and reasonably simple solution. In Reference 5, Marble extended the analysis to the direct problem of off-design operation, and to the study of mutual interference of neighboring blade rows in a multistage axial turbomachine. He provided examples of axial and conical flow, and stated that the simple linearized solution was sufficiently accurate if the vorticity effects were not large. A second order linearization was given to handle problems with greater vorticity effects. However, the computation required to find the three-dimensional flow in any particular case is rather lengthy using the linearized solutions, and involves some type of numerical integration. A simple exponential approximation was then introduced to simplify the computation, and the results using this approximation compared favorably with the detailed results of the linearized solution.

The analysis of flow in turbomachinery where the channel boundaries are purely cylindrical, or vary only slightly from a cylindrical

shape, has been extensively investigated by Rannie (References 1 and 14), Traupel (References 2 and 3), Sinnette (References 4 and 18), and others. In these analyses, the radial momentum equation used in the treatment is of the form,

$$\frac{1}{\rho}\frac{\partial p}{\partial r} = \frac{v^2}{r} \qquad (1),$$

where the radial force and other momentum terms have been neglected. The distribution of axial velocity is approximated by assuming axial symmetry, and since the centrifugal force within the rotating fluid body is balanced only by the radial pressure gradient, the resulting flow calculated in this manner is in reality that which must exist far downstream of the blades where radial velocities and accelerations have vanished. No information is provided by these analyses on how rapidly the change in velocity pattern takes place as the fluid passes through the blade row.

The purpose of this thesis is to present an approximate method for the analysis of compressible flow in modern axial turbomachines which gives sufficiently accurate information for design purposes and yet retains the simplicity necessary to be of practical value to the design engineer. This is the logical step forward from the one-dimensional method to the analysis of compressible flow in axial turbomachines. Methods which have been successfully employed in the incompressible case (Reference 1), have been modified and extended to the analysis of compressible flow in arbitrarily shaped axially-symmetric channels. It is obvious that little simplification over the so-called "numerical" methods can be obtained if the complete flow and energy fields are to be determined in the analysis. In this thesis, the flow is analyzed at the station immediately downstream of the blade row by a consideration of the upstream conditions, channel configuration, and blade shapes. The blade trailing edge angle only is considered, and the complete flow field through the blade row is not determined.

The method of analysis presented is extremely flexible and has been used to solve the direct and inverse problems, subsonic or supersonic, for arbitrary axial boundary configurations. In the solution of the direct problem, the choice of blade speed, blade spouting angle, boundary configuration, and upstream conditions can be arbitrary, and the three-dimensional velocity field, blade loading, and distribution of energy in the field are determined. In the inverse problem, for a given blade loading, blade speed, boundary configuration, and fluid state ahead of all blades, the blade spouting angle, velocity field and energy distribution can be determined. By a simple change of sign in the equations used, the method can be applied equally well to an axial compressor as to an axial turbine. Although this method is not as general as those used by Wu (Reference 9), for example, it is more flexible and practical for blading of aspect ratio greater than unity, and is sufficiently accurate in view of the assumptions used in the treatment.

The analysis is carried out on the basis of steady, axially-symmetric flow with infinitely many blades. The fluid is assumed to be compressible, but all other real fluid effects are neglected except as they may be approximated by a "polytropic efficiency" and the use of the polytropic exponent "n". As a result of this assumption, the possibility of separation of flow at the channel walls or along the blades is excluded. Boundary layer effects are also not considered in the analysis. In the supersonic solution, the occurrence of shock waves is excluded. Radial or nearly radial blades are presupposed so that the radial force can be neglected, and the radial momentum equation used in the treatment has the form,

$$\frac{1}{\rho}\frac{\partial p}{\partial r} = \frac{v^2}{r} - u\frac{\partial u}{\partial r} - w\frac{\partial u}{\partial z} \qquad (2),$$

This assumption seems justified in view of the investigations of Karlsson (Reference 19), who, by a two-dimensional analysis of incompressible flow with an infinite number of blades, showed that the effect of the radial force resulting from normal blade twist is of negligible magnitude.

The effect of downstream blades on conditions upstream is neglected, and the blade shape is specified by the trailing edge angle only. Simply stated, a blade row is assumed whose only effect on the flow is to turn it through a specified angle distribution which is a function of radius across the channel. An assumption similar to this has been used successfully in the analysis of flow through a compressor (References 1 and 14), and should be even more applicable to turbines where the blade solidity is high. The equations are particularly suited to the analysis of flows with a prescribed radial total enthalpy distribution.

Subject to the above assumptions, the resulting "exact" equations are solved by an approximate method using a simple iteration procedure. An integral for the axial velocity is derived in terms of known upstream conditions and the downstream pressure. The pressure distribution is found by integrating the radial momentum equation and applying the energy equation at a boundary. The mass flow equation is used to solve for the constant obtained from the axial velocity integral. The iteration is started by assuming an axial velocity distribution and continued until the solution is reached, i.e., until the velocity distribution produced by an iteration is the same as that assumed for that particular iteration.

II. FUNDAMENTAL EQUATIONS

A. Development of Basic Differential Equations

The differential equations are developed assuming steady, compressible flow of a fluid through an axially symmetric cylindrical channel of arbitrary shape. An infinite number of blades is assumed so that the velocity components are considered independent of angle about the axis of the machine. The fluid is assumed perfect with no losses of any sort except as these losses can be approximated by a "polytropic efficiency" and the use of the polytropic exponent "n". All boundary layer and viscosity effects are also neglected.

In order to generalize the equations for an arbitrary (but reasonable) channel shape, it is necessary to consider a special type of blading. These blades, infinite in number, have no other effect on the flow than to turn it through a prescribed angle distribution. Thus the effect of downstream blades on upstream conditions is neglected. Attention is directed to the flow patterns immediately before and after the blade rows for either the stator or the rotor.

In Figure 1, a stream annulus of small radial extent is shown, and absolute velocity components are considered at stations 1, 2, and 3. Generally, there will be a shift of the stream surface in passing through either stator or rotor blading, and three components of velocity will be present at each station.

With the above assumptions, the continuity equation is written in differential form as:

$$\rho_1 w_1 r_1 dr_1 = \rho_2 w_2 r_2 dr_2 = \rho_3 w_3 r_3 dr_3 \qquad (3).$$

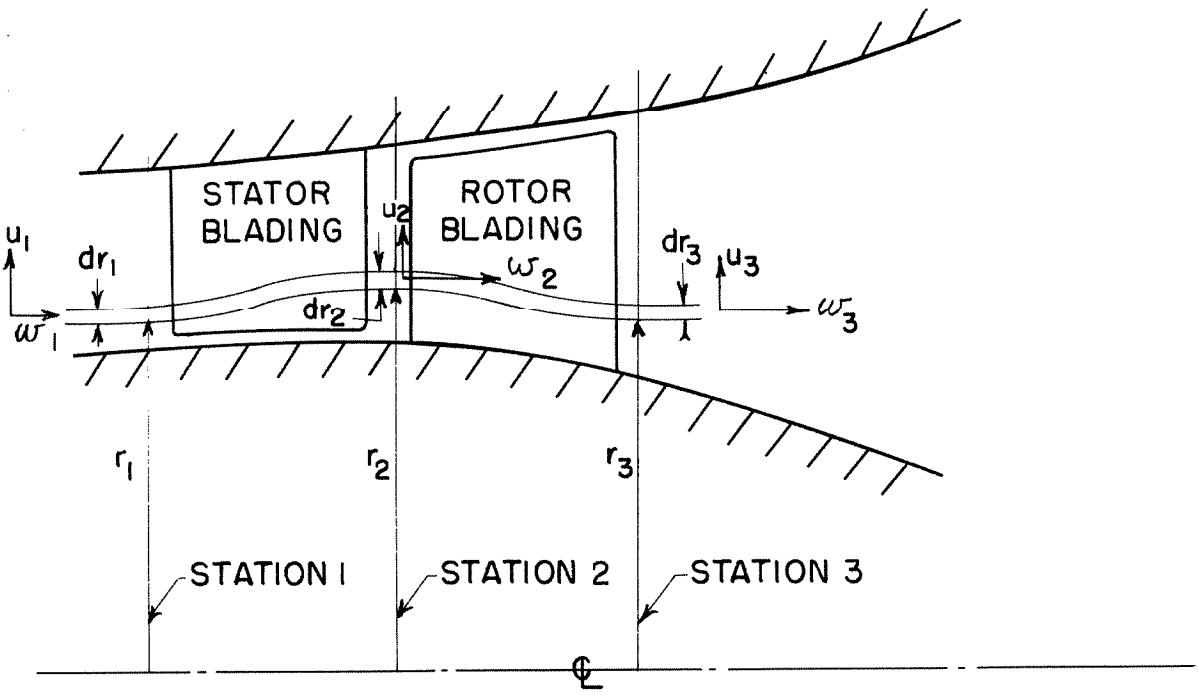

FIG. 1 — CHANNEL AND STREAM ANNULUS

For a row of stator blades, the energy equation must hold along a stream surface, and for a row of rotor blades, the energy equation must hold along a relative stream surface. Hence, in terms of absolute velocities at stations 1, 2, and 3, we have:

$$C_p T_{1t} = \frac{\gamma}{\gamma-1}\frac{p_1}{\rho_1} + \frac{1}{2}\left(u_1^2 + v_1^2 + w_1^2\right) = \frac{\gamma}{\gamma-1}\frac{p_2}{\rho_2} + \frac{1}{2}\left(u_2^2 + v_2^2 + w_2^2\right) = C_p T_{2t} \qquad (4)$$

$$\frac{\gamma}{\gamma-1}\frac{p_2}{\rho_2} + \frac{1}{2}\left(u_2^2 + v_2^2 + w_2^2 - 2\omega r_2 v_2\right) = \frac{\gamma}{\gamma-1}\frac{p_3}{\rho_3} + \frac{1}{2}\left(u_3^2 + v_3^2 + w_3^2 + 2\omega r_3 v_3\right) \qquad (5).$$

Neglecting the radial force, the radial momentum equation must hold at all stations. In absolute velocities and omitting subscripts, this equation is:

$$\frac{1}{\rho}\frac{\partial p}{\partial r} = \frac{v^2}{r} - u\frac{\partial u}{\partial r} - w\frac{\partial u}{\partial z} \qquad (2).$$

If the flow is considered to be isentropic along a relative stream-surface, the following relations must hold along this surface:

$$\frac{\rho_2}{\rho_1} = \left(\frac{p_2}{p_1}\right)^{\frac{1}{\gamma}} = \left(\frac{T_2}{T_1}\right)^{\frac{1}{\gamma-1}} \tag{6}$$

$$\frac{\rho_3}{\rho_2} = \left(\frac{p_3}{p_2}\right)^{\frac{1}{\gamma}} = \left(\frac{T_3}{T_2}\right)^{\frac{1}{\gamma-1}} \tag{7}.$$

If a polytropic flow is considered, γ will be replaced by n in Equations 6 and 7. The above equations are fundamental in the solution of the direct and inverse problems.

B. Transformation to Non-dimensional Form

For ease in handling the equations, and to avoid the use of large numbers in calculation, the derivation is completed in non-dimensional form. The notation used is given in Appendix A. Axial and radial coordinates are made non-dimensional by referring them to a standard dimension, usually the outer radius of the annulus at station 1. Velocities are made dimensionless by referring them to a standard tip speed. The following notation is used:

R_o - outer radius of the annulus at station 1.

ωR_o - reference blade speed.

$\theta = \frac{u}{\omega R_o}$ - dimensionless radial component of velocity.

$\lambda = \frac{v}{\omega R_o}$ - dimensionless tangential component of velocity.

$\phi = \frac{w}{\omega R_o}$ - dimensionless axial component of velocity.

$P = \frac{p}{p_o}$ - dimensionless pressure.

$Q = \frac{\omega^2 R_o^2}{p_o}\rho$ - dimensionless density.

$\tau = \frac{R}{\omega^2 R_o^2}T$ - dimensionless temperature.

$\frac{P}{Q} = \tau$ - gas equation.

$m = \frac{W\omega}{2\pi g p_o R_o}$ - dimensionless mass flow.

$\xi = \frac{r}{R_o}$ - dimensionless radial distance.

$\zeta = \frac{z}{R_o}$ - dimensionless axial distance.

With this notation, Equations (3), (4), (5), (2), (6), and (7) become respectively:

$$Q_1 \phi_1 \xi_1 \, d\xi_1 = Q_2 \phi_2 \xi_2 \, d\xi_2 = Q_3 \phi_3 \xi_3 \, d\xi_3 \tag{8}$$

$$\frac{\gamma}{\gamma-1} \tau_{1t} = \frac{\gamma}{\gamma-1} \frac{p_1}{Q_1} + \frac{1}{2}\left(\theta_1^2 + \lambda_1^2 + \phi_1^2\right) = \frac{\gamma}{\gamma-1} \frac{p_2}{Q_2} + \frac{1}{2}\left(\theta_2^2 + \lambda_2^2 + \phi_2^2\right) = \frac{\gamma}{\gamma-1} \tau_{2t} \tag{9}$$

$$\frac{\gamma}{\gamma-1} \frac{p_2}{Q_2} + \frac{1}{2}\left(\theta_2^2 + \lambda_2^2 + \phi_2^2 - 2\xi_2 \lambda_2\right) = \frac{\gamma}{\gamma-1} \frac{p_3}{Q_3} + \frac{1}{2}\left(\theta_3^2 + \lambda_3^2 + \phi_3^2 + 2\xi_3 \lambda_3\right) \tag{10}$$

$$\frac{1}{Q} \frac{\partial p}{\partial \xi} = \frac{\lambda^2}{\xi} - \theta \frac{\partial \theta}{\partial \xi} - \phi \frac{\partial \theta}{\partial \zeta} \tag{11}$$

$$\frac{Q_2}{Q_1} = \left(\frac{p_2}{p_1}\right)^{\frac{1}{\gamma}} = \left(\frac{\tau_2}{\tau_1}\right)^{\frac{1}{\gamma-1}} \tag{12}$$

$$\frac{Q_3}{Q_2} = \left(\frac{p_3}{p_2}\right)^{\frac{1}{\gamma}} = \left(\frac{\tau_3}{\tau_2}\right)^{\frac{1}{\gamma-1}} \tag{13}.$$

C. Equations for the Direct Problem for an Arbitrary Channel Shape

The basic integral for the axial velocity will be derived for the rotor (stations 2 to 3) for the isentropic case and simplified to the integral for the stator. The complete derivation is given in Appendix B for the isentropic direct problem and in Appendix C for the polytropic direct problem.

Differentiating the left side of Equation (10) in respect to the radius ξ_2 and the right side in respect to ξ_3 gives:

$$\left\{\frac{\gamma}{\gamma-1}\frac{d\tilde{\tau}_{2t}}{d\xi_{2}}-\frac{d(\xi_{2}\lambda_{2})}{d\xi_{2}}\right\}d\xi_{2}=\left\{\frac{\gamma}{\gamma-1}\frac{d}{d\xi_{3}}\left(\frac{\rho_{3}}{Q_{3}}\right)+\frac{1}{2}\frac{d}{d\xi_{3}}\left(\theta_{3}^{2}+\lambda_{3}^{2}+\phi_{3}^{2}\right)+\frac{d(\xi_{3}\lambda_{3})}{d\xi_{3}}\right\}d\xi_{3} \qquad (14).$$

Using Equations (8) and (13), differentiation of the first term of the right side of the above equations results in:

$$\frac{\gamma}{\gamma-1}\frac{d}{d\xi_{3}}\left(\frac{\rho_{3}}{Q_{3}}\right)=\frac{1}{Q_{3}}\frac{d\rho_{3}}{d\xi_{3}}+\frac{\gamma}{\gamma-1}\frac{\rho_{3}}{\rho_{2}^{\frac{1}{\gamma}}}\frac{d}{d\xi_{2}}\left(\frac{\rho_{2}^{\frac{1}{\gamma}}}{Q_{2}}\right)\frac{\phi_{3}\xi_{3}}{\phi_{2}\xi_{2}} \qquad (15).$$

Substituting Equations (11) and (15) into (14), and using the differential form of the mass flow relation (Equation (8)) for the ratio $\frac{d\xi_{2}}{d\xi_{3}}$, the following differential equation is obtained:

$$\frac{\lambda_{3}^{2}}{\xi_{3}}+\frac{1}{2}\frac{\partial}{\partial\xi_{3}}\left(\lambda_{3}^{2}+\phi_{3}^{2}\right)+\frac{\partial}{\partial\xi_{3}}(\xi_{3}\lambda_{3})=\left(\frac{\rho_{3}}{\rho_{2}}\right)^{\frac{1}{\gamma}}\frac{\phi_{3}\xi_{3}}{\phi_{2}\xi_{2}}\left\{\frac{\gamma}{\gamma-1}\frac{\partial\tilde{\tau}_{2t}}{\partial\xi_{2}}-\frac{\partial(\xi_{2}\lambda_{2})}{\partial\xi_{2}}\right.$$
$$\left.-\frac{\gamma}{\gamma-1}\tau_{2}\left(\frac{\rho_{3}}{\rho_{2}}\right)^{\frac{\gamma-1}{\gamma}}\frac{\partial}{\partial\xi_{2}}\left(\ln\frac{\rho_{2}^{\frac{1}{\gamma}}}{Q_{2}}\right)\right\}+\phi_{3}\frac{\partial\theta_{3}}{\partial\xi_{3}} \qquad (16).$$

For a cascade with an infinite number of blades, the exit flow is parallel to the tangent of the camber line at the trailing edge, and its direction is independent of the direction of flow approaching the cascade. For most practical applications, the direction of flow leaving the cascade is very nearly constant and independent of the inlet direction throughout the design operating range. With this assumption for the rotor, it is therefore assumed that the rotor spouting angle β_{3} is a known function of radius at station 3. Using the sign convention shown in Figure 8, it is therefore possible to describe the relation between λ_{3} and ϕ_{3} along the radius at station 3 with a function G (ξ_{3}) such that:

$$\lambda_{3}=G(\xi_{3})\phi_{3}-\xi_{3} \qquad (17).$$

Eliminating λ_3 from the differential Equation (16) by use of Equation (17) and integrating, the following integral for the rotor axial velocity for the direct problem is obtained:

$$\phi_3 = \frac{e^{+\int_{\xi_{1t}}^{\xi_3} \frac{d\xi_3}{\xi_3(1+G^2)}}}{\xi_3\sqrt{1+G^2}}\left[\int_{\xi_{1t}}^{\xi_3} e^{-\int_{\xi_{1t}}^{\xi_3}\frac{d\xi_3}{\xi_3(1+G^2)}}\left\{\frac{1}{\sqrt{1+G^2}}\left(\frac{P_3}{P_2}\right)^{\frac{1}{\gamma}}\frac{\xi_3}{\phi_2\xi_2}\left[\frac{\gamma}{\gamma-1}\frac{d\tau_{2t}}{d\xi_2}-\frac{d(\xi_2\lambda_2)}{d\xi_2}\right.\right.\right.$$

$$\left.\left.\left.-\frac{\gamma}{\gamma-1}\tau_2\left(\frac{P_3}{P_2}\right)^{\frac{\gamma-1}{\gamma}}\frac{d}{d\xi_2}\left(\ln\frac{P_2^{\frac{1}{\gamma}}}{Q_2}\right)\right]+\frac{1}{\sqrt{1+G^2}}\left(2G+\frac{d\theta_3}{d\xi_3}\right)\right\}\xi_3\,d\xi_3+C_1\right] \qquad (18).$$

It is to be noted that no linearization has been performed in arriving at the above integral. The expression for ϕ_3 is quite complicated, but its numerical evaluation by a simple iteration process to be described later is straightforward. Once a set of streamlines have been assumed, all factors involving the upstream conditions become known functions of ξ_3. In the solution of the direct problem, it is assumed that $G(\xi_3)$ is a given function of ξ_3. Thus in the integrand, P_3 and $\frac{d\theta_3}{d\zeta_3}$ are the unknowns which must be determined in the iteration process in order to evaluate the integral.

An alternate form for the square bracket in the integrand can be obtained by using the energy and radial momentum equations at station 2:

$$\left[\frac{\lambda_2^2}{\xi_2}-\phi_2\frac{d\theta_2}{d\zeta_2}+\frac{1}{2}\frac{d}{d\xi_2}\left(\lambda_2^2+\phi_2^2\right)-\frac{d}{d\xi_2}(\xi_2\lambda_2)-\frac{\gamma}{\gamma-1}\tau_2\left(\left(\frac{P_3}{P_2}\right)^{\frac{\gamma-1}{\gamma}}-1\right)\frac{d}{d\xi_2}\left(\ln\frac{P_2^{\frac{1}{\gamma}}}{Q_2}\right)\right] \qquad (19).$$

In the case that $P_{2t} = 1$ (isentropic expansion to station 2 from stagnation conditions), the bracketed term in the integrand may be further simplified to:

$$\left[\frac{\gamma}{\gamma-1}\frac{d\tau_{2t}}{d\xi_2}\left(1-\rho^{\frac{\gamma-1}{\gamma}}\right)-\frac{d}{d\xi_2}(\xi_2\lambda_2)\right] \qquad (20).$$

The constant of integration C_1 is determined by integrating Equation (8). The integrated form of this relation equates the total flow rate upstream to that at station 3:

$$m = \int_{\xi_i}^{\xi_o} \rho_2 \left(\frac{p_3}{p_2}\right)^{\frac{1}{\gamma}} \phi_3 \xi_3 \, d\xi_3 \qquad (21).$$

Using Equation (13), the integral form of the radial momentum equation becomes:

$$p_3 = \left[\frac{\gamma-1}{\gamma}\left(\frac{\rho_2}{p_2^{\frac{1}{\gamma}}}\right)\int_{\xi_i}^{\xi_3}\left(\frac{\lambda_3^2}{\xi_3} - \theta_3\frac{d\theta_3}{d\xi_3} - \phi_3\frac{d\theta_3}{d\xi_3}\right)d\xi_3 + C_2\right]^{\frac{\gamma}{\gamma-1}} \qquad (22).$$

The constant of integration C_2 is obtained by applying the energy relation (Equation (10)) at a boundary.

Having assumed a set of streamsurfaces for a particular boundary configuration, the value of $\frac{d\theta_3}{d\xi_3}$ can be approximated from the values of the slope and rate of change of slope of these streamsurfaces at station 3. At each point on a streamline at station 3, the following relation must hold:

$$\theta_3 = \phi_3\left(\frac{df}{d\zeta}\right)_3 \qquad (23),$$

where $\left(\frac{df}{d\zeta}\right)_3$ is the slope of the streamline in question. Thus the value of $\frac{d\theta_3}{d\zeta_3}$ becomes:

$$\frac{d\theta_3}{d\zeta_3} = \frac{d\phi_3}{d\zeta_3}\left(\frac{df}{d\zeta}\right)_3 + \phi_3\left(\frac{d^2f}{d\zeta^2}\right)_3 \qquad (24).$$

In order to approximate the value of $\frac{d\theta_3}{d\zeta_3}$ at points across the channel, it is therefore necessary to estimate the slope and curvature of the assumed streamlines at each point.

For the solution of the direct problem for the rotor with an arbitrary channel shape, Equations (10), (13), (17), (18), (21), (22), and (24) are applicable.

The derivation of the integral for the axial velocity in the case of the stator is carried out in a similar fashion using the form of the energy relation given as Equation (9). Using the sign convention of Figure 8, Equation (17) for the stator (stations 1 to 2) becomes:

$$\lambda_2 = F(\xi_2)\,\phi_2 \qquad (25).$$

The integral for ϕ_2 obviously takes the same form as Equation (18), and is given here only for completeness:

$$\phi_2 = \frac{e^{+\int_{\xi_i}^{\xi_2} \frac{d\xi_2}{\xi_2(1+F^2)}}}{\xi_2\sqrt{1+F^2}} \left[\int_{\xi_i}^{\xi_2} e^{-\int_{\xi_i}^{\xi_2} \frac{d\xi_2}{\xi_2(1+F^2)}} \left\{ \frac{1}{\sqrt{1+F^2}} \left(\frac{P_2}{P_1}\right)^{\frac{1}{\gamma}} \frac{\xi_2}{\phi_1 \xi_1} \left[\frac{\gamma}{\gamma-1} \frac{d\tau_{12}}{d\xi_1} - \frac{\gamma}{\gamma-1} \tau_1 \left(\frac{P_2}{P_1}\right)^{\frac{\gamma-1}{\gamma}} \frac{d}{d\xi_1}\left(\ln \frac{P_1^{\frac{1}{\gamma}}}{Q_1}\right) \right] + \frac{1}{\sqrt{1+F^2}} \frac{d\theta_2}{d\xi_2} \right\} \xi_2\, d\xi_2 + C_1 \right] \qquad (26).$$

For the solution of the direct problem for the stator with an arbitrary channel shape, Equations (9), (12), (21), (22), (24), (25), and (26) (with appropriate subscripts) are applicable.

D. Equations for the Inverse Problem for an Arbitrary Channel Shape

In the inverse problem for the rotor, the same assumptions and basic differential equations are used as in the direct problem with the exception that now the blade relation, Equation (17), is replaced by the following given function which describes the work output of the rotor as a function of the radius at station 3:

$$H(\xi_3) = \xi_2 \lambda_2 + \xi_3 \lambda_3 \qquad (27).$$

The function H (ξ_3) gives the dimensionless rate of change of angular momentum per unit mass flow at the particular radius, and represents the energy taken out of the stream. By multiplying this function by suitable constants it can readily be converted to B. T. U. per pound of mass flow.

The complete derivation of the axial velocity integral is given in Appendix D for the isentropic case and in Appendix E for the polytropic process. For the isentropic inverse problem, the derivation remains the same up to and including Equation (16), which may be written in a slightly modified form as:

$$\frac{\lambda_3^2}{\xi_3} + \frac{1}{2}\frac{\partial}{\partial \xi_3}\left(\lambda_3^2 + \phi_3^2\right) + \frac{\partial}{\partial \xi_3}\left(\xi_3 \lambda_3\right) = \left(\frac{P_3}{P_2}\right)^{\frac{1}{\gamma}} \frac{\phi_3 \xi_3}{\phi_2 \xi_2}\left\{\frac{\gamma}{\gamma-1}\frac{\partial \tau_{2t}}{\partial \xi_2} - \frac{\partial}{\partial \xi_2}\left(\xi_2 \lambda_2\right)\right.$$

$$\left. - \frac{\gamma}{\gamma-1} P_3^{\frac{\gamma-1}{\gamma}} \frac{\partial}{\partial \xi_2}\left(\frac{P_2^{\frac{1}{\gamma}}}{Q_2}\right)\right\} + \phi_3 \frac{\partial \theta_3}{\partial \xi_3} \qquad (28).$$

Using Equation (27) to eliminate λ_3, the integral is found to be:

$$\phi_3 = \int_{\xi_{1i}}^{\xi_3}\left[\left(\frac{P_3}{P_2}\right)^{\frac{1}{\gamma}} \frac{\xi_3}{\phi_2 \xi_2}\left\{\frac{\gamma}{\gamma-1}\frac{d\tau_{2t}}{d\xi_2} - \frac{\gamma}{\gamma-1} P_3^{\frac{\gamma-1}{\gamma}} \frac{d}{d\xi_2}\left(\frac{P_2^{\frac{1}{\gamma}}}{Q_2}\right) + \frac{\left(H - \xi_2 \lambda_2\right)}{\xi_3^2}\frac{d}{d\xi_2}\left(\xi_2 \lambda_2\right)\right\} + \frac{d\theta_3}{d\xi_3}\right.$$

$$\left. - \frac{1}{\phi_3}\left(1 + \frac{H - \xi_2 \lambda_2}{\xi_3^2}\right)\frac{dH}{d\xi_3}\right] d\xi_3 + C_1 \qquad (29).$$

Again the numerical evaluation of this integral by the iteration process to be described later is straightforward once a set of streamlines has been assumed. The unknown P_3 and $\frac{d\theta_3}{d\xi_3}$ appear in the integrand as in the direct problem. Because of the nature of the differential equation, however, the axial velocity ϕ_3 also appears in the integrand.

Since the mass flow and radial momentum integrals remain unchanged, Equations (10), (13), (21), (22), (24), (27), and (29) are applicable to the solution of the isentropic inverse problem.

If the inverse problem could be conceivably applied to a stator it would consist of prescribing values of λ_2 as a function of ξ_{r_2}, and solving for the resulting velocity field, distribution of energy and blade shape (as described by the blade trailing edge angle). In this case, the integral for the axial velocity simplifies to:

$$\phi_2 = \int_{\xi_{r_i}}^{\xi_{r_2}} \left[\left(\frac{P_2}{P_1}\right)^{\frac{1}{\gamma}} \frac{\xi_{r_2}}{\phi_1 \xi_{r_1}} \left\{ \frac{\gamma}{\gamma-1} \frac{d\tau_{tt}}{d\xi_{r_1}} - \frac{\gamma}{\gamma-1} P_2^{\frac{\gamma-1}{\gamma}} \frac{d}{d\xi_{r_1}} \left(\frac{P_1^{\frac{1}{\gamma}}}{\rho_1}\right) \right\} + \frac{d\theta_2}{d\xi_{r_2}} - \frac{\lambda_2}{\phi_2 \xi_{r_2}} \frac{d}{d\xi_{r_2}} (\xi_{r_2} \lambda_2) \right] d\xi_{r_2} + C_1 \tag{30}$$

where $\lambda_2(\xi_{r_2})$ is a prescribed function of the radius at station 2. Equations (9), (12), (21), (22), (24), and (30) (with appropriate subscripts) would be applicable.

E. Changes in Equations for the Compressor Solution

In the development of the equations in the preceding sections, the turbine sign convention given in Figure 8 has been adopted. If the equations are to be used for compressor design, Equation (17) for the direct rotor problem becomes, in accordance with Figure 9:

$$\lambda_3 = \xi_{r_3} - G(\xi_{r_3})\,\phi_3 \tag{31},$$

and the energy relation, Equation (10), is changed to:

$$\frac{\gamma}{\gamma-1}\frac{P_2}{\rho_2} + \frac{1}{2}\left(\theta_2^2 + \lambda_2^2 + \phi_2^2 - 2\xi_{r_2}\lambda_2\right) = \frac{\gamma}{\gamma-1}\frac{P_3}{\rho_3} + \frac{1}{2}\left(\theta_3^2 + \lambda_3^2 + \phi_3^2 - 2\xi_{r_3}\lambda_3\right) \tag{32}.$$

Using these equations, the derivation is carried out in exactly the same manner as set forth in the preceding sections for the turbine.

For the inverse problem for the compressor, the work output function (Equation (27)) becomes:

$$H(\xi_3) = \xi_2 \lambda_2 - \xi_3 \lambda_3 \qquad (33).$$

Using Equations (32) and (33) in place of Equations (10) and (27), the relations for the inverse compressor problem are derived in the same manner as for the turbine.

III. PROPOSED ITERATION PROCEDURE

A. Procedure for the Direct Problem

The general scheme of iteration is exactly the same for the direct and inverse problems, subsonic or supersonic, isentropic or polytropic. In Appendix F, one complete iteration is given for an isentropic supersonic solution (Example Vb) and a polytropic subsonic solution (Example VIII b) for the direct rotor problem. The stator solution is obtained by the same procedure using the appropriate axial velocity integral and energy equation.

In order to understand the technique of iteration for the direct problem described below, the reader is urged to refer frequently to Examples V b and VIII b of Appendix F. For an arbitrary channel shape, seven equations are used in the solution. For the rotor, these relations are Equations (10), (13), (17), (18), (21), (22), and (24). In the examples worked out in Appendix F, the functions $F(\xi_{r_2})$ and $G(\xi_{r_3})$ have been assumed to be constant and independent of radius in order to simplify the axial velocity integral and the computation. This assumption is by no means necessary. For arbitrary given functions, $F(\xi_{r_2})$ and $G(\xi_{r_3})$, the exponential integrals of Equation (18) should be evaluated at various stations across the channel by plotting the integrand and determining the value of the integral graphically.

In the solution of the direct problem, it is assumed that the boundary configuration, blade speed, blade trailing edge angle, and upstream conditions are prescribed. It is further assumed that the mass flow rate is fixed and is compatible with the given upstream conditions.

Once the problem has been set up, the first step is to assume a set of streamsurfaces as shown in Figures 3, 4, and 5. For most applications, these streamsurfaces should be chosen on the basis of equal annular areas in a plane perpendicular to the axis of the machine. The accuracy of the solution can be improved by increasing the number of stations across the channel. However, it is believed that for most purposes, six or seven steps will give sufficient accuracy for design work.

Having assumed a reasonable set of streamlines, the second step is to estimate the axial velocity distribution at the downstream station. Taking average or middle-channel values for the prescribed upstream conditions, the mass flow relation and the energy equation can be combined into one equation in terms of ϕ_3. Using average values in Equations (10) and (21), the relation is obtained as follows:

$$\overline{\tau}_3 = \overline{\tau}_{2t} - \frac{\gamma-1}{2\gamma}\left[\overline{\theta}_3^2 + \overline{\lambda}_3^2 + \overline{\phi}_3^2 + 2\left(\overline{\xi_{r_2}}\lambda_2 + \overline{\xi_{r_3}}\lambda_3\right)\right] \tag{34}$$

$$m = \overline{\rho}_2\left(\frac{\overline{\tau}_3}{\overline{\tau}_2}\right)^{\frac{1}{\gamma-1}} \overline{\phi}_3 \left(\frac{\xi_o^2 - \xi_i^2}{2}\right) \tag{35}.$$

Substituting Equation (34) into Equation (35) gives:

$$m = \overline{\rho}_2\left(\frac{\overline{\tau}_{2t} - \frac{\gamma-1}{2\gamma}\left[\overline{\theta}_3^2 + \overline{\lambda}_3^2 + \overline{\phi}_3^2 + 2\left(\overline{\xi_{r_2}}\lambda_2 + \overline{\xi_{r_3}}\lambda_3\right)\right]}{\overline{\tau}_2}\right)^{\frac{1}{\gamma-1}} \overline{\phi}_3 \left(\frac{\xi_o^2 - \xi_i^2}{2}\right) \tag{36}.$$

Using Equation (17) to eliminate $\overline{\lambda}_3$ and Equation (23) to eliminate $\overline{\theta}_3$, Equation (36) becomes a relation involving only one unknown, $\overline{\phi}_3$. The solution must be found by trial and error. In general, there will be two values of $\overline{\phi}_3$ which satisfy this

equation corresponding to the average subsonic and supersonic solutions.

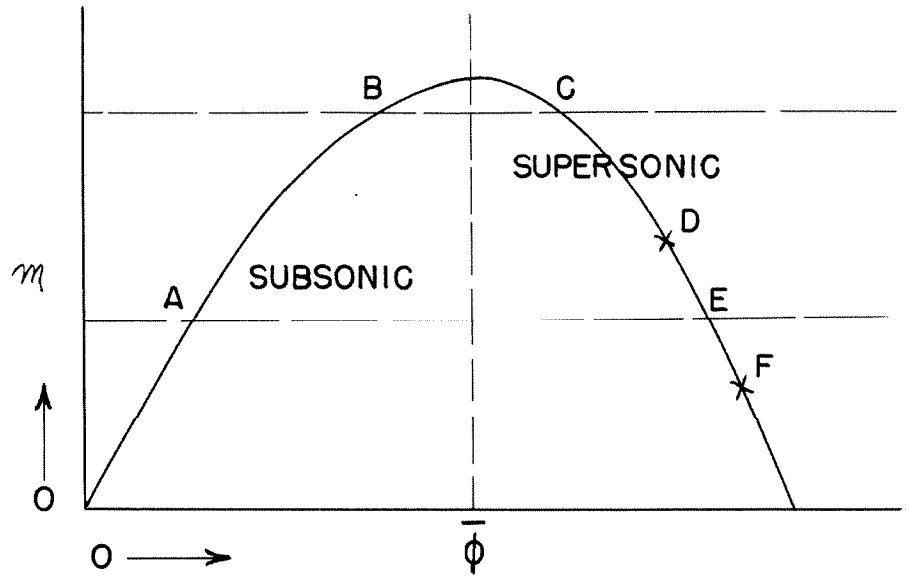

FIG. 2 — PLOT OF MASS FLOW VS. AVERAGE AXIAL VELOCITY FOR CHANNEL FLOW

If no value of $\bar{\phi}_3$ satisfies Equation (36), the prescribed mass flow cannot be forced through the channel because of choking, and the boundary configuration or upstream conditions must be altered accordingly.

Having found the average value of the axial velocity at station 3, an estimate of the distribution of this velocity across the channel can be made considering the total temperature gradient, the blade shape, and the pressure distribution expected at the downstream station.

Using the estimated distribution of ϕ_3, Equation (22) is iterated across the channel to determine the pressure gradient. The tangential velocity is found from Equation (17), the radial velocity from Equation (23), and the value of $\frac{d\theta_3}{d\zeta_3}$ from Equation (24). In order to evaluate θ_3, $\frac{d\theta_3}{d\xi_3}$, and $\frac{d\theta_3}{d\zeta_3}$ at various points across the

channel, it is necessary to estimate as accurately as possible the slope and curvature of each streamline at the station in question. Knowing the complete channel configuration, slopes and curvatures at points across the channel can be easily estimated using a simple linear distribution scheme, or a large scale drawing can be constructed and the values of slope and curvature taken graphically from this. The value of $\frac{d\phi_3}{d\zeta_3}$ in Equation (24) can be taken as the average value between stations along the axis. However, it is to be noted that even a relatively large error in the estimation of the above quantities will have little effect upon the pressure gradient obtained because of the nature of the integrated form of Equation (22). The actual pressure distribution across the channel is found by applying the energy equation at a boundary to determine the constant C_2.

With these values of P_3 and $\frac{d\theta_3}{d\zeta_3}$, the axial velocity integral can now be iterated across the channel for values of ϕ_3 in terms of the constant C_1. If the curvature of the channel is not large, the value of $\frac{d\theta_3}{d\zeta_3}$ is very small compared to the other factors in the integrand (2G, for example), and hence a relatively large error in estimating $\frac{d\theta_3}{d\zeta_3}$ has a small effect on the resulting value of ϕ_3. The constant C_1 is obtained by iterating the mass flow relation (Equation (21)) across the channel, and a new axial velocity distribution is obtained.

The above described process is the procedure for one complete iteration of the given equations. Normally in the subsonic case, the distribution of ϕ_3 thus obtained is used in the next iteration, and the process is repeated until the axial velocity distribution produced by an

iteration is the same as that assumed for that particular iteration. This is the solution. Values of τ_3 and Ω_3 are then found by use of Equation (13).

B. Procedure for the Inverse Problem

Generally, the same procedure of iteration, as described in section A above for the direct problem, is used in the solution of the inverse problem. Equations (10), (13), (21), (22), (24), (27), and (29) are applicable to the isentropic rotor. Relations used in the polytropic case are derived in Appendix E. Examples IX, X, and XI of Appendix F are typical solutions to the inverse problem. One complete iteration is given in Example IX b to illustrate the method used.

It is noted that the integrand of Equation (29) contains a term involving $\frac{1}{\phi_3}$. Since in any practical solution the axial velocity at any point across the channel will not be zero, this term does not cause any real difficulty in the iteration procedure. However, if the original estimate of the axial velocity profile at the downstream station differs greatly from the actual solution, it has been found that successive iterations will "oscillate" about the real solution, but will eventually converge as in the direct problem.

It is obvious that the work output function $H(\xi_3)$, given as Equation (27), must be prescribed reasonably. For any given channel shape, blade speed, upstream conditions and mass flow, there is a limited range of blade angles that can be used before the smooth flow over the blades is destroyed by separation effects. The limitation thus imposed by the maximum turning angle through the blade row also

limits not only the amount of work that can be extracted, but also the distribution of this work across the channel.

C. Convergence of Subsonic and Supersonic Solutions

Figure 2 indicates that, for any given setup, there is normally a supersonic as well as a subsonic solution for the direct and inverse problems. This is illustrated in Appendix F by Examples IV a and V a for the stator and Examples IV b and V b for the rotor. In these examples, for a given boundary configuration, blade spouting angle, and set of upstream conditions, both the subsonic and supersonic solutions have been obtained.

Experience in working various examples has shown that if the flow is in the low subsonic range, point A of Figure 2, for example, the iteration process converges very rapidly, and only two or three iterations are necessary to obtain accuracy of four significant figures in the solution. However as the flow becomes highly subsonic as at point B, the convergence becomes less rapid, and more iterations are necessary to obtain the solution. It is interesting to note that, in the subsonic range, the process will converge from any reasonable assumed distribution of ϕ_3. It is even possible to obtain a solution in which the flow is supersonic in one part of the channel and subsonic in the remainder (Examples I a and III a).

It has been found, however, that if the flow is completely supersonic (point E of Figure 2, for example), the iteration process diverges rapidly away from the solution. Thus if an axial velocity distribution is assumed whose average value is represented by point D, successive iterations will result in decreasing values of ϕ_3 and

eventually the subsonic solution at point A will be reached. If an axial velocity distribution corresponding to point F is assumed, successive iterations will rapidly increase ϕ_3 toward infinity. It is the realization of this phenomenon which makes it possible to obtain the isentropic supersonic solution in a given problem. Having made two successive iterations at each of the points D and F, and having noted the relative change in the constant C_1 in these iterations, a simple interpolation will give the values of ϕ_3 corresponding to the solution at point E once the solution has been "straddled".

It is important to understand the basic reason why the proposed iteration process is successful. For either the direct or inverse problems, six unknowns must be solved for at the downstream station. These are the three components of velocity (θ_3, λ_3 and ϕ_3), the pressure P_3, the density Q_3, and the temperature τ_3 . Using the isentropic (or polytropic) relation along streamsurfaces, two of these (Q_3 and τ_3) can be eliminated. The remaining four unknowns are made functions of the axial velocity ϕ_3 and the boundary and streamline configuration. The radial velocity is eliminated in terms of ϕ_3 by Equation (23), the tangential velocity λ_3 by Equation (17) or (27), and the pressure P_3 by the integral, Equation (22). Thus, effectively, only one unknown remains, the axial velocity ϕ_3 , and for any assumed distribution of ϕ_3, all other unknowns are determined. An iteration process must be used to determine ϕ_3 because of the complexity of the equations involved.

D. Correction for the Displacement of Streamlines

Having assumed a set of streamsurfaces for any particular example, and having found the corresponding solution by the proposed iteration procedure, it is possible to make a correction to determine more accurately the actual position of the streamsurfaces and thus refine the solution. The mass flow functions $m(\xi_2)$ and $m(\xi_3)$ are plotted against radius for conditions at stations 2 and 3 as shown in Figure 6. Using this diagram and fixing the radial coordinates at station 3, it is possible to estimate new corresponding upstream coordinates. With these corrected upstream radial coordinates, and the upstream conditions corresponding to them, the problem is reworked and a new solution found. It is to be emphasized that this is a small correction and that the new solution will not vary more than one or two percent from the solution based on the original streamsurfaces. An illustration of this method is given in Example V b of Appendix F.

IV. ADDITIONAL CORRECTIONS AND SIMPLIFICATIONS

A. Corrections to the Basic Solution

If it is desired to solve for the flow pattern and distribution of energy in the field at any axial station in the blade row itself, this can be done approximately by multiplying the axial velocity by a function which accounts for the blade thickness and thus reduces the effective area of the channel. Assuming a blade thickness function $t(\zeta)$ and a blade spacing s, the increased axial velocity at any point within the blade row would be:

$$(\phi)_\zeta = \phi\left(\frac{s}{s-t(\zeta)}\right) \tag{37}$$

where s and $t(\zeta)$ are assumed to be known functions at any radial position across the channel. The assumptions used in the direct problem, including that of axial symmetry, remain unchanged, except that the blade spouting angle now becomes the mean camber line at the point in question. The fundamental equations and iteration procedure remain unchanged except for the use of the above indicated expression for the axial velocity.

One of the basic assumptions used in the derivation of the fundamental equations given in Part II, is that the effects of the vorticity of the flow downstream on upstream conditions are negligible. A correction to the upstream conditions due to vorticity effects downstream could be made using the approximate theory suggested by Marble (Reference 15) for the three-dimensional case. If the hub ratio is large, the simpler two-dimensional approximation given by Rannie (Reference 1) can be used. Once the upstream conditions have

been changed using this higher order correction, the corresponding new solution can then be found by the same procedure as previously outlined in Part III.

B. Simplification of Flow Patterns

An investigation has been made to determine whether or not there are any special cases in which the equations, used in this analysis of three-dimensional, compressible flow, reduce to a simple expression for the axial velocity. Consider the integrated radial momentum equation:

$$P_3 = \left[\frac{\gamma-1}{\gamma} \left(\frac{Q_2}{P_2^{\frac{1}{\gamma}}} \right) \int_{\xi_i}^{\xi_3} \left(\frac{\lambda_3^2}{\xi_3} - \theta_3 \frac{d\theta_3}{d\xi_3} - \phi_3 \frac{d\theta_3}{d\xi_3} \right) d\xi_3 + C_2 \right]^{\frac{\gamma}{\gamma-1}} \qquad (22).$$

Since the value of P_3 appears in the integrated mass flow relation, Equation (21), to the power $\frac{1}{\gamma}$, it is clear that, generally, no simplification can be made for a channel of arbitrary shape where the values of $\theta_3 \frac{d\theta_3}{d\xi_3}$ and $\phi_3 \frac{d\theta_3}{d\xi_3}$ cannot be expressed in terms of constants and the radius ξ_3.

However, one simplification does occur in the example of a rotor in a cylindrical channel. In this case, if the velocity after the rotor is purely axial, Equation (22) reduces to $P_3 = C_2^{\frac{\gamma}{\gamma-1}}$. If, in addition, the total temperature and pressure are constant across the channel at station 2, and if $\lambda_2 = \frac{\alpha}{\xi_2}$ (vortex flow), Equation (16) for a straight channel reduces to $\phi_3 = C_1$. The constant C_2 is evaluated by applying the energy equation at a boundary, and the mass flow integral becomes:

$$m = \int_{\xi_i}^{\xi_o} \frac{1}{\tau_{2t}} \left[1 - \frac{\gamma-1}{2\gamma} \frac{C_1^2}{\tau_{2t}} \right]^{\frac{1}{\gamma-1}} C_1 \xi_1 \, d\xi_1 \qquad (38),$$

or, since τ_{2t} is constant,

$$m = \frac{C_1}{\tau_{2t}} \left[1 - \frac{\gamma-1}{2\gamma} \frac{C_1^2}{\tau_{2t}} \right]^{\frac{1}{\gamma-1}} \frac{\xi_o^2 - \xi_i^2}{2} \qquad (39).$$

Even in this simplified case, Equation (39) must be solved by trial and error for the constant C_1. This particular example gives a constant mass flow per unit area and the work is taken out uniformly across the channel.

With the exception of the above case, it can be generally stated that there are no special conditions or flow patterns in three-dimensional, compressible flow through turbomachinery using this method which result in a simple closed-form solution for the downstream axial velocity.

C. Proposed Optimum Turbine Design Condition

In the design of a turbine, the condition which normally controls the amount of heat that can be released in the combustion chamber is the limiting temperature that the first stage rotor blade root can safely withstand in continuous operation. Since the blade stresses decrease from root to tip, the allowable temperature is higher at the tip than at the root. This fact allows the possibility of increasing the amount of heat released in the combustion chamber, and hence the energy in the jet exhaust, for a fixed amount of work taken out of a turbine.

In formulating the optimum turbine design condition, reference

will be made to a one-stage turbine with an arbitrary, but fixed, boundary configuration, such as is shown in Figure 5. It is assumed that the total pressure in the combustion chamber, the blade speed, mass flow and total amount of work to be extracted by the turbine are fixed by conditions in the compressor. It is further assumed that the distribution of the maximum allowable total temperature across the channel at station 2, based on limiting blade temperatures, is known. Since the total enthalpy is conserved through the stator row, the limiting total temperature profile at station 1 is therefore known.

In order that the maximum energy be left in the exhaust gases at station 3, the condition is imposed that the velocity shall be axial after the turbine ($\lambda_3 = 0$) and that the total enthalpy shall be constant across the channel at this station ($\frac{d\tau_{3t}}{d\xi_3} = 0$).

To simplify the formulation of the proposed optimum turbine design condition, it is assumed that the known limiting total temperature profile at station 1 is linear, and that the combustion chamber can be constructed so as to give this desired total temperature variation across the channel.

The design problem can then be formulated as follows: Given a one-stage turbine with fixed boundary configuration, combustion chamber total pressure, blade speed, mass flow, and linear total temperature profile at station 1, what are the blade spouting angles of stator and rotor so that a given amount of work can be extracted by the rotor and yet leave the total temperature constant and the velocity axial at station 3?

With the above assumptions and conditions, Equation (27) can be written:

$$H(\xi_3) = \xi_{z_2} \lambda_2 \qquad (40),$$

and Equation (10) in terms of total temperatures becomes:

$$\frac{\gamma}{\gamma-1} \tau_{2t} - \xi_{z_2} \lambda_2 = \frac{\gamma}{\gamma-1} \tau_{3t} \qquad (41).$$

If τ_{3t} is to be constant at station 3, then the work must be taken out across the channel in such a way that:

$$\Delta \xi_{z_2} \lambda_2 = \Delta \frac{\gamma}{\gamma-1} \tau_{2t} \qquad (42).$$

Since the linear change in total temperature at station 2 is assumed known, the distribution of work across the channel is determined by Equation (42) and the total amount of work to be extracted. The solution to this simplified inverse problem is found in a manner similar to that illustrated by Example X of Appendix F, and the blade trailing edge angles of stator and rotor are completely determined.

In view of the discussion given in Part III, Section B, on limiting blade angles, it will obviously not always be possible to obtain the above proposed optimum condition, particularly if the upstream total temperature gradient is large. Furthermore, the above considerations could not reasonably apply to a multi-stage turbine since boundary layer effects and mixing would soon destroy the original total temperature profile. However, the designer should not overlook the possibility of increasing the gross thrust of a turbine by the use of a total enthalpy gradient based on blade limiting temperatures. (See Example XI, Appendix F.)

V. RESULTS AND CONCLUSIONS

An approximate method has been developed for the solution of three-dimensional, compressible flow in axial turbomachines. The methods and equations used are extremely flexible and can be used to solve the direct and inverse problems, subsonic or supersonic, isentropic or polytropic for either a turbine or a compressor. The upstream conditions, blade shape (as defined by the blade trailing edge angle), blade speed, and axial boundary configuration can be prescribed in the direct problem, while the upstream conditions, blade speed, blade loading, and axial boundary configuration can be prescribed in the inverse problem. In each case, six unknowns are solved for at the downstream station. These are the three components of velocity, the pressure, the density, and the temperature. In the analysis, maximum utilization has been made of the given channel configuration.

The equations are derived for a blade row with infinitely many blades, on the basis of isentropic (or polytropic), non-viscous, compressible, axially-symmetric, steady flow. Radial or nearly radial blades are assumed so that the radial force can be neglected. Separation of flow and boundary layer effects are not considered in the analysis. For an arbitrary boundary shape, a special type of blading is assumed whose only effect on the flow is to turn it through a specified blade angle distribution across the channel. Using the assumption that the blade shape is specified by the blade trailing edge angle only, and assuming that this spouting angle is very nearly independent of conditions ahead of the blade row in the operating range, the analysis of the flow has been made at the station immediately downstream of the blade

row in terms of specified conditions immediately upstream of the blade row.

This method greatly simplifies the analysis of flow in turbomachines, since, with the above assumptions, it is not necessary to solve for the complete three-dimensional flow field through the blade row, but only to consider stations immediately upstream and downstream of the blading.

The iteration process developed is simple and straightforward, and the same general procedure is used in the solution of all suggested types of problems. The calculations can be done with a slide rule, and the accuracy of the solution can be improved by increasing the number of radial steps across the channel. Corrections can be made for the displacement of the assumed streamlines and for the effect of downstream vorticity on upstream conditions to further improve the solution. It is believed that the results thus obtained by this approximate method are sufficiently accurate for design purposes.

Once the boundary configuration and other necessary conditions have been assumed for any particular problem, experience in working various examples by the proposed iteration process has shown that a basic solution for the direct problem accurate to four significant figures can be obtained for a stator in approximately four hours and obtained for a rotor in approximately six hours. The calculations for the inverse problem are somewhat simpler and less time is normally required for this solution.

In order to evaluate the term $\frac{d\theta}{d\zeta}$ which appears in both the integral for the axial velocity and the integral for the pressure in

the case of an arbitrary channel shape, it is necessary to estimate the slope and curvature of the streamlines at the station in question. It is to be noted that, for a reasonable channel shape, a relatively large error in this estimation will have little effect on the solution obtained. The term $\frac{d\theta}{d\zeta}$ appears in the general axial velocity integral for the rotor (Equation (18)) and for the stator (Equation (26)) as a small correction term, and a large error in the assumed values of slope and curvature will have a small effect on the resulting axial velocity profile. This is especially true for the rotor where the term 2G is normally dominant.

Considering the pressure integral (Equation (22)), it is to be noted that here, again, the contribution of the term $\frac{d\theta}{d\zeta}$ is small for a reasonable boundary shape. For the stator, the term $\frac{\lambda^2}{\xi}$ is the predominant one, and the terms $\theta \frac{d\theta}{d\xi}$ and $\phi \frac{d\theta}{d\zeta}$ are usually small corrections. Because of the small magnitude of the factor multiplying the integrand of Equation (22) in the iteration, a relatively large error in $\frac{d\theta}{d\zeta}$ will have but a slight effect on the resulting pressure gradient. After the rotor, where the velocity is predominantly axial, the term $\frac{\lambda^2}{\xi}$ might be of the same order of magnitude as $\theta \frac{d\theta}{d\xi}$ and $\phi \frac{d\theta}{d\zeta}$. As a result, it is possible to have a negative pressure gradient radially after a rotor if the slope and curvature of the channel is large.

It is impossible to make any general statement as to the relative contribution of the integral (Equation (18)) and the constant of integration C_1 to the resulting axial velocity profile. The relative size of the integral and the constant may be of any magnitude depending on the channel shape, total temperature gradient, blade spouting angles, and

upstream conditions of any particular example.

Several interesting observations are possible from the results of the examples given in Appendix F. The channel shapes assumed for these iterated problems are given as Figures 3, 4, and 5. In each example, the assumptions, channel configuration, upstream conditions radial coordinates, and other data are specified, and the resulting solution at the downstream station is tabulated. One complete iteration is given in Examples Vb, VIII b, and IX b to show the method used in each case.

Examples I and II use the channel configuration shown in Figure 3. In both of these examples of the direct problem, the mass flow, blade speed, blade spouting angles, and total heat content in the flow are the same. Example I, however, has no radial total temperature gradient at station 1, while Example II has a large radial enthalpy gradient. The effect of a total temperature gradient across the channel in changing the axial velocity profile is clearly evident from the results obtained. Normally for a stator, it is to be expected that the positive pressure gradient would make the axial velocity higher at the root than at the tip. This is the case in Example I a for no temperature gradient. However, Example II a shows that the effect of the positive total gradient imposed is to make the axial velocity higher at the tip than at the root, and reduce the Mach number slightly at all stations across the channel. Also, the resulting total pressure at station 3 has been increased by the use of the radial enthalpy gradient.

Examples IV and V use the channel configuration of Figure 5, and have the same mass flow, blade speed, blade spouting angles, and

conditions at station 1. Example IVa is the subsonic stator solution while Example Va is the supersonic solution for the same stator. Examples IVb and Vb are the subsonic and supersonic rotor solutions, respectively, for conditions after the subsonic stator of Example IVa. The mass flow functions for the subsonic and supersonic rotor examples are plotted in Figure 6. From this graph, the position of the displaced streamlines has been estimated and plotted on Figure 7. This plot of the streamline shift in each case, clearly indicates that the shift is in one direction when the "governing" Mach number is subsonic, and in the opposite direction when the "governing" Mach number is supersonic. The "governing" Mach number has been defined by Monroe (Reference 7, page 51) as the Mach number based on the meridional velocity instead of the total velocity. The results shown in Figure 7 clearly agree with Monroe's observation that the deflection of the "meridional Mach surfaces" is in different directions for subsonic and supersonic "governing" Mach numbers, and that the deflection of the streamsurfaces will be less if the governing velocity is transonic than if it is entirely subsonic or entirely supersonic.

Examples VI, VII, and VIII use the channel configuration of Figure 5, the same conditions at station 1, and the same blade speed, blade spouting angles, and mass flow. Example VI is the isentropic case, Example VII is a polytropic solution with $n = 1.37$ ($\eta = 94.5$ percent), and Example VIII is a polytropic solution with $n = 1.33$ ($\eta = 86.8$ percent). From these examples, the effect of a decrease in "polytropic efficiency" on the three-dimensional velocity field and distribution of energy in the flow can clearly be seen. When the

"efficiency" has dropped to 94.5 percent, the average axial velocity at station 3 has increased 2.7 percent, the average total pressure has decreased 2.5 percent, and the work output has increased 4.7 percent when compared with the isentropic solution. As the "polytropic efficiency" drops to 86.8 percent, the results of Example VIII show that the average axial velocity at station 3 has increased 8.2 percent, the average total pressure has decreased 8.0 percent, and the work output has increased 17.0 percent when compared with the isentropic solution.

The results of these examples clearly show the reason for the "loading up" of the first stages of a multi-stage turbine as the efficiency drops. As the efficiency decreases, more work is taken out in the initial stage, and less total pressure is left for the remaining turbine stages. Thus, the last stage of a multi-stage turbine may well act as a compressor if the efficiency of the system has dropped sufficiently. In view of this phenomenon, it is obvious that the design engineer should design his machine for the expected efficiency in the operating range, and not on the basis of isentropic flow.

Example XI has been constructed to illustrate the increase in gross thrust obtainable by the use of a radial total temperature gradient. Assuming a one-stage turbine configuration similar to that shown in Figure 3, and keeping the mass flow, combustion chamber total pressure, blade speed, and work extracted constant in each case, the gross thrust of the jet exhaust has been calculated with and without a total temperature gradient. In order to give the example more physical meaning, blades were used which were tapered in cross-sectional area from hub to tip. Having calculated the centrifugal stress at various radial points

along the blades, and using the high temperature data for "Vitallium" (H.S. 21) (NR-10) given in References 16 and 17, it was estimated that the rotor blade root could safely stand a temperature of 1450°F, while the blade tip temperature could be 1850°F.

Using this data, the gross thrust of the turbine was calculated for: (a) A constant radial total temperature of 1450°F, and (b) a linear total temperature gradient of 400°F with the same root total temperature of 1450°F. The results of these examples show that an increase in gross thrust of 917.8 pounds, or 7.7 percent, was obtained by the use of the radial total temperature gradient indicated.

REFERENCES

1. Bowen, J. T., Sabersky, R. H. and Rannie, W. D.: "Theoretical and Experimental Investigations of Axial Flow Compressors." Report on Research Conducted under Navy Contract N6-ORI-102, Task Order IV. Mechanical Engineering Laboratory, California Institute of Technology.

2. Traupel, W.: "New General Theory of Multistage Axial Flow Turbomachines", NavShips 250-445-1, Navy Dept. (Translated by C. W. Smith, General Electric Corp.)

3. Traupel, W.: "Kömpressible Strömung durch Turbinen", Schweizer Archiv, pp. 176-186. June 1950.

4. Sinnette, J. T., Costello, G. R. and Cummings, R. L.: "Expressions for Measuring the Accuracy of Approximate Solutions to Compressible Flow through Cascades of Blades". NACA T.N. 2501, 1951.

5. Marble, F. E. and Michelson, I.: "Analytical Investigation of Some Three-Dimensional Flow Problems in Turbomachines". Final Report on NACA Contract NAw-5665, C.I.T., May 1950.

6. Fabri, J. and Seistrunck, R.: "Ecoulements Tourbillonnaires dans les Machines Axiales". France, Office National d'Etudes et de Recherches Aeronautiques, Publication No. 45, 1950.

7. Monroe, G. M., Lt. U.S. Navy: "A Study of Compressible Fluid Motion in Turbomachines with Infinitely Many Blades". Ph.D. Thesis, California Institute of Technology, 1951.

8. Vavra, M. H.: "Steady Flow of Nonviscous Elastic Fluids in Axially Symmetric Channels". Journal of the Aeronautical Sciences, Vol. 17, No. 3, March 1950, pp. 149-156, 172.

9. Wu, Chung-Hua: NACA T.N. 1795, 2214, 2302, 2407, 2455, 2492, 2604, 2702.

10. Reissner, H.: "Blade Systems of Circular Arrangement in Steady, Compressible Flow". Courant Anniversary Volume-Studies and Essays, Interscience Publishers, Inc., 1948.

11. Goldstein, A. W.: "Axisymmetric Supersonic Flow in Rotating Impellers". NACA T.N. 2388, 1951.

12. Wislicenus, G. F.: "Fluid Mechanics of Turbomachinery", Mc-Graw-Hill Book Co., Inc. (New York) 1947.

13. Traugott, S. C., Smith, L. H. Jr., and Wislicenus, G.F.: "A Practical Solution of a Three-Dimensional Flow Problem of Axial-Flow Turbomachinery". Published by the Department of Mechanical Engineering, Johns Hopkins University, 1952.

14. Bowen, J. T., Sabersky, R. H., and Rannie, W. D.: "Investigations of Axial Flow Compressors". Am. Soc. of Mech. Eng., Preprint No. 49-A-102.

15. Marble, F. E.: "The Flow of a Perfect Fluid Through an Axial Turbomachine with Prescribed Blade Loading"; J.A.S., Vol. 15, No. 8, pp. 473-485, Aug. 1948.

16. Sweeney, W. O.: "Haynes Alloys for High-Temperature Service", Trans. Am. Soc. Mech. Engrs., Vol. 69, 569 (1947).

17. Clark, F. H.: "Metals at High Temperatures", pp. 208-211, Reinhold Pub. Co., 1950.

18. Sinnette, J. T., Jr.: "Increasing the Range of Axial Flow Compressors by Use of Adjustable Stator Blades". Jour. Aero. Sci., Vol. 14, No. 5, pp. 269-282, May 1947.

19. Karlsson, T.: "On the Influence of Radial Components of Blade Forces in Axial Turbomachines", M.E. Thesis, Calif. Inst. of Technology, 1953.

APPENDIX A

SYMBOLS AND DEFINITIONS

β_2 - Stator spouting angle measured from the plane perpendicular to the axis.

β_3 - Rotor spouting angle measured relative to the rotating wheel.

c - Axial distance between stations in feet.

C_1 - Constant obtained from axial velocity integral.

C_2 - Constant obtained from radial momentum integral.

C_p - Specific heat at constant pressure.

Δ - Used to denote incremental changes of a quantity in the radial direction.

$F(\xi_2)$ - Cotangent of stator spouting angle β_2 as a function of radius. $F(\xi_2) = \frac{\lambda_2}{\phi_2}$

$G(\xi_3)$ - Cotangent of rotor relative spouting angle β_3 as a function of radius. $G(\xi_3) = \frac{\lambda_3 + \xi_3}{\phi_3}$

γ - Ratio of specific heats.

g - Acceleration of gravity (32.17 ft/sec^2).

$H(\xi_3)$ - Dimensionless work output of rotor as a function of radius. $H(\xi_3) = \xi_2 \lambda_2 + \xi_3 \lambda_3$

m - Dimensionless mass flow. $m = \frac{W\omega}{2\pi g p_t R_o}$

M - Mach number based on total velocity. $M = \frac{\phi}{\sqrt{\gamma\tau}}$

Mg - "Governing" Mach number as defined on p. 87 of Reference 7. $M_g = \sqrt{\frac{\phi^2 + \theta^2}{\gamma\tau}}$

n - Polytropic exponent.

η - Polytropic efficiency. $\left(\frac{\gamma}{\gamma-1}\right)\eta = \frac{n}{n-1}$

ω - Angular velocity of rotor in radians per second.

p - Pressure in pounds per square foot.

P - Dimensionless pressure. $P = \frac{p}{p_o}$

ρ - Density (lb. sec.^{2}/ft.^{4}).

Q - Dimensionless density. $Q = \frac{\omega^2 R_o^2 \rho}{p_t}$

R - Gas constant ($1715 \frac{ft^2}{sec^2 {}^oF}$).

R_o - Reference radius in feet.

r - Radius from the axis in feet.

ξ - Dimensionless radius. $\xi = \frac{r}{R_o}$

T - Absolute temperature in degrees Rankine.

τ - Dimensionless temperature. $\tau = \frac{R}{\omega^2 R_o^2} T$

u - Radial component of absolute velocity in feet per second.

θ - Dimensionless radial component of absolute velocity. $\theta = \frac{u}{\omega R_o}$

v - Tangential component of absolute velocity in feet per second.

λ - Dimensionless tangential component of absolute velocity. $\lambda = \frac{v}{\omega R_o}$

w - Axial component of absolute velocity in feet per second.

ϕ - Dimensionless axial component of absolute velocity. $\phi = \frac{w}{\omega R_o}$

$\underline{\Phi}$ - Dimensionless total absolute velocity. $\underline{\Phi} = \sqrt{\phi^2 + \lambda^2 + \theta^2}$

W - Mass flow in pounds per second.

z - Axial distance along axis of rotor from reference point in feet.

ζ - Dimensionless axial distance. $\zeta = \frac{z}{R_o}$

$( )_1$ - Subscript to denote station immediately upstream of stator.

$( )_2$ - Subscript to denote station immediately downstream of stator and immediately upstream of rotor.

$( )_3$ - Subscript to denote station immediately after rotor.

$( )_i$ - Subscript to denote inner boundary of channel.

$( )_o$ - Subscript to denote outer boundary of channel.

$\frac{\partial f}{\partial \zeta}$ - Slope of streamline.

$\frac{\partial^2 f}{\partial \zeta}$ - Rate of change of slope of streamline.

APPENDIX B

Note: In Appendices B, C, D, E and F, Equations of lower number than 43 refer to relations previously given in the text. The numbering of equations is consistent throughout the thesis.

Development of Equations for Direct Problem (Isentropic).

The equations are derived for a rotor with infinitely many blades on the basis of isentropic, non-viscous, compressible, axially-symmetric, steady flow. Radial or nearly radial blades are assumed so that the radial force can be neglected. The channel shape, blade shape, mass flow, and upstream conditions are assumed specified in any particular example.

The derivation follows the general procedure given in Reference 1, Section 2:2.2 for the incompressible case. The energy equation is written for any two points (for example, b_2 and b_3, Fig. 5) on a streamline surface between stations 2 and 3. Using absolute velocities, the equation in dimensionless form is:

$$\frac{\gamma}{\gamma-1}\tau_{2t} - \xi_2\lambda_2 = \frac{\gamma}{\gamma-1}\tau_3 + \frac{1}{2}\left[\theta_3^2 + \left(\lambda_3 + \xi_3\right)^2 + \phi_3^2\right] - \frac{1}{2}\xi_3^2 \qquad (43)$$

where

$$\frac{\gamma}{\gamma-1}\tau_{2t} = \frac{\gamma}{\gamma-1}\tau_2 + \frac{1}{2}\left(\theta_2^2 + \lambda_2^2 + \phi_2^2\right),$$

and

$$\frac{\gamma}{\gamma-1}\tau_{3t} = \frac{\gamma}{\gamma-1}\tau_3 + \frac{1}{2}\left(\theta_3^2 + \lambda_3^2 + \phi_3^2\right).$$

The energy equation is now differentiated in respect to the radius at stations 2 and 3:

$$\left\{\frac{\gamma}{\gamma-1}\frac{d\tau_{2t}}{d\xi_{2}} - \frac{d}{d\xi_{2}}\left(\xi_{2}\lambda_{2}\right)\right\}d\xi_{2} = \left\{\frac{\gamma}{\gamma-1}\frac{d}{d\xi_{3}}\tau_{3} + \frac{1}{2}\frac{d}{d\xi_{3}}\left(\theta_{3}^{2}+\lambda_{3}^{2}+\phi_{3}^{2}\right) + \frac{d}{d\xi_{3}}\left(\xi_{3}\lambda_{3}\right)\right\}d\xi_{3} \qquad (44).$$

Using the gas equation, $\tau_3 = \frac{p_3}{\rho_3}$, the first term of the right side of Equation (44) becomes, with the isentropic relation:

$$\frac{\rho_3}{\rho_2} = \left(\frac{p_3}{p_2}\right)^{\frac{1}{\gamma}} = \left(\frac{\tau_3}{\tau_2}\right)^{\frac{1}{\gamma-1}} \qquad (13)$$

$$\frac{\gamma}{\gamma-1}\frac{d\tau_3}{d\xi_3} = \frac{\gamma}{\gamma-1}\frac{d}{d\xi_3}\left(\frac{p_3}{\rho_3}\right) = \frac{\gamma}{\gamma-1}\frac{d}{d\xi_3}\left(\frac{p_2^{\frac{1}{\gamma}}}{\rho_2}p_3^{\frac{\gamma-1}{\gamma}}\right) \qquad (45).$$

Using the differential form of the continuity equation for a stream cylinder of small radial extent,

$$\phi_2\rho_2\xi_2\,d\xi_2 = \phi_3\rho_3\xi_3\,d\xi_3 \qquad (8)$$

and differentiating Equation (45) as a product, the following is obtained:

$$\frac{\gamma}{\gamma-1}\frac{d}{d\xi_3}\left(\frac{p_3}{\rho_3}\right) = \frac{p_2^{\frac{1}{\gamma}}}{\rho_2 p_3^{\frac{1}{\gamma}}}\frac{dp_3}{d\xi_3} + \frac{\gamma}{\gamma-1}p_3^{\frac{\gamma-1}{\gamma}}\frac{d}{d\xi_3}\left(\frac{p_2^{\frac{1}{\gamma}}}{\rho_2}\right)$$

$$\frac{\gamma}{\gamma-1}\frac{d}{d\xi_3}\left(\frac{p_3}{\rho_3}\right) = \frac{1}{\rho_3}\frac{dp_3}{d\xi_3} + \frac{\gamma}{\gamma-1}\frac{p_3}{p_2^{\frac{1}{\gamma}}}\frac{d}{d\xi_2}\left(\frac{p_2^{\frac{1}{\gamma}}}{\rho_2}\right)\frac{\phi_3\xi_3}{\phi_2\xi_2} \qquad (15).$$

Using the radial momentum equation at station 3,

$$\frac{1}{\rho_3}\frac{\partial p_3}{\partial \xi_3} = \frac{\lambda_3^2}{\xi_3} - \theta_3\frac{\partial\theta_3}{\partial\xi_3} - \phi_3\frac{\partial\theta_3}{\partial\zeta_3} \qquad (11)$$

and combining Equations (8), (11), (15) and (44), the following differential equation results:

$$\left\{\frac{1}{Q_3}\frac{dP_3}{d\xi_3}+\frac{\gamma}{\gamma-1}\frac{P_3}{P_2^{\frac{1}{\gamma}}}\frac{d}{d\xi_2}\left(\frac{P_2^{\frac{1}{\gamma}}}{Q_2}\right)\frac{\phi_3\xi_3}{\phi_2\xi_2}+\frac{1}{2}\frac{d}{d\xi_3}\left(\theta_3^2+\lambda_3^2+\phi_3^2\right)+\frac{d(\xi_3\lambda_3)}{d\xi_3}\right\}d\xi_3$$

$$=\left\{\frac{\gamma}{\gamma-1}\frac{d\tau_{2t}}{d\xi_2}-\frac{d(\xi_2\lambda_2)}{d\xi_2}\right\}d\xi_2$$

$$\left\{\frac{\lambda_3^2}{\xi_3}-\phi_3\frac{\partial\theta_3}{\partial\xi_3}+\frac{1}{2}\frac{\partial}{\partial\xi_3}\left(\lambda_3^2+\phi_3^2\right)+\frac{\partial(\xi_3\lambda_3)}{\partial\xi_3}\right\}$$

$$=\left(\frac{P_3}{P_2}\right)^{\frac{1}{\gamma}}\frac{\phi_3\xi_3}{\phi_2\xi_2}\left\{\frac{\gamma}{\gamma-1}\frac{\partial\tau_{2t}}{\partial\xi_2}-\frac{\partial(\xi_2\lambda_2)}{\partial\xi_2}-\frac{\gamma}{\gamma-1}\frac{Q_2}{Q_3}\frac{P_3}{P_2^{\frac{1}{\gamma}}}\frac{\partial}{\partial\xi_2}\left(\frac{P_2^{\frac{1}{\gamma}}}{Q_2}\right)\right\} \qquad (46).$$

For the direct problem it is assumed that the rotor spouting angle β_3 is known as a function of radius at station 3. It is therefore possible to describe the relation between λ_3 and ϕ_3 along the radius with a function G(ξ_3) such that:

$$\lambda_3 = G(\xi_3)\phi_3-\xi_3 \qquad (17).$$

Eliminating λ_3 from Equation (46) with this relation the following differential equation is obtained:

$$\frac{(G\phi_3-\xi_3)^2}{\xi_3}+\frac{1}{2}\frac{\partial}{\partial\xi_3}\left[(G\phi_3-\xi_3)^2+\phi_3^2\right]+\frac{\partial}{\partial\xi_3}\left[\xi_3(G\phi_3-\xi_3)\right]$$

$$=\left(\frac{P_3}{P_2}\right)^{\frac{1}{\gamma}}\frac{\phi_3\xi_3}{\phi_2\xi_2}\left\{\frac{\gamma}{\gamma-1}\frac{\partial\tau_{2t}}{\partial\xi_2}-\frac{\partial(\xi_2\lambda_2)}{\partial\xi_2}-\frac{\gamma}{\gamma-1}\tau_2\left(\frac{P_3}{P_2}\right)^{\frac{\gamma-1}{\gamma}}\frac{\partial}{\partial\xi_2}\left(\ell_n\frac{P_2^{\frac{1}{\gamma}}}{Q_2}\right)\right\}+\phi_3\frac{\partial\theta_3}{\partial\xi_3}$$

$$\frac{G^2\phi_3}{\xi_3}+G\frac{\partial}{\partial\xi_3}(G\phi_3)+\frac{\partial\phi_3}{\partial\xi_3}$$

$$=\left(\frac{P_3}{P_2}\right)^{\frac{1}{\gamma}}\frac{\xi_3}{\phi_2\xi_2}\left\{\frac{\gamma}{\gamma-1}\frac{\partial\tau_{2t}}{\partial\xi_2}-\frac{\partial(\xi_2\lambda_2)}{\partial\xi_2}-\frac{\gamma}{\gamma-1}\tau_2\left(\frac{P_3}{P_2}\right)^{\frac{\gamma-1}{\gamma}}\frac{\partial}{\partial\xi_2}\left(\ell_n\frac{P_2^{\frac{1}{\gamma}}}{Q_2}\right)\right\}+\frac{\partial\theta_3}{\partial\xi_3}+2G$$

$$\frac{\partial\phi_3}{\partial\xi_3}+\phi_3\left[\frac{G^2}{\xi_3(1+G^2)}+\frac{1}{2(1+G^2)}\frac{\partial(1+G^2)}{\partial\xi_3}\right]$$

$$=\left(\frac{P_3}{P_2}\right)^{\frac{1}{\gamma}}\frac{\xi_3}{\phi_2\xi_2}\left\{\frac{\gamma}{\gamma-1}\frac{\partial\tau_{2t}}{\partial\xi_2}-\frac{\partial(\xi_2\lambda_2)}{\partial\xi_2}-\frac{\gamma}{\gamma-1}\tau_2\left(\frac{P_3}{P_2}\right)^{\frac{\gamma-1}{\gamma}}\frac{\partial}{\partial\xi_2}\left(\ell_n\frac{P_2^{\frac{1}{\gamma}}}{Q_2}\right)\right\}+\frac{\partial\theta_3}{\partial\xi_3}+2G \qquad (47).$$

If P_3, ξ_{η_3}, $\frac{\partial \theta_3}{\partial \zeta_3}$ and the known quantities at station 2 are considered to be functions of ξ_{η_3} (to be determined in the iteration process) the integral for ϕ_3 can be immediately written down as:

$$\phi_3 = \frac{e}{\xi_{\eta_3}\sqrt{1+G^2}}\left[\int_{\xi_{\eta_i}}^{\xi_{\eta_3}} e^{+\int_{\xi_{\eta_i}}^{\xi_{\eta_3}} \frac{d\xi_{\eta_3}}{\xi_{\eta_3}(1+G^2)} - \int_{\xi_{\eta_i}}^{\xi_{\eta_3}} \frac{d\xi_{\eta_3}}{\xi_{\eta_3}(1+G^2)}} \left\{ \frac{1}{\sqrt{1+G^2}}\left(\frac{P_3}{P_2}\right)^{\frac{1}{\gamma}} \frac{\xi_{\eta_3}}{\phi_2 \xi_{\eta_2}} \left[\frac{\gamma}{\gamma-1}\frac{d\tau_{2t}}{d\xi_{\eta_2}} - \frac{d(\xi_{\eta_2}\lambda_2)}{d\xi_{\eta_2}} \right.\right.\right.$$

$$\left.\left.\left. - \frac{\gamma}{\gamma-1}\tau_2\left(\frac{P_3}{P_2}\right)^{\frac{\gamma-1}{\gamma}} \frac{d}{d\xi_{\eta_2}}\left(\ln \frac{P_2^{\frac{1}{\gamma}}}{Q_2}\right)\right] + \frac{1}{\sqrt{1+G^2}}\left(2G + \frac{d\theta_3}{d\zeta_3}\right)\right\} \xi_{\eta_3} d\xi_{\eta_3} + C_1 \right] \qquad (18).$$

An alternate form for the square bracket in the above integrand can be obtained by using the energy and radial momentum equations at station 2:

$$\left[\frac{\lambda_2^2}{\xi_{\eta_2}} - \phi_2 \frac{d\theta_2}{d\zeta_2} + \frac{1}{2}\frac{d}{d\xi_{\eta_2}}\left(\lambda_2^2 + \phi_2^2\right) - \frac{d(\xi_{\eta_2}\lambda_2)}{d\xi_{\eta_2}} - \frac{\gamma}{\gamma-1}\tau_2\left(\left(\frac{P_3}{P_2}\right)^{\frac{\gamma-1}{\gamma}} - 1\right)\frac{d}{d\xi_{\eta_2}}\left(\ln \frac{P_2^{\frac{1}{\gamma}}}{Q_2}\right)\right] \qquad (19).$$

In the case that $P_{2t} = 1$ (isentropic expansion to station 2 from stagnation conditions), the bracketed term in the integrand may be further simplified to:

$$\left[\frac{\gamma}{\gamma-1}\frac{d\tau_{2t}}{d\xi_{\eta_2}}\left(1 - P_3^{\frac{\gamma-1}{\gamma}}\right) - \frac{d}{d\xi_{\eta_2}}\left(\xi_{\eta_2}\lambda_2\right)\right] \qquad (20).$$

The integral form of the mass flow equation is:

$$m = \int_{\xi_{\eta_i}}^{\xi_{\eta_o}} Q_2\left(\frac{P_3}{P_2}\right)^{\frac{1}{\gamma}} \phi_3 \xi_{\eta_3}\, d\xi_{\eta_3} \qquad (21),$$

and the integral form of the radial momentum equation is:

$$\rho_3 = \left[\frac{\gamma-1}{\gamma} \left(\frac{Q_2}{P_2^{\frac{1}{\gamma}}} \right) \int_{\xi_i}^{\xi_3} \left(\frac{\lambda_3^2}{\xi_{r3}} - \theta_3 \frac{d\theta_3}{d\xi_3} - \phi_3 \frac{d\theta_3}{d\xi_3} \right) d\xi_{r3} + C_2 \right]^{\frac{\gamma}{\gamma-1}} \qquad (22).$$

Equations (10), (13), (17), (18), (21), (22), and (24) are used in the solution of the direct problem for the rotor (isentropic).

In the case of a stator, Equation (17) becomes:

$$\lambda_2 = F(\xi_{r2})\, \phi_2 \qquad (25),$$

G is replaced by F in Equation (18) and the terms $\frac{d(\xi_2 \lambda_2)}{d\xi_{r2}}$ and 2G are omitted. Equation (18) becomes Equation (26) for the isentropic stator. Equations (13), (21), (22), and (24) (with appropriate subscripts) remain unchanged, and the energy relation becomes Equation (9).

APPENDIX C

Development of Equations for Direct Problem (Polytropic).

The equations for a polytropic process through a rotor are derived with the same assumptions as used in Appendix B with the exception that the isentropic relation (13) is now replaced by:

$$\frac{Q_3}{Q_2} = \left(\frac{\rho_3}{\rho_2}\right)^{\frac{1}{n}} = \left(\frac{\tau_3}{\tau_2}\right)^{\frac{1}{n-1}} \tag{48}$$

where n is related to the so-called polytropic efficiency η for an expansion ($n < \gamma$) by: (see Reference 12, p. 449)

$$\frac{n}{n-1}\eta = \frac{\gamma}{\gamma-1} \tag{49}.$$

The energy equation (10), the continuity equation (8), the radial momentum equation (11), and the blade relation (17) remain the same in differential form.

The first term of the right side of Equation (44) now becomes:

$$\frac{\gamma}{\gamma-1}\frac{d}{d\xi_3}\left(\frac{\rho_3}{Q_3}\right) = \frac{\gamma}{\gamma-1}\frac{1}{Q_3}\frac{d\rho_3}{d\xi_3} - \frac{\gamma}{\gamma-1}\frac{\rho_3}{Q_3^2}\frac{dQ_3}{d\xi_3}$$

$$\frac{\gamma}{\gamma-1}\frac{d}{d\xi_3}\left(\frac{\rho_3}{Q_3}\right) = \frac{1}{Q_3}\frac{d\rho_3}{d\xi_3} + \frac{1}{\gamma-1}\frac{1}{Q_3}\frac{d\rho_3}{d\xi_3} - \frac{\gamma}{\gamma-1}\frac{\rho_3}{Q_3^2}\frac{dQ_3}{d\xi_3}.$$

But,

$$\frac{1}{\gamma-1}\frac{1}{Q_3}\frac{d\rho_3}{d\xi_3} - \frac{\gamma}{\gamma-1}\frac{\rho_3}{Q_3^2}\frac{dQ_3}{d\xi_3} = \frac{\gamma}{\gamma-1}\rho_3^{\frac{\gamma-1}{\gamma}}\frac{d}{d\xi_3}\left(\frac{\rho_3^{\frac{1}{\gamma}}}{Q_3}\right).$$

So, as before,

$$\frac{\gamma}{\gamma-1}\frac{d}{d\xi_3}\left(\frac{\rho_3}{Q_3}\right) = \frac{1}{Q_3}\frac{d\rho_3}{d\xi_3} + \frac{\gamma}{\gamma-1}\rho_3^{\frac{\gamma-1}{\gamma}}\frac{d}{d\xi_3}\left(\frac{\rho_3^{\frac{1}{\gamma}}}{Q_3}\right) \tag{50}.$$

The right side of the differential equation is obtained in the same form as Equation (46) with a correction term as follows:

$$\frac{P_3^{\frac{1}{\gamma}}}{Q_3} = \left(\frac{P_3^{\frac{1}{n}}}{Q_3}\right) P_3^{\frac{n-\gamma}{\gamma n}}$$

$$\frac{\gamma}{\gamma-1} P_3^{\frac{\gamma-1}{\gamma}} \frac{d}{d\xi_{f_3}} \left(\frac{P_3^{\frac{1}{\gamma}}}{Q_3}\right) = \frac{\gamma}{\gamma-1} P_3^{\frac{\gamma-1}{\gamma}} \left[P_3^{\frac{n-\gamma}{\gamma n}} \frac{d}{d\xi_{f_3}} \left(\frac{P_2^{\frac{1}{n}}}{Q_2}\right) + \frac{P_2^{\frac{1}{n}}}{Q_2} \frac{d}{d\xi_{f_3}} P_3^{\frac{n-\gamma}{\gamma n}} \right] \quad (51).$$

Using the differential form of the continuity equation (8), Equation (51) finally becomes:

$$\frac{\gamma}{\gamma-1} P_3^{\frac{\gamma-1}{\gamma}} \frac{d}{d\xi_{f_3}} \left(\frac{P_3^{\frac{1}{\gamma}}}{Q_3}\right) = \frac{\gamma}{\gamma-1} P_3^{\frac{n-1}{n}} \frac{d}{d\xi_{f_2}} \left(\frac{P_2^{\frac{1}{n}}}{Q_2}\right) \left(\frac{P_3}{P_2}\right)^{\frac{1}{n}} \frac{\phi_3 \xi_{f_3}}{\phi_2 \xi_{f_2}} - \frac{(\gamma-n)}{(\gamma-1)(n-1)} \left(\frac{P_2^{\frac{1}{n}}}{Q_2}\right) \frac{d}{d\xi_{f_3}} P_3^{\frac{n-1}{n}} \quad (52).$$

The differential equation corresponding to Equation (46) for the isentropic case now is:

$$\left\{ \frac{\lambda_3^2}{\xi_{f_3}} + \frac{1}{2} \frac{\partial}{\partial \xi_{f_3}} (\lambda_3^2 + \phi_3^2) + \frac{\partial (\xi_{f_3} \lambda_3)}{\partial \xi_{f_3}} \right\} = \left(\frac{P_3}{P_2}\right)^{\frac{1}{n}} \frac{\phi_3 \xi_{f_3}}{\phi_2 \xi_{f_2}} \left\{ \frac{\gamma}{\gamma-1} \frac{\partial \tau_{2t}}{\partial \xi_{f_2}} - \frac{\partial (\xi_{f_2} \lambda_2)}{\partial \xi_{f_2}} \right.$$

$$\left. - \frac{\gamma}{\gamma-1} P_3^{\frac{n-1}{n}} \frac{\partial}{\partial \xi_{f_2}} \left(\frac{P_2^{\frac{1}{n}}}{Q_2}\right) \right\} + \phi_3 \frac{\partial \theta_3}{\partial \xi_{f_3}} + \frac{(\gamma-n)}{(\gamma-1)(n-1)} \left(\frac{P_2^{\frac{1}{n}}}{Q_2}\right) \frac{\partial}{\partial \xi_{f_3}} P_3^{\frac{n-1}{n}} \quad (53).$$

The relation corresponding to Equation (47) becomes:

$$\frac{\partial \phi_3}{\partial \xi_{f_3}} + \phi_3 \left[\frac{G^2}{\xi_{f_3}(1+G^2)} + \frac{1}{2(1+G^2)} \frac{\partial (1+G^2)}{\partial \xi_{f_3}} \right] = \left(\frac{P_3}{P_2}\right)^{\frac{1}{n}} \frac{\xi_{f_3}}{\phi_2 \xi_{f_2}} \left\{ \frac{\gamma}{\gamma-1} \frac{\partial \tau_{2t}}{\partial \xi_{f_2}} - \frac{\partial (\xi_{f_2} \lambda_2)}{\partial \xi_{f_2}} \right.$$

$$\left. - \frac{\gamma}{\gamma-1} P_3^{\frac{n-1}{n}} \frac{\partial}{\partial \xi_{f_2}} \left(\frac{P_2^{\frac{1}{n}}}{Q_2}\right) \right\} + \frac{\partial \theta_3}{\partial \xi_{f_3}} + 2G + \frac{1}{\phi_3} \frac{\gamma-n}{(\gamma-1)(n-1)} \left(\frac{P_2^{\frac{1}{n}}}{Q_2}\right) \frac{\partial P_3^{\frac{n-1}{n}}}{\partial \xi_{f_3}} \quad (54).$$

The integral equation corresponding to Equation (18) is:

$$\phi_3 = \frac{e^{+\int_{\xi_i}^{\xi_3} \frac{d\xi_3}{\xi_3(1+G^2)}}}{\xi_3\sqrt{1+G^2}} \left[\int_{\xi_i}^{\xi_3} e^{-\int_{\xi_i}^{\xi_3} \frac{d\xi_3}{\xi_3(1+G^2)}} \left\{ \frac{1}{\sqrt{1+G^2}} \left(\frac{\rho_3}{\rho_2}\right)^{\frac{1}{n}} \frac{\xi_3}{\phi_2 \xi_2} \left[\frac{\gamma}{\gamma-1} \frac{d\tau_{2t}}{d\xi_2} - \frac{d(\xi_2\lambda_2)}{d\xi_2} \right.\right.\right.$$

$$\left.\left.\left. - \frac{\gamma}{\gamma-1}\rho_3^{\frac{n-1}{n}} \frac{d}{d\xi_2}\left(\frac{\rho_2^{\frac{1}{n}}}{Q_2}\right)\right] + \frac{1}{\sqrt{1+G^2}}\left(2G + \frac{d\theta_3}{d\xi_3} + \frac{1}{\phi_3}\frac{(\gamma-n)}{(\gamma-1)(n-1)}\left(\frac{\rho_2^{\frac{1}{n}}}{Q_2}\right)\frac{d\rho_3^{\frac{n-1}{n}}}{d\xi_3}\right)\right\} \xi_3 d\xi_3 + C_1 \right] \quad (55).$$

If $P_{2t} = 1$ at station 2, the square bracket under the integral will be:

$$\left[\frac{\gamma}{\gamma-1} \frac{d\tau_{2t}}{d\xi_2}\left(1 - \rho_3^{\frac{n-1}{n}}\right) - \frac{d(\xi_2\lambda_2)}{d\xi_2} \right] \quad (56).$$

The integrated form of the mass flow equation is

$$m = \int_{\xi_i}^{\xi_o} Q_2 \left(\frac{\rho_3}{\rho_2}\right)^{\frac{1}{n}} \phi_3 \xi_3 d\xi_3 \quad (57)$$

and the integral form of the radial momentum equation is:

$$\rho_3 = \left[\frac{n-1}{n}\left(\frac{Q_2}{\rho_2^{\frac{1}{n}}}\right) \int_{\xi_i}^{\xi_3} \left(\frac{\lambda_3^2}{\xi_3} - \theta_3 \frac{d\theta_3}{d\xi_3} - \phi_3 \frac{d\theta_3}{d\xi_3} \right) d\xi_2 + C_2 \right]^{\frac{n}{n-1}} \quad (58).$$

Equations (10), (17), (24), (48), (55), (57) and (58) are used in the solution of the polytropic direct problem for the rotor.

In the case of the stator, Equation (25) is used in place of Equation (17), and the terms $\frac{d}{d\xi_2}(\xi_2\lambda_2)$ and 2G are omitted in Equation (55). Equations (10), (24), (48), (57) and (58) remain unchanged (with appropriate subscripts).

APPENDIX D

Development of Equations for the Inverse Problem (Isentropic).

The following equations are derived with the same assumptions as given in Appendix B with the exception that now the blade relation, Equation (17), is replaced by the following given function which describes the work output of the rotor as a function of the radius ξ_3 :

$$H(\xi_3) = \xi_2 \lambda_2 + \xi_3 \lambda_3 \tag{27}$$

For the isentropic case, the derivation remains unchanged up to an including Equation (46), which may be written as:

$$\frac{\lambda_3^2}{\xi_3} + \frac{1}{2}\frac{\partial}{\partial \xi_3}\left(\lambda_3^2 + \phi_3^2\right) + \frac{\partial(\xi_3\lambda_3)}{\partial \xi_3} = \left(\frac{P_3}{P_2}\right)^{\frac{1}{\gamma}} \frac{\phi_3 \xi_3}{\phi_2 \xi_2}\left\{\frac{\gamma}{\gamma-1}\frac{\partial \tau_{2t}}{\partial \xi_2} - \frac{\partial(\xi_2\lambda_2)}{\partial \xi_2} - \frac{\gamma}{\gamma-1} P_3^{\frac{\gamma-1}{\gamma}} \frac{\partial}{\partial \xi_2}\left(\frac{P_2^{\frac{1}{\gamma}}}{Q_2}\right)\right\} + \phi_3 \frac{\partial \theta_3}{\partial \zeta_3} \tag{28}$$

Using Equation (27) to eliminate λ_3 , the differential equation corresponding to (47) is developed as follows:

$$\frac{\lambda_3^2}{\xi_3} + \frac{1}{2}\frac{d\lambda_3^2}{d\xi_3} = \frac{\xi_3\lambda_3}{\xi_3^2}\frac{d(\xi_3\lambda_3)}{d\xi_3}$$

$$\phi_3 \frac{d\phi_3}{d\xi_3} + \left(1 + \frac{\xi_3\lambda_3}{\xi_3^2}\right)\frac{d}{d\xi_3}(\xi_3\lambda_3) = \left(\frac{P_3}{P_2}\right)^{\frac{1}{\gamma}} \frac{\phi_3\xi_3}{\phi_2\xi_2}\left\{\frac{\gamma}{\gamma-1}\frac{d\tau_{2t}}{d\xi_2} - \frac{d(\xi_2\lambda_2)}{d\xi_2} - \frac{\gamma}{\gamma-1} P_3^{\frac{\gamma-1}{\gamma}} \frac{d}{d\xi_2}\left(\frac{P_2^{\frac{1}{\gamma}}}{Q_2}\right)\right\} + \phi_3 \frac{d\theta_3}{d\zeta_3}$$

$$\frac{d}{d\xi_3}\left(H - \xi_2\lambda_2\right) = \frac{dH}{d\xi_3} - \left(\frac{P_3}{P_2}\right)^{\frac{1}{\gamma}} \frac{\phi_3\xi_3}{\phi_2\xi_2}\frac{d}{d\xi_2}(\xi_2\lambda_2) \tag{59}$$

$$\frac{d\phi_3}{d\xi_3} = \left(\frac{P_3}{P_2}\right)^{\frac{1}{\gamma}} \frac{\xi_3}{\phi_2 \xi_2} \left\{ \frac{\gamma}{\gamma-1} \frac{d\tau_{2t}}{d\xi_2} - \frac{\gamma}{\gamma-1} P_3^{\frac{\gamma-1}{\gamma}} \frac{d}{d\xi_2}\left(\frac{P_2^{\frac{1}{\gamma}}}{Q_2}\right) \right.$$

$$\left. + \left(\frac{H-\xi_2\lambda_2}{\xi_3^2}\right) \frac{d}{d\xi_2}(\xi_2\lambda_2) \right\} + \frac{d\theta_3}{d\xi_3} - \frac{1}{\phi_3}\left(1 - \frac{H-\xi_2\lambda_2}{\xi_3^2}\right)\left(\frac{\partial H}{\partial \xi_3}\right) \qquad (60).$$

Assuming that the right side of the above Equation (60) is a known function of ξ_3 (to be determined in the iteration process), the integral equation for the axial velocity can be written as:

$$\phi_3 = \int_{\xi_{1i}}^{\xi_3} \left[\left(\frac{P_3}{P_2}\right)^{\frac{1}{\gamma}} \frac{\xi_3}{\phi_2 \xi_2} \left\{ \frac{\gamma}{\gamma-1} \frac{d\tau_{2t}}{d\xi_2} - \frac{\gamma}{\gamma-1} P_3^{\frac{\gamma-1}{\gamma}} \frac{d}{d\xi_2}\left(\frac{P_2^{\frac{1}{\gamma}}}{Q_2}\right) + \frac{(H-\xi_2\lambda_2)}{\xi_3^2} \frac{d}{d\xi_2}(\xi_2\lambda_2) \right\} + \frac{d\theta_3}{d\xi_3} \right.$$

$$\left. - \frac{1}{\phi_3}\left(1 + \frac{H-\xi_2\lambda_2}{\xi_3^2}\right) \frac{dH}{d\xi_3} \right] d\xi_3 + C_1 \qquad (29).$$

Since the mass flow integral and the radial momentum integral remain the same, Equations (10), (13), (21), (22), (24), (27) and (29) are used in the solution of the isentropic inverse problem for the rotor.

APPENDIX E

Development of Equations for the Inverse Problem (Polytropic).

The following derivation is made assuming the same conditions for a rotor as given in Appendix C. The work output of the rotor as a function of radius is again given by Equation (27).

The differential equation (53) still holds, which is:

$$\frac{\lambda_3^2}{\xi_3} + \frac{1}{2}\frac{\partial}{\partial \xi_3}\left(\lambda_3^2 + \phi_3^2\right) + \frac{\partial}{\partial \xi_3}\left(\xi_3 \lambda_3\right) = \left(\frac{\rho_3}{\rho_2}\right)^{\frac{1}{n}} \frac{\phi_3 \xi_3}{\phi_2 \xi_2}\left\{\frac{\gamma}{\gamma-1}\frac{\partial \tau_{2t}}{\partial \xi_2} - \frac{\partial(\xi_2 \lambda_2)}{\partial \xi_2}\right.$$

$$\left. - \frac{\gamma}{\gamma-1}\rho_3^{\frac{n-1}{n}}\frac{\partial}{\partial \xi_2}\left(\frac{P_2^{\frac{1}{n}}}{Q_2}\right)\right\} + \phi_3 \frac{\partial \theta_3}{\partial \xi_3} + \frac{\gamma - n}{(\gamma-1)(n-1)}\left(\frac{P_2^{\frac{1}{n}}}{Q_2}\right)\frac{\partial}{\partial \xi_3}\left(\rho_3^{\frac{n-1}{n}}\right) \qquad (53).$$

The resulting integral equation is similar to Equation (29) with the addition of a correction term:

$$\phi_3 = \int_{\xi_{3i}}^{\xi_3}\left[\left(\frac{P_3}{P_2}\right)^{\frac{1}{n}}\frac{\xi_3}{\phi_2 \xi_2}\left\{\frac{\gamma}{\gamma-1}\frac{d\tau_{2t}}{d\xi_2} - \frac{\gamma}{\gamma-1}\rho_3^{\frac{n-1}{n}}\frac{d}{d\xi_2}\left(\frac{P_2^{\frac{1}{n}}}{Q_2}\right) + \frac{(H-\xi_2\lambda_2)}{\xi_3^2}\frac{d}{d\xi_2}(\xi_2\lambda_2)\right\} + \frac{d\theta_3}{d\xi_3}\right.$$

$$\left. + \frac{1}{\phi_3}\left\{\frac{(\gamma-n)}{(\gamma-1)(n-1)}\left(\frac{P_2^{\frac{1}{n}}}{Q_2}\right)\frac{d}{d\xi_3}\rho_3^{\frac{n-1}{n}} - \left(1 + \frac{H-\xi_2\lambda_2}{\xi_3^2}\right)\frac{dH}{d\xi_3}\right\}\right] d\xi_3 + C_1 \qquad (61).$$

The mass flow and radial momentum equations remain the same as in Appendix C, and Equations (10), (24), (27), (48), (57), (58) and (61) are used to solve the polytropic inverse problem for the rotor.

APPENDIX F

Iterated Examples

The following data are used for Examples I-X inclusive:

ω = 734 rad/sec (7000 RPM) $\quad p_{lt} = 16{,}300 \frac{lb}{ft^2} \quad R_o = 1.2500$ ft.

$\gamma = 1.40 \quad \omega R_o = 917.5$ ft/sec $\quad C_p = .2396 \frac{BTU}{lb\,^oF}$

$R = 1715 \frac{ft^2}{sec^2\,^oF} \quad \omega^2 R_o^2 = .8418 \times 10^6 \frac{ft^2}{sec^2} \quad c = .250$ ft

Example Ia.

Solution for the stator of Fig. 3 (cylindrical channel), with no radial total temperature distribution and coordinates for equal areas in the plane perpendicular to the axis. This is a solution for the direct problem (F (ξ_2) given) for the isentropic, subsonic case.

For the stator with F constant, $P_{lt} = 1$, and $\theta = 0$, Equations (18), (21), (22), (13), (25) and (43) of Appendix B become:

$$\phi_2 = \frac{1}{\xi_2^{\frac{F^2}{1+F^2}}(1+F^2)} \left[\int_{\xi_i}^{\xi_2} \left(\frac{\rho_2}{\rho_1}\right)^{\frac{1}{\gamma}} \frac{1}{\phi_1} \left[\frac{\gamma}{\gamma-1} \frac{d\tau_{lt}}{d\xi_1} \left(1 - \rho_2^{\frac{\gamma-1}{\gamma}}\right) \right] \xi_2^{\frac{F^2}{1+F^2}} d\xi_2 \right] + \frac{C_1}{\xi_2^{\frac{F^2}{1+F^2}}} \tag{62}$$

$$m = \int_{\xi_i}^{\xi_o} Q \left(\frac{\rho_2}{\rho_1}\right)^{\frac{1}{\gamma}} \phi_2 \xi_2 \, d\xi_2 \tag{63}$$

$$\rho_2 = \left[\frac{\gamma-1}{\gamma} \frac{1}{\tau_{lt}} \int_{\xi_i}^{\xi_2} \frac{\lambda_2^2}{\xi_2} d\xi_2 + C_2 \right]^{\frac{\gamma}{\gamma-1}} \tag{64}$$

$$\frac{Q_2}{Q_1} = \left(\frac{\rho_2}{\rho_1}\right)^{\frac{1}{\gamma}} = \left(\frac{\tau_2}{\tau_1}\right)^{\frac{1}{\gamma-1}} \tag{65}$$

$$\lambda_2 = F\,\phi_2 \qquad (F = \text{const.}) \qquad (66)$$

$$\frac{\gamma}{\gamma-1}\tau_{1t} = \frac{\gamma}{\gamma-1}\tau_2 + \frac{1}{2}\left(\lambda_2^2 + \phi_2^2\right) \qquad (67)$$

$$M = \frac{\Phi}{\sqrt{\gamma\tau}} \qquad (\text{Mach number}) \qquad (68).$$

Conditions at station 1: (given)

$P_{1t} = 1.00$ $\quad \Omega_{1t} = .23828$ $\quad \tau_{1t} = 4.1968$ $\quad \phi_1 = .4857$

$P_1 = .9723$ $\quad \Omega_1 = .23354$ $\quad \tau_1 = 4.1631$ $\quad \lambda_1 = 0$

$\frac{d\tau_{1t}}{d\xi_1} = 0$ $\quad F = 2.75$ $\quad m = .020417$ $\quad W = 114.7\ \frac{\text{lb}}{\text{sec}}$ $\quad T_{1t} = 2060^{\circ}\text{R}$

Solution at station 2:

	a_2	b_2	c_2	d_2	e_2
ξ_2	.8000	.8544	.9055	.9539	1.0000
ϕ_2	.7926	.7479	.7105	.6785	.6508
λ_2	2.1796	2.0567	1.9539	1.8659	1.7897
P_2	.4928	.5365	.5730	.6041	.6307
τ_2	3.4283	3.5128	3.5794	3.6340	3.6789
Ω_2	.14372	.15274	.16007	.16623	.17144
M	1.059	.986	.929	.880	.841
$\Delta\tau_2$	+.0001	-.0002	-.0001	-.0004	-.0002

$C_1 = .6508$ $\quad P_{2t} = P_{1t}$ $\quad \tau_{2t} = \tau_{1t}$ $\quad \Omega_{2t} = \Omega_{1t}$ $\quad \theta_2 = 0$

$C_2 = .8169$

Note: The column headed $\Delta\tau_2$ above represents the difference between τ_2 as calculated by the iteration process and τ_2 obtained by applying the energy equation along the streamlines indicated after the solution has been reached. The same applies in the solution of the following examples. This is a rough check on the accuracy of the solution. Obviously, if an exact solution had been found, $\Delta\tau$ would be zero.

Example Ib.

Solution for the rotor of Fig. 3 (cylindrical channel) with no radial total temperature gradient and radial coordinates for equal areas. This is an isentropic, subsonic solution for the direct problem (G (ξ_3) given) for a rotor.

For the rotor with G constant and $P_{2t} = 1$, the applicable relations are Equations (63), (64), (65) (with appropriate subscripts) and the following three equations:

$$\phi_3 = \frac{1}{\xi_3^{\frac{G^2}{1+G^2}}(1+G^2)}\left[\int_{\xi_i}^{\xi_3}\left\{\left(\frac{P_3}{P_2}\right)^{\frac{1}{\gamma}}\frac{1}{\phi_2}\left[\frac{\gamma}{\gamma-1}\frac{d\tau_{2t}}{d\xi_2}\left(1-P_3^{\frac{\gamma-1}{\gamma}}\right)-\frac{d}{d\xi_2}\left(\xi_2\lambda_2\right)\right]+2G\right\}\xi_3^{\frac{G^2}{1+G^2}}d\xi_3\right]+\frac{C_1}{\xi_3^{\frac{G^2}{1+G^2}}} \quad (69)$$

$$\lambda_3 = G\phi_3 - \xi_3 \qquad (G = \text{const.}) \quad (70)$$

$$\frac{\gamma}{\gamma-1}\tau_{2t} - \xi_2\lambda_2 = \frac{\gamma}{\gamma-1}\tau_3 + \frac{1}{2}\left(\lambda_3^2+\phi_3^2\right)+\xi_3\lambda_3 \quad (71).$$

Conditions at station 2 are the same as after the stator, Example Ia.

$$G = 1.411 \qquad \frac{d\tau_{2t}}{d\xi_2} = 0 \qquad m = .020417$$

Solution at station 3:

	a_3	b_3	c_3	d_3	e_3
ξ_3	.8000	.8544	.9055	.9539	1.0000
ϕ_3	.6624	.6779	.6955	.7146	.7346
λ_3	.1346	.1021	.0759	.0544	.0365
P_3	.5862	.5865	.5865	.5865	.5865
τ_3	3.6025	3.6034	3.6034	3.6035	3.6035
Q_3	.16269	.16278	.16276	.16276	.16277
P_{3t}	.6244	.6254	.6264	.6273	.6284
τ_{3t}	3.6679	3.6699	3.6717	3.6734	3.6751
Q_{3t}	.17019	.17041	.17061	.17077	.17099
$\Delta\tau_3$	0	-.0007	-.0017	-.0035	-.0058

$C_1 = .5710$ $C_2 = .8585$

Example IIa.

Solution for the stator of Fig. 3 (cylindrical channel) with the same conditions and assumptions as given in Problem Ia except with a radial total temperature gradient.

Equations (62) - (68) of Example Ia are applicable.

Conditions at station 1: (given)

	a_1	b_1	c_1	d_1	e_1
ξ_1	.8000	.8544	.9055	.9539	1.000
τ_{1t}	3.3819	3.8252	4.2415	4.6361	5.0118
P_{1t}	1.00	1.00	1.00	1.00	1.00
Q_{1t}	.29569	.26142	.23577	.21570	.19953
P_1	.9723	.9723	.9723	.9723	.9723
τ_1	3.3548	3.7946	4.2076	4.5990	4.9717
Q_1	.28981	.25622	.23108	.21141	.19556
ϕ_1	.4355	.4628	.4871	.5096	.5298
λ_1	0	0	0	0	0

$F = 2.75$ $m = .020417$ $\frac{d\tau_{1t}}{d\xi_1} = +8.1495$

Solution at station 2:

	a_2	b_2	c_2	d_2	e_2
ξ_2	.8000	.8544	.9055	.9539	1.0000
ϕ_2	.6778	.6805	.6829	.6848	.6864
λ_2	1.8639	1.8714	1.8780	1.8832	1.8876
P_2	.5295	.5713	.6061	.6355	.6611
τ_2	2.8200	3.2599	3.6762	4.0729	4.4527
Q_2	.18777	.17525	.16488	.15602	.14845
M	.999	.930	.883	.842	.805
$\Delta\tau_2$	0	-.0012	-.0052	-.0104	-.0172

$C_1 = .5565$ $C_2 = .8339$

$P_{2t} = P_{1t}$, $\tau_{2t} = \tau_{1t}$, $Q_{2t} = Q_{1t}$, $\theta_2 = 0$

Example IIb

Solution for the rotor of Fig. 3 (cylindrical channel) with the same conditions and assumptions given in Problem Ib except with a radial total temperature gradient. Equations (63), (64), (65), (69), (70) and (71) of Example I (with appropriate subscripts) are applicable. Conditions at station 2 are the same as after the stator, Example IIa, above.

$G = 1.411$, $\frac{d\tau_{2t}}{d\xi_2} = 8.1495$, $m = .020417$

Solution at station 3:

	a_3	b_3	c_3	d_3	e_3
ξ_3	.8000	.8544	.9055	.9539	1.0000
ϕ_3	.5377	.6174	.6920	.7628	.8303
λ_3	-.0413	.0168	.0709	.1224	.1716
P_3	.6009	.6009	.6009	.6009	.6012
τ_3	2.9237	3.3072	3.6670	4.0081	4.3334
Q_3	.20551	.18168	.16386	.14990	.13871
P_{3t}	.6313	.6381	.6422	.6447	.6461
Q_{3t}	.21289	.18964	.17184	.15759	.14603
τ_{3t}	2.9653	3.3643	3.7373	4.0895	4.4235
$\Delta\tau_3$	0	+.0035	+.0012	-.0039	-.0126

$C_1 = .4635$ $C_2 = .8646$

After correcting the upstream conditions at station 2 for the displacement of the streamlines from the position originally assumed, the following corrected solution at station 3 is obtained: (See Problem Vb for method.)

	a_3	b_3	c_3	d_3	e_3
ξ_3	.8000	.8544	.9055	.9539	1.0000
ϕ_3	.5311	.6106	.6853	.7560	.8234
λ_3	-.0506	.0072	0615	.1128	.1618
P_3	.6029	.6029	.6029	.6029	.6032
τ_3	2.9268	3.2771	3.6296	3.9868	4.3374
Q_3	.20602	.18411	.16623	.15127	.13917
P_{3t}	.6327	.6378	.6417	.6453	.6476
τ_{3t}	2.9675	3.3303	3.6951	4.0648	4.4263
Q_{3t}	.21325	.19166	.17381	.15879	.14641
$\Delta\tau_3$	0	-.0001	-.0022	- 0055	-.0118

$C_1 = .4578$ $\qquad$ $C_2 = .8654$

Example IIIa.

Solution for the stator of Fig. 4 (divergent channel with straight walls) with a radial total temperature gradient. This is an isentropic, subsonic solution for the direct problem for a stator ($F(\xi_2)$ given).

For the stator with F constant and $P_{1t} = 1$, Equations (63), (65) and (66) are applicable in addition to the following four relations:

$$\phi_2 = \frac{1}{\xi_2^{\frac{F^2}{1+F^2}}(1+F^2)}\left[\int_{\xi_1}^{\xi_2}\left\{\left(\frac{P_2}{P_1}\right)^{\frac{1}{\gamma}}\frac{\xi_2}{\phi_1\xi_1}\left[\frac{\gamma}{\gamma-1}\frac{d\tau_{1t}}{d\xi_1}\left(1-P_2^{\frac{\gamma-1}{\gamma}}\right)\right]+\frac{d\theta_2}{d\xi_2}\right\}\xi_2^{\frac{F^2}{1+F^2}}d\xi_2\right]+\frac{C_1}{\xi_2^{\frac{F^2}{1+F^2}}} \quad (72)$$

$$\rho_2 = \left[\frac{\gamma-1}{\gamma} \frac{1}{\tau_{1t}} \int_{\xi_i}^{\xi_2} \left(\frac{\lambda_2^2}{\xi_2} - \theta_2 \frac{d\theta_2}{d\xi_2} - \phi_2 \frac{d\theta_2}{d\xi_2} \right) d\xi_2 + C_2 \right]^{\frac{\gamma}{\gamma-1}} \tag{73}$$

$$\frac{\gamma}{\gamma-1}\tau_{1t} = \frac{\gamma}{\gamma-1}\tau_2 + \frac{1}{2}\left(\theta_2^2 + \lambda_2^2 + \phi_2^2\right) \tag{74}$$

$$\frac{\partial \theta_2}{\partial \xi_2} = \frac{\partial \phi_2}{\partial \xi_2}\left(\frac{\partial f}{\partial \xi}\right)_2 + \phi_2\left(\frac{\partial^2 f}{\partial \xi^2}\right)_2 \tag{75}.$$

Conditions at station 1: (given)

	a_1	b_1	c_1	d_1	e_1
ξ_1	.80	.85	.90	.95	1.00
τ_{1t}	3.9931	4.0950	4.1968	4.2987	4.4006
Q_{1t}	.25043	.24420	.23828	.23263	.22724
P_{1t}	1.00	1.00	1.00	1.00	1.00
P_1	.9696	.9696	.9696	.9696	.9696
τ_1	3.9581	4.0591	4.1600	4.2610	4.3620
Q_1	.24497	.23888	.23309	.22756	.22229
ϕ_1	.4944	.5014	.5069	.5112	.5142
θ_1	-.0247	.0000	.0253	.0511	.0771
λ_1	0	0	0	0	0

$F = 2.75 \qquad \frac{d\tau_{1t}}{d\xi_1} = +2.0375 \qquad m = .024639 \qquad W = 138.4 \ \frac{lb}{sec}$

$c = .25$ ft

Solution at station 2:

	a_2	b_2	c_2	d_2	e_2
ξ_{r2}	.790	.850	.910	.970	1.30
ϕ_2	.7410	.7046	.6735	.6469	.6236
λ_2	2.0377	1.9376	1.8521	1.7790	1.7149
θ_2	-.0370	0	.0337	.0647	.0935
P_2	.5247	.5716	.6122	.6472	.6777
τ_2	3.3212	3.4904	3.6479	3.7966	3.9376
Q_2	.15798	.16378	.16782	.17051	.17210
M	1.004	.930	.870	.817	.779
$\Delta\tau_2$	0	-.0027	-.0061	-.0103	-.0138

$C_1 = .6017 \quad C_2 = .8317 \quad P_{2t} = P_{1t}, \; Q_{2t} = Q_{1t}, \; \tau_{2t} = \tau_{1t}$

Example IIIb.

Solution for the rotor of Fig. 4 (divergent channel with straight walls) with a radial total temperature gradient. This is an isentropic, subsonic solution for the direct problem for the rotor (G (ξ_3) given).

Equations (63), (65), (70), (73), (75)(with appropriate subscripts) and the following two relations are applicable:

$$\phi_3 = \frac{1}{\frac{G^2}{\xi_{r3}^{\frac{G^2}{1+G^2}}(1+G^2)}} \left[\int_{\xi_{r2}}^{\xi_{r3}} \left\{ \left(\frac{P_3}{P_2}\right)^{\frac{1}{\gamma}} \frac{\xi_{r3}}{\phi_2 \xi_{r2}} \left[\frac{\gamma}{\gamma-1} \frac{d\tau_{2t}}{d\xi_{r2}} \left(1 - P_3^{\frac{\gamma-1}{\gamma}}\right) - \frac{d}{d\xi_{r2}}(\xi_{r2}\lambda_2) \right] + 2G + \frac{d\theta_3}{d\xi_{r3}} \right\} \xi_{r3}^{\frac{G^2}{1+G^2}} d\xi_{r3} + \frac{C_1}{\xi_{r3}^{\frac{G^2}{1+G^2}}} \right] \quad (76)$$

$$\frac{\gamma}{\gamma-1}\tau_{2t} - \xi_{r2}\lambda_2 = \frac{\gamma}{\gamma-1}\tau_3 + \frac{1}{2}\left(\theta_3^2 + \lambda_3^2 + \phi_3^2\right) + \xi_{r3}\lambda_3 \quad (77).$$

Conditions at station 2 are the same as after the stator, Example IIIa above.

$$G = 1.411 \quad m = .024639 \quad \frac{d\tau_{2t}}{d\xi_{r2}} = +1.6979 \quad c = .25 \text{ ft.}$$

Solution at station 3:

	a_3	b_3	c_3	d_3	e_3
ξ_3	.780	.850	.920	.990	1.060
ϕ_3	.4567	.4987	.5423	.5873	.6347
θ_3	-.0228	0	.0271	.0587	.0952
λ_3	-.1356	-.1463	-.1548	-.1613	-.1644
P_3	.6500	.6500	.6505	.6508	.6508
Q_3	.18409	.17954	.17525	.17119	.16720
τ_3	3.5308	3.6209	3.7117	3.8027	3.8923
P_{3t}	.6712	.6749	.6780	.6804	.6828
Q_{3t}	.18836	.18442	.18051	.17672	.17304
τ_{3t}	3.5634	3.6600	3.7560	3.8514	3.9459
$\Delta\tau_3$	+.0001	+.0005	-.0013	-.0048	-.0092

$C_1 = .3871$ $\quad C_2 = .8842$

Example IVa

Solution for the stator of Fig. 5 (divergent curved channel walls) with a radial total temperature gradient. This is an isentropic, subsonic solution for the direct problem for a stator ($F(\xi_2)$ given). The same equations as used in Example IIIa are applicable.

Conditions at station 1: (given)

	a_1	b_1	c_1	d_1	e_1	f_1
ξ_1	.80	.84	.88	.92	.96	1.00
τ_{1t}	3.7894	3.9524	4.1152	4.2783	4.4413	4.6043
P_{1t}	1.00	1.00	1.00	1.00	1.00	1.00
Q_{1t}	.26389	.25301	.24299	.23374	.22516	.21719
P_1	.9400	.9400	.9400	.9400	.9400	.9400
τ_1	3.7231	3.8832	4.0433	4.2034	4.3636	4.5237
Q_1	.25248	.24207	.23248	.22363	.21542	.20780
ϕ_1	.6804	.6960	.7090	.7205	.7293	.7365
θ_1	-.0340	0	.0354	.0720	.1094	.1473
λ_1	0	0	0	0	0	0

$F = 2.75$ $\quad \frac{d\tau_{1t}}{d\xi_1} = 4.0746$ $\quad m = .029242$ $\quad W = 164.2 \frac{lb}{sec}$

$c = .250$ ft.

Solution at station 2:

	a_2	b_2	c_2	d_2	e_2	f_2
ξ_2	.785	.842	.899	.956	1.013	1.070
ϕ_2	.7051	.6763	.6531	.6344	.6192	.6072
λ_2	1.9390	1.8598	1.7960	1.7446	1.7028	1.6698
θ_2	-.0705	.0135	.0914	.1649	.2353	.3036
P_2	.5417	.5860	.6222	.6518	.6761	.6962
τ_2	3.1805	3.3928	3.5937	3.7860	3.9713	4.1519
Ω_2	.17032	.17272	.17313	.17217	.17022	.16767
M	.977	.909	.854	.809	.776	.747
$\Delta\tau_2$	0	0	-.0013	-.0039	-.0069	-.0118

$$C_1 = .5694 \qquad C_2 = .8393$$

$$P_{2t} = P_{1t}\ ,\quad \tau_{2t} = \tau_{1t}\ ,\quad \Omega_{2t} = \Omega_{1t}$$

Example IVb

Solution for the rotor of Fig. 5 (divergent curved channel walls) with a radial total temperature gradient. This is an isentropic, subsonic solution of the direct problem for the rotor ($G(\xi_3)$ given). The same equations as used in Example IIIb are applicable.

Conditions at station 2 are the same as after the stator, Example IVa.

$$G = 1.730 \qquad \frac{d\tau_{2t}}{d\xi_2} = 2.8593 \qquad m = .029242$$

Solution at station 3:

	a_3	b_3	c_3	d_3	e_3	f_3
ξ_3	.760	.848	.936	1.024	1.112	1.200
ϕ_3	.1958	.2641	.3260	.3852	.4458	.5117
λ_3	-.4213	-.3911	-.3720	-.3576	-.3408	-.3148
θ_3	-.0294	.0106	.0750	.1617	.2719	.4094
P_3	.6948	.6981	.7010	.7027	.7010	.6927
τ_3	3.4149	3.5669	3.7180	3.8682	4.0126	4.1461
Q_3	.20346	.19573	.18852	.18167	.17466	.16707
τ_{3t}	3.4660	3.5998	3.7535	3.9064	4.0568	4.2018
Q_{3t}	.21117	.20027	.19303	.18619	.17950	.17272
P_{3t}	.7320	.7209	.7246	.7274	.7283	.7257
M	.212	.210	.219	.236	.266	.302
$\Delta\tau_3$	0	+.0010	-.0003	-.0049	-.0113	-.0196

$C_1 = .1594$ $C_2 = .9012$

Example Va.

Supersonic isentropic solution for the stator of Example IVa (divergent curved channel walls and radial total temperature gradient). The conditions at station 1, the data, and the applicable equations are the same as for Example IVa.

Solution at station 2:

	a_2	b_2	c_2	d_2	e_2	f_2
ϕ_2	.9303	.8906	.8601	.8371	.8201	.8087
λ_2	2.5583	2.4491	2.3653	2.3020	2.2553	2.2239
θ_2	-.0930	.0178	.1204	.2176	.3116	.4043
P_2	.3171	.3715	.4169	.4547	.4856	.5102
τ_2	2.7294	2.9784	3.2051	3.4157	3.6131	3.7990
Q_2	.11617	.12471	.13007	.13310	.13440	.13430
M	1.367	1.274	1.188	1.123	1.080	1.038
$\Delta\tau_2$	0	+.0039	+.0034	-.0012	-.0082	-.0178

$C_1 = .7512$ $C_2 = .7203$ $P_{2t} = P_{1t}$, $Q_{2t} = Q_{1t}$, $\tau_{2t} = \tau_{1t}$

Example Vb.

Supersonic isentropic solution for the rotor of Example IVb (divergent curved channel walls and radial total temperature gradient). The conditions at station 2 are assumed the same as after the subsonic stator of Example IVa. The data and equations used are the same as that used for Example IVb.

One complete approximation for this problem is given below to show the method of iteration. The procedure of correcting for the displacement of the assumed streamlines is then given to show the method for this correction.

The iteration is started by assuming an axial velocity distribution across the channel. The tangential velocity is then calculated using Equation (70). The value of $\frac{\partial \theta_3}{\partial \zeta_3}$ is found from Equation (75) and the pressure distribution from Equation (73) and the application of Equation (77) at the inner channel boundary. The axial velocity distribution is then determined using Equation (76) and the constant is determined by the mass flow Equation (63). The iteration is continued until the values of ϕ_3 assumed agree with those resulting from the iteration process. It is important to note that in the supersonic case, the iteration diverges rapidly away from the solution. Thus if an axial velocity distribution is assumed that is greater than the solution, successive iterations will increase ϕ_3 until the pressure P_3 has reached zero. If an axial velocity distribution is assumed which is less than the solution, successive iterations will result in decreasing values of ϕ_3 and eventually the subsonic solution will be reached. The supersonic solution is found by a simple interpolation once the solution has been "straddled".

The reverse is true for the subsonic solution for a given setup. The iteration process will converge toward the solution from any reasonable assumed distribution of ϕ_3.

Data used in the solution:

$\Delta\xi_3 = .088$ $\quad \frac{\gamma}{\gamma-1}\frac{d\tau_{2t}}{d\xi_2} = 10.0075$ $\quad G = 1.730$ $\quad 2G = 3.460$

$\frac{G^2}{1+G^2} = .7496$

	a_3	b_3	c_3	d_3	e_3	f_3
ξ_3	.760	.848	.936	1.024	1.112	1.200
$\left(\frac{\partial f}{\partial \xi}\right)_3$	-.150	.040	.230	.420	.610	.800
$\left(\frac{\partial^2 f}{\partial \xi^2}\right)_3$	-.250	.100	.450	.800	1.150	1.500
Factor	.02117	.02125	.02133	.02138	.02144	
$\frac{\overline{\xi_3}}{\phi_2 \xi_2}$	1.4310	1.5415	1.6411	1.7305	1.8098	
$\frac{1}{\xi_3^{.7496}}$	1.2283	1.1316	1.0509	.9824	.9235	.8722
$\overline{Q_2}\frac{(\xi_i^2 - \xi_{i-1}^2)}{2}$	.01299	.01357	.01489	.01694	.01719	
$-\frac{d}{d\xi_{\tau_2}}(\xi_{\tau_2}\lambda_2)$	-.7702	-.8526	-.9333	-1.0018	-1.0842	
$\frac{\gamma-1}{\gamma}\frac{1}{\overline{\tau}_{2t}}(\xi_i - \xi_{i-1})$	.006498	.006235	.005993	.005768	.005560	

("Factor" above $= \dfrac{1}{\xi_3^{\frac{G^2}{1+G^2}}(1+G^2)} \displaystyle\int_{\xi_{i-1}}^{\xi_i} \xi_3^{\frac{G^2}{1+G^2}} d\xi_3$

Try $C_1 = 1.3920$

	a_3	b_3	c_3	d_3	e_3	f_3
ϕ_3	1.7098	1.6727	1.6943	1.7698	1.9004	2.0912
$G\phi_3$	2.9580	2.8938	2.9311	3.0618	3.2877	3.6178
λ_3	2.1980	2.0458	1.9951	2.0378	2.1757	2.4178
θ_3	-.2565	.0669	.3897	.7433	1.1592	1.6730
λ_3^2	4.8312	4.1853	3.9804	4.1526	4.7337	5.8458
$\frac{\lambda_3^2}{\xi_3}$	6.3568	4.9354	4.2525	4.0553	4.2569	4.8715
$\frac{\overline{\lambda_3^2}}{\xi_3}$		5.6461	4.5939	4.1539	4.1561	4.5642
$\overline{\theta_3}$		-.0948	.2283	.5665	.9512	1.4161
$\frac{\partial \theta_3}{\partial \xi_3}$		3.6750	3.6681	4.0181	4.7261	5.8386
$-\overline{\theta_3}\frac{\partial \theta_3}{\partial \xi_3}$		+.3484	-.8374	-2.2763	-4.4955	-8.2680
$\frac{\partial \phi_3}{\partial \xi_3}$	5.0235	4.9820	5.2060	5.6770	6.4060	7.4200
$\frac{\partial \phi_3}{\partial \xi_3}\left(\frac{\partial f}{\partial \xi}\right)_3$	-.7535	.1993	1.1974	2.3843	3.9077	5.9360
$\phi_3\left(\frac{\partial^2 f}{\partial \xi^2}\right)_3$	-.4274	.1673	.7624	1.4158	2.1855	3.1368
$\frac{\partial \theta_3}{\partial \xi_3}$	-1.1809	.3666	1.9598	3.8001	6.0932	9.0728
$-\phi_3\frac{\partial \theta_3}{\partial \xi_3}$	+2.0191	-.6132	-3.3205	-6.7254	-11.5795	-18.9730
$-\overline{\phi_3\frac{\partial \theta_3}{\partial \xi_3}}$		+.7030	-1.9668	-5.0229	-9.1524	-15.2762
$\Delta p_3^{\frac{\gamma-1}{\gamma}}$		+.04352	+ .01116	- .01885	- .05475	- .10553

The constant C_2 is found by applying Equation (77) at the inner channel boundary:

$$\tau_3 = 3.7894 - .14286\left[4.8312+2.9234+.0658+2(1.5221+1.6705)\right] = 1.7600$$

$$P_3 = .5417(.5534)^{\frac{\gamma}{\gamma-1}} = .0683 \qquad C_2 = (.0683)^{\frac{\gamma-1}{\gamma}} = .4645$$

	a_3	b_3	c_3	d_3	e_3	f_3
$\rho_3^{\frac{\gamma-1}{\gamma}}$	.4645	.5080	.5192	.5003	.4456	.3400
ρ_3	.0683	.0934	.1008	.0886	.0591	.0229
$\frac{\rho_3}{\rho_2}$	.1261	.1594	.1620	.1359	.0874	.0329
$\left(\frac{\rho_3}{\rho_2}\right)^{\frac{1}{\gamma}}$	.2278	.2694	.2725	.2404	.1754	.0873
Average	.2486	.2709	.2564	.2079	.1313	
$(1-\rho_3^{\frac{\gamma-1}{\gamma}})$	.5355	.4920	.4809	.4996	.5543	.6601
Average	.5137	.4864	.4902	.5269	.6072	

The axial velocity integral is iterated in steps across the channel as follows:

	$\Delta\phi_3$	ϕ_3	Average
$.02117\left[.3557(5.1414-.7702)+3.46-.4073\right] =$	.09754	.09754	.04877
$.02125\left[.4176(4.8681-.8526)+3.46+1.1633\right] =$	.13388	.23142	.16448
$.02133\left[.4208(4.9062-.9333)+3.46+2.8802\right] =$	.17090	.40232	.31687
$.02138\left[.3598(5.2735-1.0018)+3.46+4.9470\right] =$	.21260	.61492	.50862
$.02144\left[.2376(6.0766-1.0842)+3.46+7.5834\right] =$	.26220	.87712	.74602

The mass flow equation is iterated to solve for C_1 as follows:

$$.029242 = .003229(.04877+1.1799C_1)+.003676(.16448+1.0912C_1)$$
$$+.003818(.31687+1.0166C_1)+.003522(.50862+.9529C_1)$$
$$+.002257(.74602+.8978C_1)$$

$$C_1 = \frac{.023790}{.017089} = 1.3920$$

Solution at station 3:

	a_3	b_3	c_3	d_3	e_3	f_3
ϕ_3	1.7098	1.6727	1.6943	1.7698	1.9004	2.0912
λ_3	2.1980	2.0458	1.9951	2.0378	2.1757	2.4178
θ_3	-.2565	.0669	.3897	.7433	1.1592	1.6730
P_3	.0683	.0934	.1008	.0886	.0591	.0229
τ_3	1.7601	2.0079	2.1365	2.1406	1.9793	1.5653
Q_3	.03880	.04653	.04718	.04139	.02986	.01464
τ_{3t}	2.8773	3.0093	3.1204	3.2056	3.2572	3.2649
Q_{3t}	.13256	.12794	.12162	.11358	.10373	.09198
P_{3t}	.3815	.3849	.3795	.3641	.3379	.3000
M	1.780	1.570	1.540	1.620	1.880	2.420
M_g	1.100	.993	1.005	1.110	1.340	1.810
$\Delta\tau_3$	+.0001	+.0028	-.0170	-.0548	-.1065	-.1603

Correction of supersonic solution for displacement of streamlines:

$$m(\xi_2) = \int_{\xi_i}^{\xi_2} Q_2 \phi_2 \xi_2 \, d\xi_2$$

	a_2	b_2	c_2	d_2	e_2	f_2
ξ_2	.785	.842	.899	.956	1.013	1.070
$m(\xi_2)$	0	.005498	.011201	.017071	.023095	.029242

$$m(\xi_3) = \int_{\xi_{2i}}^{\xi_3} Q_3 \phi_3 \xi_3 \, d\xi_3$$

	a_3	b_3	c_3	d_3	e_3	f_3
ξ_3	.760	.848	.936	1.024	1.112	1.200
$m(\xi_3)$	0	.005258	.011609	.018374	.024639	.029242

The functions $m(\xi_2)$ and $m(\xi_3)$ are plotted against radius on Fig. 6. From this graph, a corrected ξ_2 is obtained and, hence, new conditions at station 2.

Corrected values at station 2:

	a_2	b_2	c_2	d_2	e_2	f_2
ξ_2	.785	.839	.902	.968	1.026	1.070
ϕ_2	.7051	.6778	.6322	.6305	.6157	.6072
λ_2	1.9390	1.8640	1.7926	1.7338	1.6933	1.6698
θ_2	-.0705	.0090	.0955	.1804	.2514	.3036
τ_{2t}	3.7894	3.9438	4.1240	4.3127	4.4785	4.6043
P_2	.5417	.5837	.6241	.6580	.6816	.6962
τ_2	3.1805	3.3815	3.6043	3.8266	4.0135	4.1519
Q_2	.17032	.17259	.17315	.17197	.16978	.16767

Corrected solution at station 3:

	a_3	b_3	c_3	d_3	e_3	f_3
ϕ_3	1.7398	1.7007	1.7151	1.7686	1.8722	2.0493
λ_3	2.2499	2.0942	2.0311	2.0357	2.1269	2.3453
θ_3	-.2610	.1020	.2573	.4422	.9361	1.6394
P_3	.0605	.0842	.0953	.0959	.0733	.0295
τ_3	1.7003	1.9450	2.1067	2.2072	2.1223	1.6832
Q_3	.03558	.04330	.04523	.04344	.03452	.01754
τ_{3t}	2.8660	2.9896	3.1189	3.2376	3.3064	3.2898
Q_{3t}	.13104	.12665	.12076	.11325	.10449	.09375
P_{3t}	.3643	.3790	.3763	.3666	.3458	.3071
$\Delta\tau_3$	+.0006	+.0033	-.0069	-.0368	-.0881	-.1032

$C_1 = 1.4165$ $C_2 = .4487$

Note: Examples VI, VII and VIII use the channel configuration of Fig. 5 and the same conditions at station 1. Example VI is the isentropic solution ($\gamma = 1.40$), Example VII is a polytropic solution for n = 1.37, and Example VIII is for n = 1.33. From these examples it is possible to see clearly the effect of a decrease in polytropic efficiency on the solution for the same mass flow, upstream conditions and channel configuration.

Example VIa.

Solution for the stator of Fig. 5 (divergent curved channel walls) with a radial total temperature gradient. This is an isentropic ($\gamma = 1.40$) subsonic solution for the direct problem for a stator ($F(\xi_{\gamma_2})$ given). The radial coordinates have been chosen for equal areas in the plane perpendicular to the axis. The same equations as used in Example IIIa are applicable.

Conditions at station 1: (given)

	a_1	b_1	c_1	d_1	e_1	f_1
ξ_{γ_1}	.8000	.8438	.8854	.9252	.9633	1.0000
τ_{1t}	3.7894	3.9679	4.1374	4.2995	4.4548	4.6043
P_{1t}	1.000	1.000	1.000	1.000	1.000	1.000
Q_{1t}	.26389	.25202	.24170	.23258	.22448	.21719
P_1	.9500	.9500	.9500	.9500	.9500	.9500
Q_1	.25439	.24295	.23300	.22421	.21640	.20937
τ_1	3.7343	3.9102	4.0772	4.2369	4.3900	4.5373
ϕ_1	.6202	.6355	.6481	.6583	.6657	.6716
θ_1	-.0310	.0030	.0367	.0701	.1026	.1343

$F = 2.75$ $\quad m = .026865$ $\quad \frac{d\tau_{1t}}{d\xi_{\gamma_1}} = 4.0746$ $\quad \lambda_1 = 0$

Solution at station 2: ($\gamma = 1.40$)

	a_2	b_2	c_2	d_2	e_2	f_2
ξ_{γ_2}	.7850	.8496	.9098	.9661	1.0194	1.0700
ϕ_2	.5772	.5513	.5317	.5166	.5046	.4948
λ_2	1.5873	1.5161	1.4622	1.4206	1.3876	1.3607
θ_2	-.0577	.0198	.0865	.1453	.1986	.2474
P_2	.6712	.7095	.7378	.7592	.7763	.7898
Q_2	.19848	.19723	.19451	.19103	.18732	.18349
τ_2	3.3814	3.5974	3.7930	3.9738	4.1437	4.3041
M_2	.775	.754	.675	.668	.630	.609
$\Delta\tau_2$	0	-.0013	-.0025	-.0037	-.0061	-.0080

$\tau_{2t} = \tau_{1t}$, $P_{2t} = P_{1t}$, $Q_{2t} = Q_{1t}$ $\quad C_1 = .4661$ $\quad C_2 = .8923$

Example VIb

Solution for the rotor of Fig. 5 (divergent curved channel walls) with a radial total temperature gradient. This is an isentropic (γ=1.40) subsonic solution for the direct problem for the rotor ($G(\xi_3)$ given). The radial coordinates are for equal areas. The same equations as used in Example IIIb are applicable.

Conditions at station 2 are the same as after the stator, Example VIa.

$G = 1.96$ $\quad m = .026865$ $\quad \frac{d\tau_{2t}}{d\xi_2} = 2.8593$

Solution at station 3: ($\gamma = 1.40$)

	a_3	b_3	c_3	d_3	e_3	f_3
ξ_3	.7600	.8661	.9605	1.0464	1.1258	1.2000
ϕ_3	.1652	.2370	.2982	.3543	.4089	.4658
θ_3	-.0248	.0187	.0844	.1660	.2616	.3726
λ_3	-.4362	-.4016	-.3760	-.3520	-.3244	-.2870
P_3	.7550	.7595	.7626	.7635	.7606	.7532
τ_3	3.4970	3.6683	3.8290	3.9802	4.1197	4.2460
Q_3	.21589	.20707	.19916	.19181	.18460	.17738
τ_{3t}	3.5281	3.6993	3.8605	4.0126	4.1549	4.2867
P_{3t}	.7788	.7824	.7847	.7853	.7837	.7788
Q_{3t}	.22073	.21150	.20326	.19572	.18859	.18167
$\Delta\tau_3$	-.0001	-.0002	-.0024	-.0072	-.0135	-.0219

$C_1 = .1329$ $\quad C_2 = .9228$

Example VIIa

Solution for the same channel configuration, mass flow, and conditions at station 1 as for Example VIa, except for a polytropic process ($n = 1.37$, $\eta = 94.5\%$) through the stator.

Equations (48), (57), (58), (66), (74), (75) and the following integral are applicable for the polytropic stator (F = const):

$$\phi_2 = \frac{}{\xi_{\eta 2}^{\frac{F^2}{1+F^2}}(1+F^2)}\left[\int_{\xi_{\eta 1}}^{\xi_{\eta 2}}\left\{\left(\frac{\rho_2}{\rho_1}\right)^{\frac{1}{n}}\frac{\xi_{\eta 2}}{\phi_1\,\xi_{\eta 1}}\left[\frac{\gamma}{\gamma-1}\frac{d\tau_{1t}}{d\xi_{\eta 1}}\left(1-\rho_2^{\frac{n-1}{n}}\right)\right]+\frac{d\theta_2}{d\xi_{\eta 2}}+\frac{(\gamma-n)}{(\gamma-1)(n-1)}\frac{\tau_{1t}}{\phi_2}\frac{d\rho_2^{\frac{n-1}{n}}}{d\xi_{\eta 2}}\right\}\xi_{\eta 2}^{\frac{F^2}{1+F^2}}d\xi_{\eta 2}\right]+\frac{C_1}{\xi_{\eta 2}^{\frac{F^2}{1+F^2}}} \quad (78).$$

$F = 2.75$ $\quad m = .026865$ $\quad \frac{d\tau_{1t}}{d\xi_{\eta 1}} = 4.0746$

Solution at station 2: (n = 1.37)

	a_2	b_2	c_2	d_2	e_2	f_2
$\xi_{\eta 2}$	.7850	.8496	.9098	.9661	1.0194	1.0700
ϕ_2	.5897	.5652	.5469	.5330	.5222	.5135
λ_2	1.6216	1.5543	1.5040	1.4657	1.4360	1.4121
θ_2	-.0590	.0203	.0890	.1499	.2055	.2567
P_2	.6450	.6837	.7127	.7347	.7523	.7662
τ_2	3.3635	3.5778	3.7726	3.9526	4.1218	4.2814
Q_2	.19176	.19110	.18889	.18585	.18251	.17895
P_{2t}	.9789	.9821	.9845	.9863	.9874	.9882
Q_{2t}	.25834	.24751	.23793	.22938	.22164	.21461
$\Delta\tau_2$	+.0001	-.0017	-.0022	-.0038	-.0066	-.0090

$C_1 = .4762$ $\quad C_2 = .8883$ $\quad \tau_{2t} = \tau_{1t}$

Example VIIb

Solution for the same channel configuration, blade shape, and mass flow as for Example VIb, except for a polytropic process through the rotor (n = 1.37, η = 94.5%).

Conditions at station 2 are the same as after the stator, Example VIIa.

Equations (48), (57), (58), (70), (75), (77) and the following integral are applicable for the polytropic rotor (G = const, $P_{2t} \neq 1$):

$$\phi_3 = \frac{1}{\xi_{1_3}^{\frac{G^2}{1+G^2}}(1+G^2)}\left[\int_{\xi_{1_2}}^{\xi_{1_3}}\left\{\left(\frac{P_3}{P_2}\right)^{\frac{1}{n}}\frac{\xi_3}{\phi_2\xi_{1_2}}\left[\frac{\gamma}{\gamma-1}\frac{d\tau_{2t}}{d\xi_{1_2}} - \frac{\gamma}{\gamma-1}\rho_3^{\frac{n-1}{n}}\frac{d}{d\xi_{1_2}}\left(\frac{P_2^{\frac{1}{n}}}{Q_2}\right) - \frac{d}{d\xi_{1_2}}(\xi_{1_2}\lambda_2)\right] + 2G\right.\right.$$

$$\left.\left. + \frac{d\theta_3}{d\xi_{1_3}} + \frac{1}{\phi_3}\frac{(\gamma-n)}{(\gamma-1)(n-1)}\left(\frac{P_2^{\frac{1}{n}}}{Q_2}\right)\frac{dP_3^{\frac{n-1}{n}}}{d\xi_{1_3}}\right\}\xi_{1_3}^{\frac{G^2}{1+G^2}}d\xi_{1_3}\right] + \frac{C_1}{\xi_{1_3}^{\frac{G^2}{1+G^2}}} \qquad (79).$$

$G = 1.96$ $\quad m = .026865$ $\quad \frac{d\tau_{2t}}{d\xi_{1_2}} = 2.8593$

Solution at station 3: (n = 1.37)

	a_3	b_3	c_3	d_3	e_3	f_3
ξ_{1_3}	.7600	.8661	.9605	1.0464	1.1258	1.2000
ϕ_3	.1664	.2496	.3120	.3637	.4097	.4514
λ_3	-.4339	-.3769	-.3490	-.3335	-.3228	-.3153
θ_3	-.0250	.0197	.0883	.1704	.2621	.3611
P_3	.7387	.7430	.7457	.7463	.7439	.7379
τ_3	3.4890	3.6590	3.8190	3.9694	4.1094	4.2382
Q_3	.21172	.20306	.19524	.18799	.18101	.17410
τ_{3t}	3.5199	3.6839	3.8422	3.9947	4.1404	4.2807
P_{3t}	.7620	.7608	.7617	.7632	.7636	.7640
Q_{3t}	.21646	.20653	.19823	.19102	.18443	.17849
$\Delta\tau_3$	0	-.0044	-.0092	-.0137	-.0177	-.0194

$C_1 = .1338$ $\quad C_2 = .9215$

It is interesting to note that, compared to the isentropic case (Examples VIa, b), the polytropic flow through the identical stator and rotor results in the following percentage changes at station 3 (maximum):

ϕ_3: +5.3°/o $\quad$ τ_3: -0.3°/o

λ_3: +7.7°/o $\quad$ P_{3t}: -3.0°/o

P_3: -2.3°/o $\quad$ Work out: +6.6°/o

Example VIIIa

Solution for the same channel configuration, mass flow, and conditions at station 1 as for Example VIa, except for a polytropic process (n = 1.33, η = 86.8°/o) through the stator. The equations used in Example VIIa are applicable.

F = 2.75 m = .026865 $\frac{d\tau_{1t}}{d\xi_1}$ = 4.0746

Solution at station 2: (n = 1.33)

	a_2	b_2	c_2	d_2	e_2	f_2
ξ_2	.7850	.8496	.9098	.9661	1.0194	1.0700
ϕ_2	.6225	.5994	.5828	.5704	.5613	.5545
λ_2	1.7119	1.6483	1.6027	1.5686	1.5436	1.5249
θ_2	-.0622	.0216	.0948	.1605	.2209	.2772
P_2	.5878	.6280	.6584	.6817	.7000	.7146
τ_2	3.3149	3.5286	3.7225	3.9022	4.0695	4.2279
Q_2	.17731	.17796	.17685	.17470	.17199	.16902
P_{2t}	.9387	.9470	.9532	.9571	.9608	.9631
Q_{2t}	.24770	.23863	.23035	.22262	.21564	.20918
$\Delta\tau_2$	-.0001	-.0002	-.0019	-.0044	-.0071	-.0107

$\tau_{2t} = \tau_{1t}$ C_1 = .5027 C_2 = .8765

Example VIIIb

Solution for the same channel configuration, blade shape, and mass flow as for Example VIb, except for a polytropic process through the rotor (n = 1.33, η = 86.8°/o).

Conditions at station 2 are the same as after the stator, Example VIIIa. The equations used in Example VIIb are applicable. One complete approximation for the polytropic, subsonic, direct problem for the rotor is given below to demonstrate the iteration procedure.

Data used in the solution:

$m = .026865 \qquad G = 1.96 \qquad 2G = 3.9200 \qquad \frac{G^2}{1+G^2} = .7935$

$\frac{\gamma}{\gamma-1}\frac{d\tau_{2t}}{d\xi_2} = 10.0075$

	a_3	b_3	c_3	d_3	e_3	f_3
ξ_3	.7600	.8661	.9505	1.0464	1.1258	1.2000
$\left(\frac{\partial f}{\partial \zeta}\right)_3$	-.1500	.0791	.2829	.4684	.6398	.8000
$\left(\frac{\partial^2 f}{\partial \zeta^2}\right)_3$	-.2500	.1720	.5474	.8891	1.2049	1.5000
Factor	.02083	.01874	.01716	.01593	.01495	
$\frac{\overline{\xi_3}}{\phi_2 \xi_2}$	1.6278	1.7561	1.8551	1.9330	1.9949	
$\frac{d}{d\xi_2}\left(\frac{\gamma}{\gamma-1}\tau_{2t} - \xi_2\lambda_2\right)$	9.1313	9.0490	8.9897	8.9174	8.8593	
$\frac{\gamma}{\gamma-1}\frac{d}{d\xi_2}\left(\frac{\rho_2^{\frac{1}{n}}}{Q_2}\right)$	9.6600	9.8311	10.0646	10.2042	10.2714	
$\frac{(\gamma-n)}{(\gamma-1)(n-1)}\left(\frac{\overline{\rho_2^{\frac{1}{n}}}}{Q_2}\right)$	2.0529	2.1450	2.2328	2.3169	2.3975	
$\frac{1}{\xi_3^{.7935}}$	1.2433	1.1208	1.0325	.9646	.9102	.8653
$\overline{Q_2}\frac{(\xi_i^2 - \xi_{i-1}^2)}{2}$	.01532	.01530	.01516	.01495	.01470	
$\frac{n-1}{n}\left(\frac{Q_2}{\rho_2^{\frac{1}{n}}}\right)(\xi_i - \xi_{i-1})$	.006801	.006099	.005064	.004509	.004072	

(For definition of "Factor" above, see Problem Vb).

Try $C_1 = .1568$

	a_3	b_3	c_3	d_3	e_3	f_3
ϕ_3	.1949	.2717	.3312	.3775	.4164	.4524
$G\phi_3$	.3820	.5325	.6492	.7399	.8161	.8867
λ_3	-.3780	-.3336	-.3113	-.3065	-.3097	-.3133
θ_3	-.0292	.0215	.0937	.1768	.2664	.3619
$\frac{\lambda_3^2}{\xi_3}$	.1880	.1285	.1009	.0898	.0852	.0818
$\overline{\frac{\lambda_3^2}{\xi_3}}$	.1582	.1147	.0953	.0875	.0835	
$\overline{\theta_3}$	-.0039	.0576	.1352	.2216	.3141	
$-\overline{\theta_3}\frac{\partial\theta_3}{\partial\xi_3}$	+.0019	-.0418	-.1308	-.2501	-.4043	
$\frac{\partial\phi_3}{\partial\zeta_3}\left(\frac{\partial f}{\partial\zeta}\right)_3$	+.3207	-.1296	-.3559	-.4518	-.4635	-.4084
$\phi_3\left(\frac{\partial^2 f}{\partial\zeta^2}\right)_3$	-.0487	.0467	.1813	.3356	.5017	.6786
$\frac{\partial\theta_3}{\partial\zeta_3}$	+.2720	-.0829	-.1746	-.1162	+.0382	+.2702
$\overline{\frac{\partial\theta_3}{\partial\zeta_3}}$	+.0946	-.1287	-.1454	-.0390	+.1542	
$-\overline{\phi_3}\overline{\frac{\partial\theta_3}{\partial\zeta_3}}$	-.0221	+.0388	+.0515	+.0155	-.0670	
$\Delta P_3^{\frac{n-1}{n}}$	1.00094	+.00068	+.00008	-.00066	-.00158	

The constant C_2 is found by applying Equation (77) at the inner channel boundary.

$$\tau_3 = 3.7894 - .14286\left[.1429 + .0380 + .0009 + 2(1.3438 - .2873)\right] = 3.4616$$

$$P_3 = .5878(1.0443)^{\frac{n}{n-1}} = .7000 \qquad C_2 = (.7000)^{\frac{n-1}{n}} = .9153$$

	a_3	b_3	c_3	d_3	e_3	f_3
$P_3^{\frac{n-1}{n}}$	.9153	.9162	.9169	.9170	.9163	.9148
P_3	.7000	.7028	.7049	.7052	.7031	.6984
$(\frac{P_3}{P_2})$	1.1909	1.1191	1.0706	1.0345	1.0044	.9773
$(\frac{P_3}{P_2})^{\frac{1}{n}}$	1.1404	1.0883	1.0526	1.0258	1.0033	.9829
Av.	1.1143	1.0704	1.0392	1.0145	.9931	
$\overline{P_3}^{\frac{n-1}{n}}$	.9157	.9165	.9169	.9166	.9155	
$\frac{1}{\phi_3}\frac{d}{d\xi_3}\rho_3^{\frac{n-1}{n}}$	+.0380	+.0227	+.0026	-.0209	-.0490	

The axial velocity integral is iterated in steps across the channel as follows:

	$\Delta\phi_3$	ϕ_3	Average
$.02083\left[1.8139(9.1313-8.8461)+3.92+.0946+.0780\right]$	= .09602	.09602	.04801
$.01874\left[1.8797(9.0490-9.0107)+3.92-.1287+.0487\right]$	= .07331	.16933	.13267
$.01716\left[1.9278(8.9897-9.2287)+3.92-.1454+.0058\right]$	= .05697	.22630	.19781
$.01593\left[1.9610(8.9174-9.3537)+3.92-.0390-.0484\right]$	= .04742	.27372	.25001
$.01495\left[1.9811(8.8593-9.4040)+3.92+.1542-.1175\right]$	= .04302	.31674	.29523

The mass flow equation is iterated to solve for C_1 as follows:

$$.026865 = .017071(.04801 + 1.1820C_1) + .016377(.13267 + 1.0766C_1)$$
$$+ .015754(.19781 + .9985C_1) + .015167(.25001 + .9374C_1)$$
$$+ .014597(.29523 + .8877C_1)$$
$$C_1 = \frac{.012654}{.080717} = .1568$$

Solution at station 3: (n = 1.33)

	a_3	b_3	c_3	d_3	e_3	f_3
ξ_3	.7600	.8661	.9605	1.0464	1.1258	1.2000
ϕ_3	.1949	.2717	.3312	.3775	.4164	.4524
λ_3	-.3780	-.3336	-.3113	.3065	-.3097	-.3133
θ_3	-.0292	.0215	.0937	.1768	.2664	.3619
P_3	.7000	.7028	.7049	.7052	.7031	.6984
τ_3	3.4617	3.6285	3.7862	3.9354	4.0740	4.2038
Q_3	.20220	.19367	.18615	.17921	.17275	.16518
τ_{3t}	3.4876	3.6503	3.8062	3.9582	4.1049	4.2456
P_{3t}	.7185	.7177	.7181	.7204	.7219	.7229
Q_{3t}	.20600	.19659	.18863	.18183	.17605	.16929
$\Delta\tau_3$	-.0001	-.0047	-.0108	-.0155	-.0178	-.0202

Compared to the isentropic case (Examples VIa, b), the polytropic flow with n = 1.33 through the same stator and rotor results in the following maximum percentage changes at station 3:

ϕ_3: +18.0°/o — τ_3: -1.1°/o

λ_3: +20.8°/o — P_{3t}: -9.3°/o

P_3: - 8.3°/o — Work out: +19.5°/o

Example IXa

Solution for the stator of Fig. 5 (divergent curved channel walls) with a radial total temperature gradient and radial coordinates for equal areas. This is an isentropic, subsonic solution for the direct problem for the stator. The resulting solution at station 2 is used in

Example IXb as the upstream conditions for a solution of the inverse problem for a rotor.

The equations used in Example IIIa are applicable.

Conditions at station 1: given

	a_1	b_1	c_1	d_1	e_1	f_1
ξ_1	.8000	.8438	.8854	.9252	.9633	1.0000
τ_{1t}	3.7894	3.9679	4.1374	4.2995	4.4548	4.6043
P_{1t}	1.00	1.00	1.00	1.00	1.00	1.00
Q_{1t}	.26389	.25202	.24170	.23258	.22448	.21719
P_1	.9400	.9400	.9400	.9400	.9400	.9400
τ_1	3.7231	3.8985	4.0650	4.2243	4.3768	4.5237
Q_1	.25249	.24113	.23126	.22253	.21478	.20781
θ_1	-.0340	.0033	.0403	.0768	.1125	.1473
ϕ_1	.6804	.6970	.7108	.7215	.7303	.7365

$F = 2.75$ $\quad m = .029242$ $\quad \frac{d\tau_{1t}}{d\xi_1} = 4.0746$ $\quad \lambda_1 = 0$

Solution at station 2:

	a_2	b_2	c_2	d_2	e_2	f_2
ξ_2	.7850	.8496	.9098	.9661	1.0194	1.0700
ϕ_2	.7008	.6688	.6452	.6275	.6139	.6033
λ_2	1.9272	1.8392	1.7743	1.7256	1.6882	1.6591
θ_2	-.0701	.0241	.1050	.1765	.2416	.3016
P_2	.5460	.5954	.6322	.6601	.6822	.6997
τ_2	3.1879	3.4217	3.6292	3.8183	3.9938	4.1577
Q_2	.17126	.17402	.17419	.17286	.17081	.16828
$\Delta\tau_2$	0	-.0010	-.0026	-.0049	-.0083	-.0116

$\tau_{2t} = \tau_{1t}$ $\quad P_{2t} = P_{1t}$, $\quad Q_{2t} = Q_{1t}$

$C_1 = .5659$ $\quad C_2 = .8412$

Example IXb

Solution for the rotor of Fig. 5 (divergent curved channel walls) with a radial temperature gradient and radial coordinates for

equal areas. This is an isentropic, subsonic solution for the inverse problem ($H(\xi_3)$ given) for the rotor. One complete approximation for the inverse problem for the rotor is given below to illustrate the iteration procedure.

Equations (63), (65), (73), (75), (77) (with appropriate subscripts) and the following two relations are used:

$$\phi_3 = \int_{\xi_{1i}}^{\xi_3} \left[\left(\frac{P_3}{P_2}\right)^{\frac{1}{\gamma}} \frac{\xi_3}{\phi_2 \xi_{2i}} \left\{ \frac{\gamma}{\gamma-1} \frac{d\tau_{2t}}{d\xi_2} \left(1 - P_3^{\frac{\gamma-1}{\gamma}}\right) + \frac{(H-\xi_2\lambda_2)}{\xi_3^2} \frac{d(\xi_2\lambda_2)}{d\xi_2} \right\} - \frac{1}{\phi_3}\left(1 + \frac{H-\xi_2\lambda_2}{\xi_3^2}\right)\frac{dH}{d\xi_3} + \frac{d\theta_3}{d\zeta_3} \right] d\xi_3 + C_1 \quad (80)$$

$$H(\xi_3) = \xi_2\lambda_2 + \xi_3\lambda_3 \quad (27).$$

When iterated across the channel, Equation (80) becomes:

$$\phi_3 = \sum_1^n \left(\frac{P_3}{P_2}\right)^{\frac{1}{\gamma}} \frac{1}{\phi_2 \xi_2} \left[\frac{\gamma}{\gamma-1} \frac{d\tau_{2t}}{d\xi_2} \left(1 - P_3^{\frac{\gamma-1}{\gamma}}\right) \left(\frac{\xi_i^2 - \xi_{i-1}^2}{2}\right) + (H-\xi_2\lambda_2) \frac{d(\xi_2\lambda_2)}{d\xi_2} \ln \frac{\xi_i}{\xi_{i-1}} \right] - \frac{1}{\phi_3}(H_i - H_{i-1}) \quad (81).$$

$$+ \frac{1}{\phi_3}(H-\xi_2\lambda_2)\frac{dH}{d\xi_3}\left(\frac{1}{\xi_i} - \frac{1}{\xi_{i-1}}\right) + \frac{d\theta_3}{d\xi_3}(\xi_i - \xi_{i-1}) + C_1$$

Conditions at station 2 are the same as after the stator, Example IXa above. The work output function $H(\xi_3)$ is given in this example, and the blade shape (spouting angle) is determined.

Data used in the iteration:

$m = .029242$ $\qquad \frac{d\tau_{2t}}{d\xi_2} = 2.8593$ $\qquad H(\xi_3) = 1.300$ (constant-given)

$(H_i - H_{i-1}) = 0$ $\qquad \frac{dH}{d\xi_3} = 0$

	a_3	b_3	c_3	d_3	e_3	f_3
ξ_3	.7600	.8661	.9605	1.0464	1.1258	1.2000
$H(\xi_3)$	1.3000	1.3000	1.3000	1.3000	1.3000	1.3000
$\xi_2 \lambda_2$	1.5129	1.5626	1.6143	1.6671	1.7210	1.7752
$\xi_3 \lambda_3$	-.2129	-.2626	-.3143	-.3671	-.4210	-.4752
λ_3	-.2801	-.3032	-.3272	-.3508	-.3739	-.3960
$\frac{\overline{1}}{\Phi_2 \xi_2}$	1.7889	1.7317	1.6766	1.6238	1.5736	
$\frac{\gamma}{\gamma-1} \frac{d\tau_{2t}}{d\xi_2} \frac{(\xi_i^2 - \xi_{i-1}^2)}{2}$	.86305	.86305	.86305	.86305	.86305	
$\left(H - \xi_2 \lambda_2\right) \frac{d(\xi_2 \lambda_2)}{d\xi_2} \ln \frac{\xi_i}{\xi_{i-1}}$	-.02931	-.02801	-.02751	-.02681	-.02631	
$(\xi_i - \xi_{i-1})$	.1061	.0944	.0859	.0794	.0742	
$\bar{Q}_2 \frac{(\xi_i^2 - \xi_{i-1}^2)}{2}$	.01489	.01501	.01496	.01482	.01462	
$\frac{\gamma-1}{\gamma} \frac{1}{\tau_{2t}} (\xi_i - \xi_{i-1})$	.007820	.006658	.005821	.005185	.004682	

Try $C_1 = .1039$.

	a_3	b_3	c_3	d_3	e_3	f_3
ϕ_3	.1039	.2379	.3295	.4159	.5242	.6891
λ_3	-.2801	-.3032	-.3272	-.3508	-.3739	-.3960
θ_3	-.0156	.0188	.0932	.1948	.3354	.5513
$\frac{\overline{\lambda_3^2}}{\xi_3}$		.1047	.1088	.1145	.1209	.1274
$\overline{\theta}_3$		.0016	.0560	.1440	.2651	.4433
$\frac{\partial \theta_3}{\partial \xi_3}$		.3242	.7881	1.1827	1.7707	2.9097
$-\overline{\theta}_3 \frac{\partial \theta_3}{\partial \xi_3}$		-.0005	-.0441	-.1703	-.4694	-1.2889
$\frac{\partial \phi_3}{\partial \zeta_3}$	-2.9845	-2.1545	-1.5785	-1.0580	-.4485	+.4290
$\frac{\partial \phi_3}{\partial \zeta_3}\left(\frac{\partial f}{\partial \zeta^*}\right)_3$	+.4477	-.1704	-.4466	-.4956	-.2870	+.3432
$\phi_3\left(\frac{\partial^2 f}{\partial \zeta^{*2}}\right)_3$	-.0260	.0409	.1804	.3698	.6316	1.0336
$\frac{\partial \theta_3}{\partial \zeta_3}$	+.4217	-.1295	-.2662	-.1258	+.3446	+1.3768
$\frac{\partial \overline{\theta_3}}{\partial \zeta_3}$		+.1461	-.1978	-.1960	+.1094	+.8607
$-\overline{\phi}_3 \frac{\partial \overline{\theta_3}}{\partial \zeta_3}$		-.0065	+.0592	+.0700	-.0642	-.5647
$\Delta \rho_3^{\frac{\gamma-1}{\gamma}}$		+.00076	+.00082	+.00008	-.00214	-.00809

The constant C_2 is found by applying Equation (77) at the inner channel boundary.

$$\zeta_3 = 3.7894 - .14286 \left[.0785 + .0108 + .0002 + 2.600\right] = 3.4052$$

$$P_3 = .5460 \ (1.0682)^{\frac{\gamma}{\gamma-1}} = .6878 \qquad C_2 = (.6878)^{\frac{\gamma-1}{\gamma}} = .8986$$

	a_3	b_3	c_3	d_3	e_3	f_3
$P_3^{\frac{\gamma-1}{\gamma}}$	.8986	.8994	.9002	.9003	.8981	.8900
P_3	.6878	.6900	.6921	.6924	.6865	.6651
$\left(\frac{\rho_3}{\rho_2}\right)$	1.2597	1.1589	1.0947	1.0489	1.0063	.9506
$\left(\frac{\rho_3}{\rho_2}\right)^{\frac{1}{\gamma}}$	1.1793	1.1111	1.0668	1.0347	1.0045	.9645
Av.	1.1452	1.0889	1.0507	1.0196	.9845	
$\left(1-\rho_3^{\frac{\gamma-1}{\gamma}}\right)$	.1014	.1006	.0998	.0997	.1019	.1100
Av.	.1010	.1002	.0998	.1008	.1059	

The axial velocity integral is iterated in steps across the channel as follows:

	$\Delta\phi_3$	ϕ_3	Average
2.0486 (.08717- .02931) + .01550 =	.13403	.13403	.06701
1.8856 (.08648 -.02801) - .01867 =	.09158	.22561	.17982
1.7616 (.08613 -.02751) - .01684 =	.08642	.31203	.26882
1.6556 (.08700 -.02681) +.00869 =	.10834	.42037	.36620
1.5492 (.09140 - .02631) +.06386 =	.16470	.58507	.50272

The mass flow equation is iterated to solve for C_1 as follows:

$$.029242 = .017052\,(.06701 + C_1) + .016344\,(.17982 + C_1) + .015718\,(.26882 + C_1) + .015110\,(.36620 + C_1) + .014393\,(.50272 + C_1)$$

$$C_1 = \frac{.008166}{.078617} = .1039$$

Solution at station 3:

	a_3	b_3	c_3	d_3	e_3	f_3
ξ_3	.7600	.8661	.9605	1.0464	1.1258	1.2000
ϕ_3	.1039	.2379	.3295	.4159	.5243	.6890
λ_3	-.2801	-.3032	-.3272	-.3508	-.3739	-.3960
θ_3	-.0156	.0188	.0932	.1948	.3354	.5512
P_3	.6878	.6900	.6921	.6924	.6865	.6651
τ_3	3.4052	3.5688	3.7243	3.8706	4.0010	4.0978
Q_3	.20197	.19335	.18583	.17886	.17158	.16231
$G(\xi_3)$	4.619	2.366	1.922	1.672	1.434	1.167
β_3	12°12'	22°55'	27°30'	30°55'	34°53'	40°35'
$\Delta\tau_3$	0	+.0064	+.0096	+.0097	+.0070	+.0014

Note: A supersonic solution is indicated for problem IXb by using average values in the mass flow and energy equations ($\phi_3 \cong 3.780$). However, the supersonic solution is impossible in this case since the pressure goes to zero at the outer channel boundary before the solution is reached.

Example Xa.

Examples Xa, b are the isentropic, subsonic solutions for the stator and rotor of Fig. 5. This is an example of the inverse problem in which $H(\xi_3)$ and $\lambda_3 = 0$ are specified and the blade shapes of both the stator and rotor are thus determined.

Equations (27), (63), (65), (73), (74), (75) (with appropriate subscripts) are applicable for the stator in addition to the following relation:

$$\left(\lambda_3 = 0\,,\ H(\xi_3) = \xi_2 \lambda_2\right)$$

$$\phi_2 = \int_{\xi_{1i}}^{\xi_2} \left[\left(\frac{\rho_2}{\rho_1}\right)^{\frac{1}{\gamma}} \frac{\xi_2}{\phi_1 \xi_1} \frac{\gamma}{\gamma-1} \frac{d\tau_{1t}}{d\xi_1} \left(1-\rho_2^{\frac{\gamma-1}{\gamma}}\right) + \frac{d\theta_2}{d\zeta_2^*} - \frac{1}{\phi_2} \frac{\lambda_2}{\xi_2} \frac{d(\xi_2 \lambda_2)}{d\xi_2} \right] d\xi_2 + C_1 \qquad (82).$$

Conditions at station 1 are assumed the same as for Example IXa.

	a_2	b_2	c_2	d_2	e_2	f_2
$H(\xi_2)$ (given)	1.3000	1.3561	1.4061	1.4515	1.4935	1.5328
λ_2	1.6561	1.5962	1.5455	1.5024	1.4651	1.4325

$$m = .029242 \qquad F(\xi_2) = \frac{\lambda_2}{\phi_2}$$

$$\frac{d\tau_{1t}}{d\xi_1} = 4.0746$$

Solution at station 2:

	a_2	b_2	c_2	d_2	e_2	f_2
ξ_2	.7850	.8496	.9098	.9661	1.0194	1.0700
ϕ_2	.6791	.6327	.6004	.5760	.5532	.5311
λ_2 (given)	1.6561	1.5962	1.5455	1.5024	1.4651	1.4325
θ_2	-.0679	.0228	.0977	.1620	.2177	.2656
P_2	.6367	.6780	.6932	.7308	.7489	.7635
τ_2	3.3310	3.5501	3.7485	3.9310	4.1015	4.2627
Q_2	.19116	.19093	.18604	.18590	.18279	.17912
$F(\xi_2)$	2.439	2.523	2.574	2.608	2.648	2.697
β_2	22°18'	21°36'	21°15'	20°59'	20°41'	20°21'
$\Delta\tau_2$	0	-.0035	-.0052	-.0051	-.0038	-.0019

$C_1 = .6791$ $\quad C_2 = .8790$ $\quad P_{2t} = P_{1t}$, $Q_{2t} = Q_{1t}$, $\tau_{2t} = \tau_{1t}$

Example Xb.

Solution for the rotor of Fig. 5 for the inverse problem in which H (ξ_3) and $\lambda_3 = 0$ are specified and the blade shape G (ξ_3) is to be determined.

Equations (27), (63), (65), (73), (75), (77) (with appropriate subscripts are applicable for the rotor in addition to the following relation :

$$\phi_3 = \int_{\xi_{1i}}^{\xi_3} \left[\left(\frac{P_3}{P_2}\right)^{\frac{1}{\gamma}} \frac{\xi_3}{\phi_2 \xi_2} \left\{ \frac{\gamma}{\gamma-1} \frac{d\tau_{2t}}{d\xi_2} \left(1 - P_3^{\frac{\gamma-1}{\gamma}}\right) - \frac{d}{d\xi_2}(\xi_2 \lambda_2) \right\} + \frac{d\theta_3}{d\xi_3} \right] d\xi_3 + C_1 \qquad (83).$$

Conditions at station 2 are the same as after the stator, Example Xa.

m = .029242 $\qquad \frac{d\tau_{2t}}{d\xi_2} = 2.8593 \qquad \lambda_3 = 0 \qquad G(\xi_3) = \frac{\xi_3}{\phi_3}$

Solution at station 3:

	a_3	b_3	c_3	d_3	e_3	f_3
ξ_3	.7600	.8661	.9605	1.0464	1.1258	1.2000
ϕ_3	.2985	.3398	.3627	.3830	.4110	.4602
θ_3	-.0048	.0269	.1026	.1794	.2630	.3682
λ_3	0	0	0	0	0	0
P_3	.6876	.6873	.6868	.6857	.6825	.6758
Q_3	.20196	.19280	.18481	.17763	.17105	.16416
τ_3	3.4049	3.5639	3.7388	3.8602	3.9940	4.1165
$G(\xi_3)$	2.546	2.549	2.648	2.732	2.739	2.608
β_3	21°25'	21°23'	20°41'	20°07'	20°02'	20°57'
$\Delta\tau_3$	0	-.0001	+.0011	-.0010	+.0001	+.0002

$C_1 = .2985 \qquad C_2 = .8985$

Example XI

This example has been constructed to illustrate the increase in gross thrust obtainable by the use of a radial total temperature gradient.

A hypothetical one-stage turbine consisting of a stator and a rotor has been assumed similar to that shown in Fig. 3. In order to give this example more physical meaning, rotor blades have been used which are tapered linearly in area in such a way that the ratio of hub to tip cross-sectional area is three. Using a rotor tip speed of 1100 feet per second, the stress due to centrifugal forces was calculated at various points along the blade. Using the high-temperature data for "Vitallium", (H. S. 21) (NR-10), given in References 16 and 17, it was then estimated that the blade root could safely stand a temperature of $1450^{\circ}F$, while the blade tip temperature could be $1850^{\circ}F$.

Using this data, the thrust of this turbine is calculated for two conditions: (a) A constant radial total temperature of $1450^{\circ}F$, and (b) a linear temperature gradient of $400^{\circ}F$ with the same root total temperature of $1450^{\circ}F$. The mass flow, boundary configuration, combustion chamber total pressure, and work extracted are the same in both cases.

Example XIa.

Solution for the stator and rotor of Fig. 3 with no radial total temperature gradient and equal area coordinates. This is an isentropic, subsonic solution to the inverse problem ($H\left(\xi_3\right)$ given).

For no radial total temperature gradient, $H(\xi_3) = \xi_2 \lambda_2$ = constant, and a cylindrical channel, Equation (82) reduces to $\phi_2 = C_1$. Equations (63), (64), (65) and (67) are also used in the solution for the stator.

Conditions at station 1: (given)

$\tau_{1t} = 2.7071$	$P_{1t} = 1.00$	$Q_{1t} = .36940$	$\phi_1 = .4915$
$\tau_1 = 2.6726$	$P_1 = .9562$	$Q_1 = .35775$	$\lambda_1 = 0$
$\omega = 880 \frac{rad}{sec}$	$T_{1t} = 1910^{\circ}R$ (const.)		$W = 148.26 \frac{lb}{sec}$
$\omega R_o = 1100 \frac{ft}{sec}$	$p_{1t} = 16,300 \frac{lb}{ft^2}$		$H(\xi_3) = 1.3964$ (const.)
$R_o = 1.25$ ft	$m = .031650$		$\lambda_3 = 0$

Solution at station 2:

	a_2	b_2	c_2	d_2	e_2
ξ_2	.8000	.8544	.9055	.9539	1.0000
ϕ_2	.7260	.7260	.7260	.7260	.7260
λ_2	1.7455	1.6342	1.5421	1.4639	1.3964
P_2	.4812	.5236	.5585	.5879	.6125
Q_2	.21909	.23268	.24369	.25277	.26027
τ_2	2.1965	2.2501	2.2921	2.3259	2.3533
$F = \frac{\lambda_2}{\phi_2}$	2.404	2.251	2.124	2.016	1.923
β_2	$22^{\circ}34'$	$23^{\circ}59'$	$25^{\circ}13'$	$26^{\circ}25'$	$27^{\circ}30'$
M_2	1.071	1.005	.951	.904	.873
$\Delta\tau_2$	0	+.0002	0	-.0003	-.0001

$C_1 = .7620$ $\qquad \tau_{2t} = \tau_{1t}$, $P_{2t} = P_{1t}$, $Q_{2t} = Q_{1t}$

$C_2 = .8114$

For the rotor with no radial total temperature gradient, $H(\xi_2)$ = constant, and $\lambda_3 = 0$, the solution at station 3 is easily found to be:

ϕ_3	= .7806	Q_3	= .22525
λ_3	= 0	τ_{3t}	= 2.3081
P_3	= .5003	Q_{3t}	= .24798
τ_3	= 2.2211	P_{3t}	= .5724

	a_3	b_3	c_3	d_3	e_3
$G = \frac{\xi_3}{\phi_3}$	1.025	1.095	1.160	1.222	1.281
β_3	44°20'	42°25'	40°46'	39°17'	37°56'

Assuming isentropic expansion to atmospheric pressure through an ideal nozzle, the total gross thrust is found to be 11,966 pounds.

Example XIb.

Solution for the same stator and rotor as Example XIa except with a linear radial total temperature gradient of 400°F. The mass flow, combustion chamber total pressure, and work extracted are the same as in the above example.

Equations (27), (63), (64), (65), (67), and (82) are applicable.

Conditions at station 1: (given)

	a_1	b_1	c_1	d_1	e_1
ξ_1	.8000	.8544	.9055	.9539	1.0000
τ_{1t}	2.7071	2.8614	3.0062	3.1434	3.2741
P_{1t}	1.00	1.00	1.00	1.00	1.00
Q_{1t}	.36940	.34948	.33265	.31813	.30543
P_1	.9512	.9512	.9512	.9512	.9512
τ_1	2.6687	2.8208	2.9635	3.0988	3.2276
Q_1	.35643	.33721	.32097	.30696	.29471
ϕ_1	.5185	.5331	.5467	.5587	.5705
λ_1	0	0	0	0	0

m = .031650 $\quad \frac{d\tau_{1t}}{d\xi_1} = 2.8350 \quad H(\xi_3) = 1.3964$ (const), $\lambda_3 = 0$

Solution at station 2 :

	a_2	b_2	c_2	d_2	e_2
ϕ_2	.5844	.6975	.7955	.8819	.9589
λ_2	1.7455	1.6342	1.5421	1.4639	1.3964
P_2	.5018	.5443	.5774	.6036	.6249
τ_2	2.2231	2.4050	2.5697	2.7212	2.8625
Q_2	.22574	.22632	.22474	.22183	.21829
$F = \frac{\lambda_2}{\phi_2}$	2.987	2.342	1.938	1.659	1.467
β_2	18°30'	23°07'	27°18'	31°09'	34°19'
M_2	1.044	.974	.920	.878	.850
$\Delta\tau_2$	-.0001	+.0054	+.0064	+.0049	+.0017

$C_1 = .5844$ $\qquad \tau_{2t} = \tau_{1t}$, $P_{2t} = P_{1t}$, $Q_{2t} = Q_{1t}$

$C_2 = .8212$

For the rotor with H (ξ_3) = constant and $\lambda_3 = 0$, Equation (64) reduces to P_3 = constant. Equations (63), (65), (71), and the following integral are applicable:

$$\phi_3 = \int_{\xi_{1i}}^{\xi_3} \left(\frac{\rho_3}{\rho_2}\right)^{\frac{1}{\gamma}} \frac{1}{\phi_2} \frac{\gamma}{\gamma-1} \frac{d\tau_{2t}}{d\xi_2} \left(1-\rho_3^{\frac{\gamma-1}{\gamma}}\right) d\xi_3 + C_1 \qquad (84).$$

Solution at station 3:

	a_3	b_3	c_3	d_3	e_3
ϕ_3	.6002	.7426	.8514	.9397	1.0141
λ_3	0	0	0	0	0
P_3	.5289	.5289	.5289	.5289	.5289
τ_3	2.2566	2.3853	2.5060	2.6203	2.7293
Q_3	.23435	.22171	.21103	.20182	.19376
τ_{3t}	2.3081	2.4624	2.6072	2.7444	2.8751
P_{3t}	.5724	.5912	.6075	.6220	.6345
Q_{3t}	.24798	.24005	.23300	.22658	.22067
$G = \frac{\xi_3}{\phi_3}$	1.333	1.151	1.064	1.015	.986
β_3	36°52'	40°58'	43°13'	44°35'	45°22'
$\Delta\tau_3$	0	-.0017	-.0023	-.0020	-.0011

$C_1 = .6002$ $C_2 = .8336$

Assuming isentropic expansion to atmospheric pressure through an ideal nozzle, and summing the thrust by stream tubes, the total gross thrust is found to be 12,883.8 pounds. This is an increase of 917.8 pounds, or 7.7 percent, over than found in Example XIa.

	ξ_1, ξ_2, ξ_3
a	.8200
b	.8584
c	.9055
d	.9539
e	1.0000

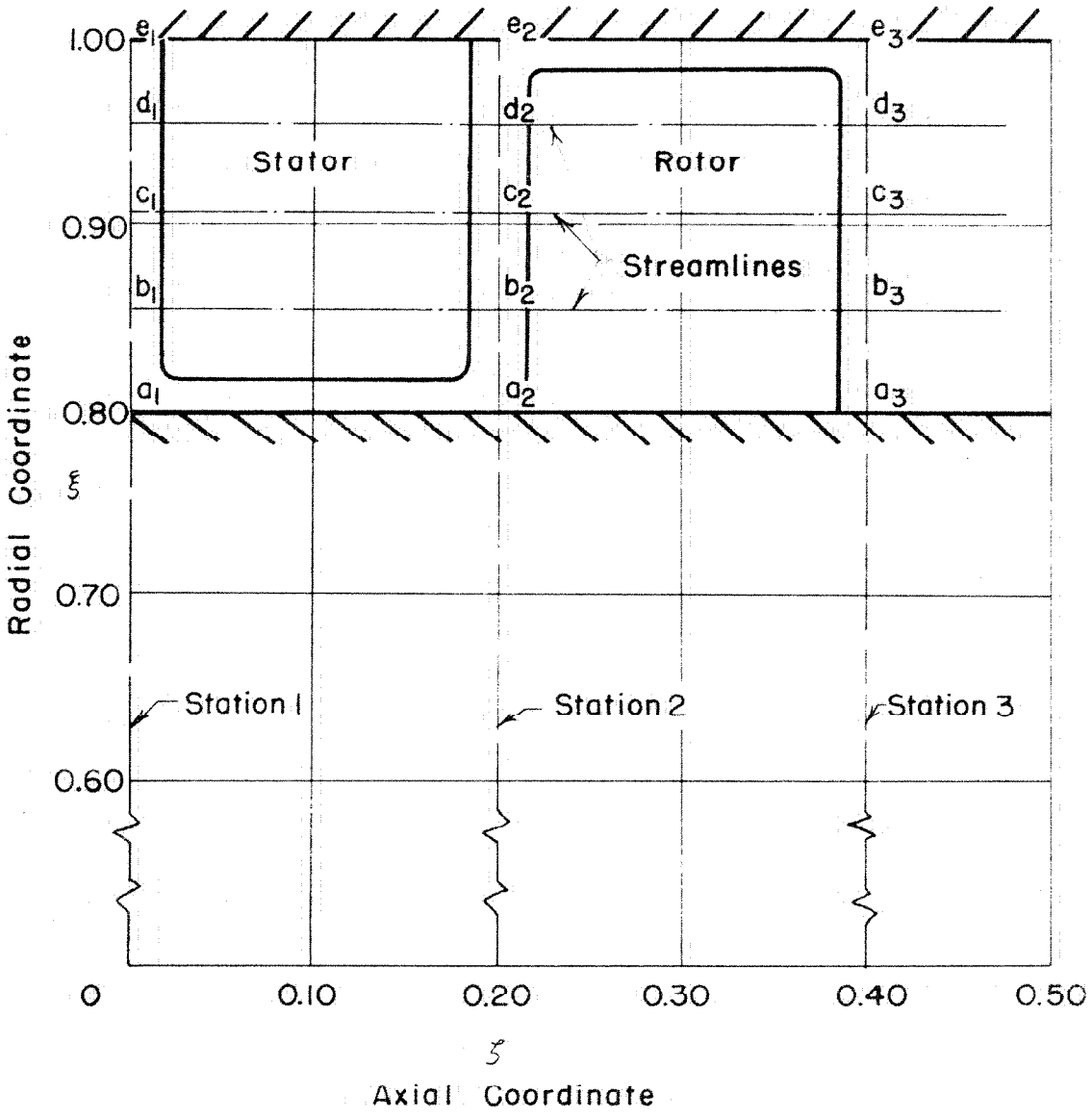

FIG. 3 — CHANNEL CONFIGURATION AND COORDINATES FOR EXAMPLES I, II, AND XI

	ξ_1	ξ_2	ξ_3	$\left(\frac{\partial f}{\partial \xi}\right)_{1,2,3}$
a	.800	.790	.780	-.050
b	.850	.850	.850	0
c	.900	.910	.920	+.050
d	.950	.970	.990	+.100
e	1.000	1.030	1.060	+.150

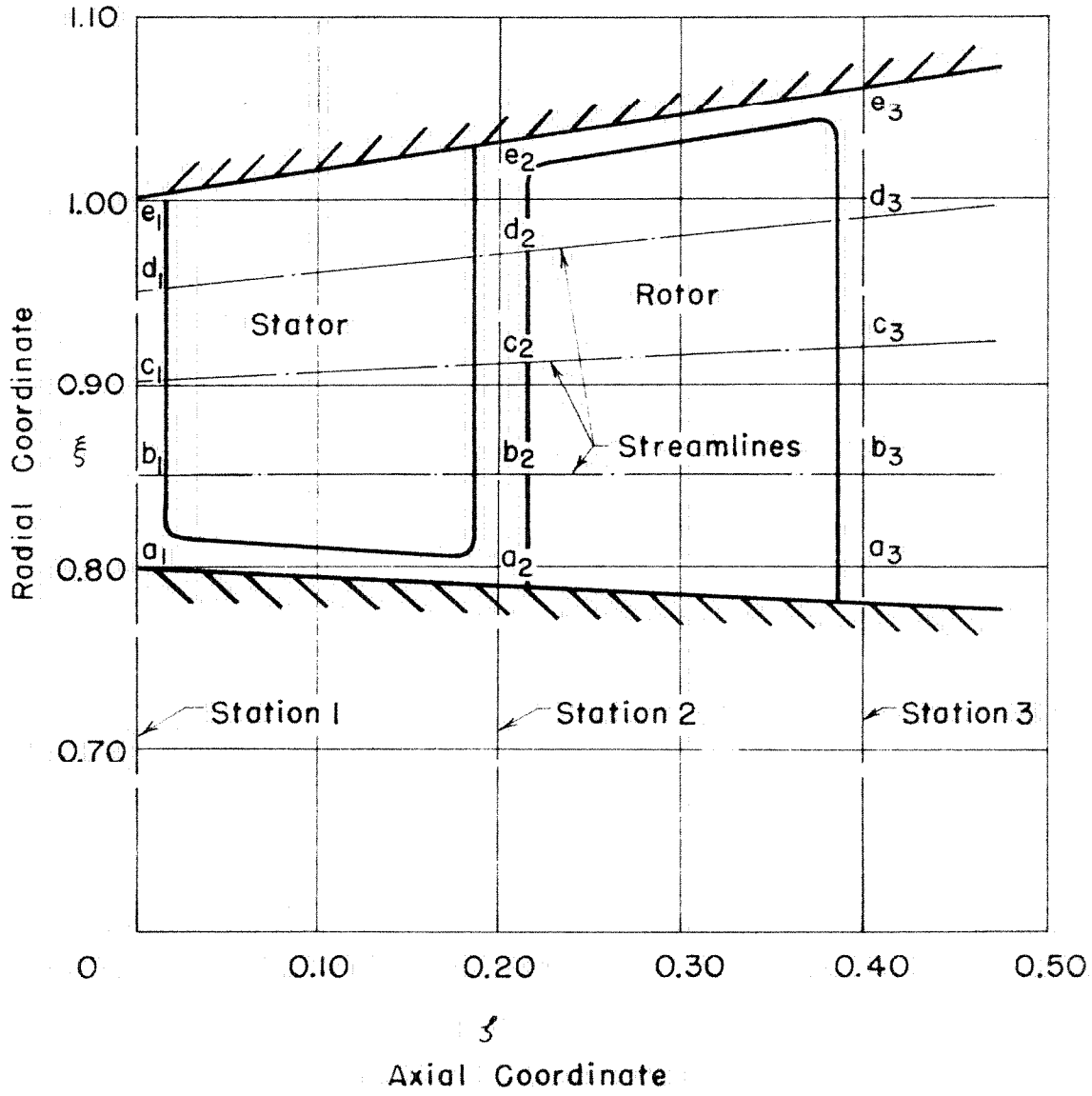

FIG. 4 — CHANNEL CONFIGURATION AND COORDINATES FOR EXAMPLE III

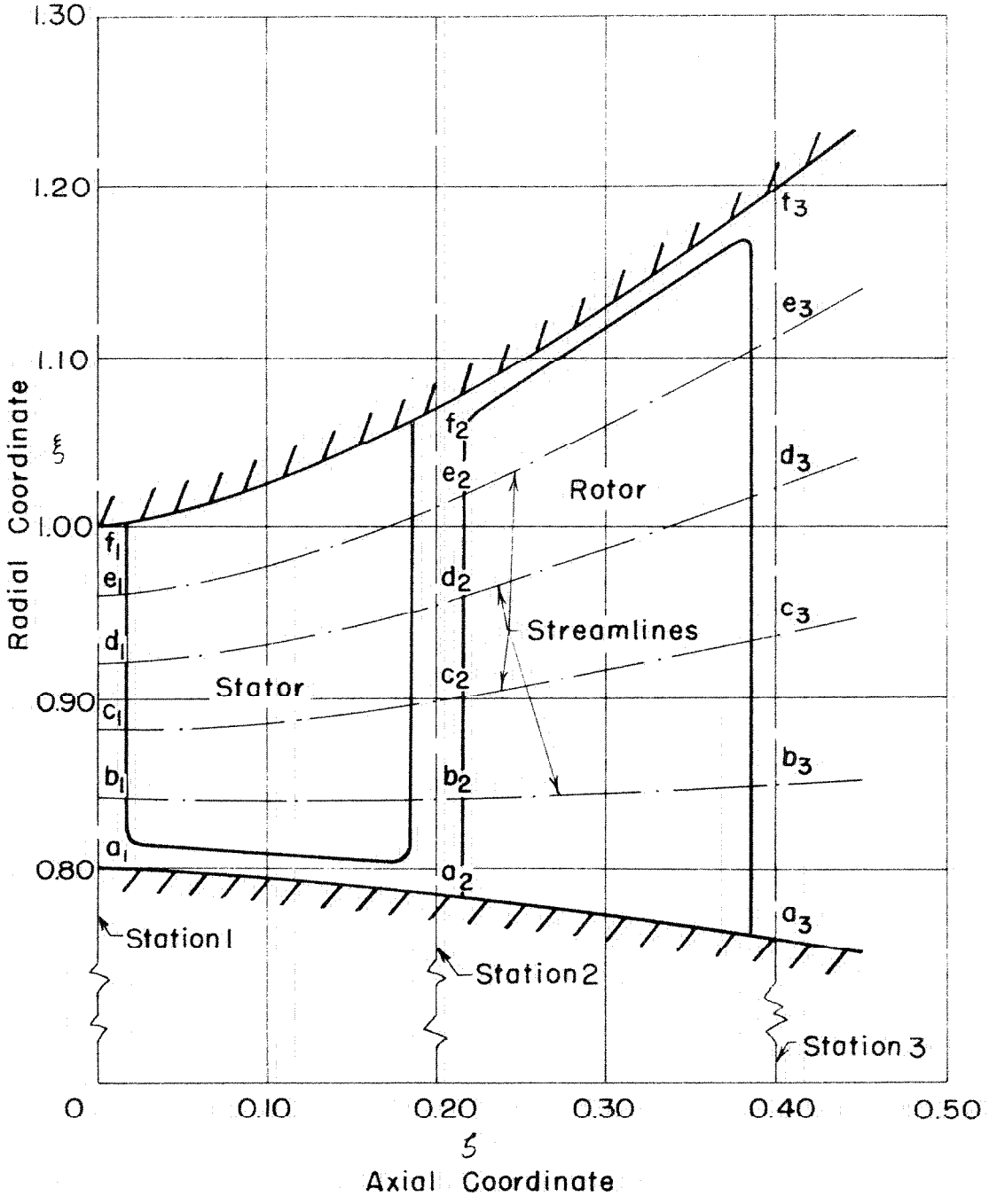

FIG.5 – CHANNEL CONFIGURATION AND COORDINATES FOR EXAMPLES IV – X

Examples IV, V

ξ_1	ξ_1	ξ_2	ξ_3	$\left(\frac{\partial f}{\partial \xi}\right)_1$	$\left(\frac{\partial f}{\partial \xi}\right)_2$	$\left(\frac{\partial f}{\partial \xi}\right)_3$	$\left(\frac{\partial^2 f}{\partial \xi^2}\right)_{1,2,3}$
a	.800	.785	.760	-.05	-.10	-.15	-.25
b	.840	.842	.848	0	.02	.04	.10
c	.880	.899	.936	.05	.14	.23	.45
d	.920	.956	1.024	.10	.26	.42	.80
e	.960	1.013	1.112	.15	.38	.61	1.15
f	1.000	1.070	1.200	.20	.50	.80	1.50

Examples VI - X

	ξ_1	ξ_2	ξ_3	$\left(\frac{\partial f}{\partial \xi}\right)_1$	$\left(\frac{\partial f}{\partial \xi}\right)_2$	$\left(\frac{\partial f}{\partial \xi}\right)_3$	$\left(\frac{\partial^2 f}{\partial \xi^2}\right)_1$	$\left(\frac{\partial^2 f}{\partial \xi^2}\right)_2$	$\left(\frac{\partial^2 f}{\partial \xi^2}\right)_3$
a	.8000	.7850	.7600	-.0500	-.1000	-.1500	-.2500	-.2500	-.2500
b	.8438	.8496	.8661	.0047	.0360	.0791	.1332	.1467	.1720
c	.8854	.9098	.9605	.0567	.1627	.2829	.4972	.5163	.5474
d	.9252	.9661	1.0464	.1065	.2813	.4684	.8455	.8620	.8891
e	.9633	1.0194	1.1258	.1541	.3935	.6398	1.1789	1.1893	1.2049
f	1.0000	1.0700	1.2000	.2000	.5000	.8000	1.5000	1.5000	1.5000

TABLE I – STREAMSURFACE COORDINATES, SLOPES AND CURVATURES USED FOR EXAMPLES IV - X AND FIGURE 5

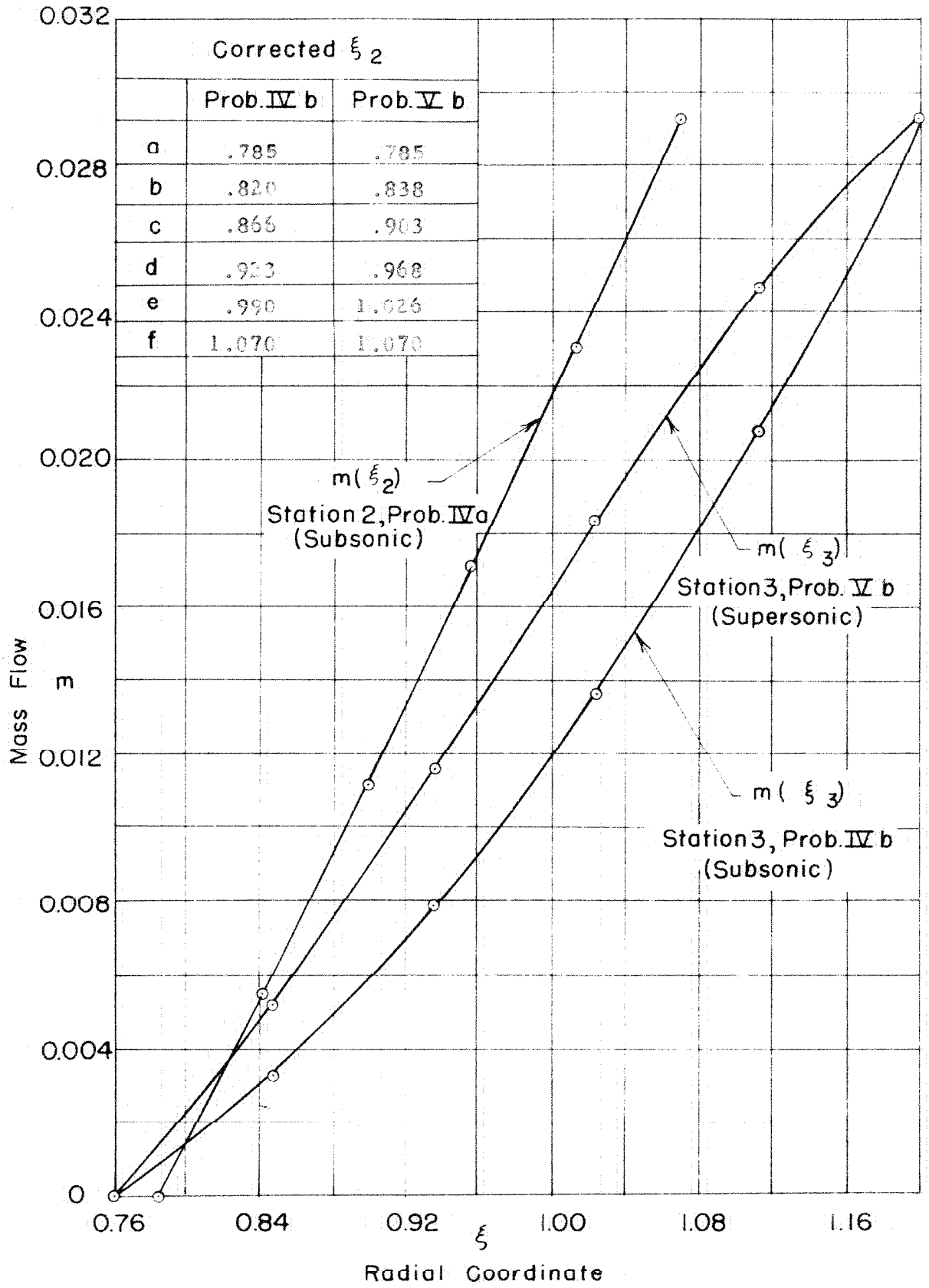

FIG. 6 – MASS FLOW FUNCTION FOR SUBSONIC AND SUPERSONIC ROTOR FROM SUBSONIC STATOR

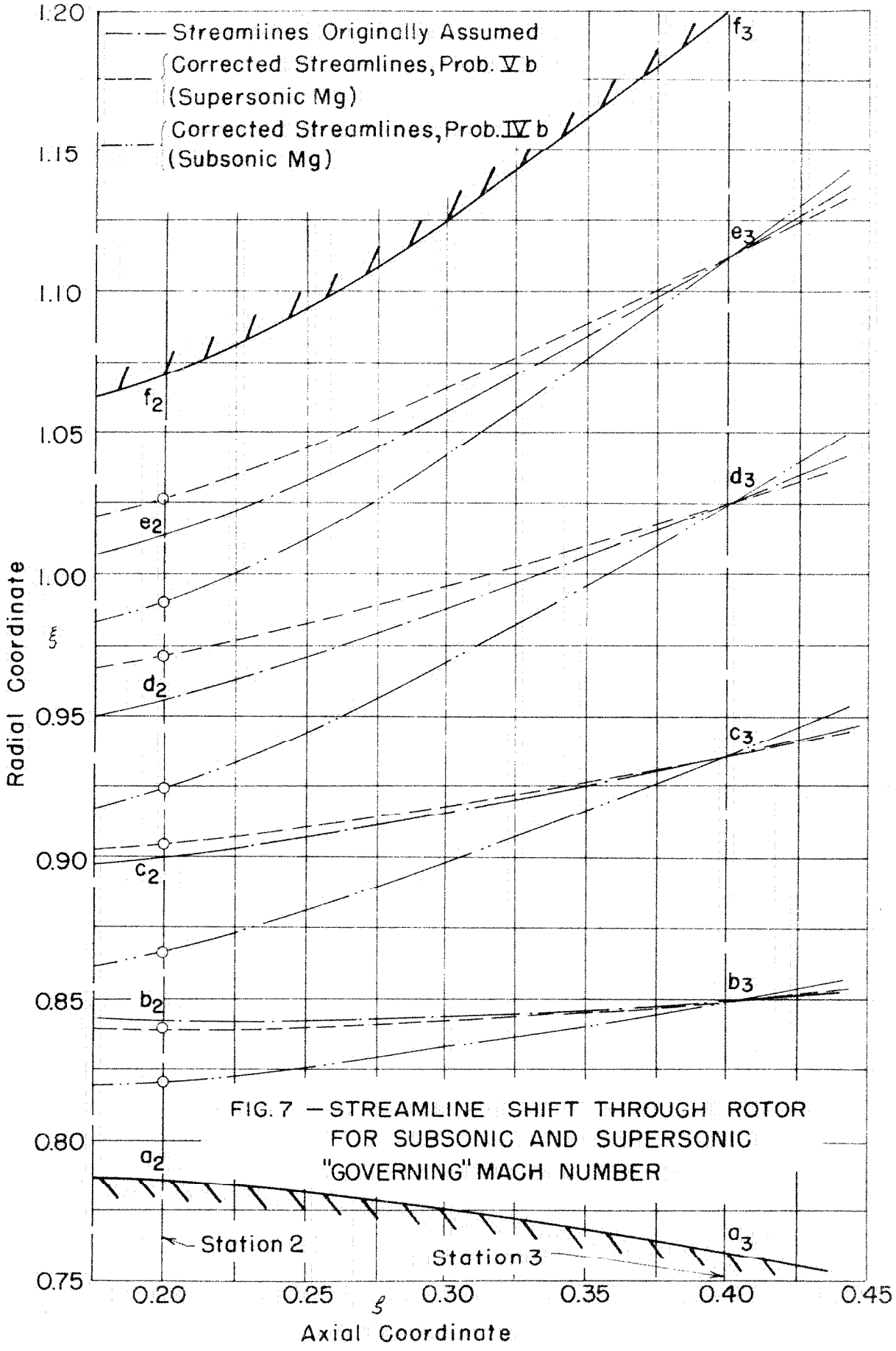

FIG. 7 — STREAMLINE SHIFT THROUGH ROTOR FOR SUBSONIC AND SUPERSONIC "GOVERNING" MACH NUMBER

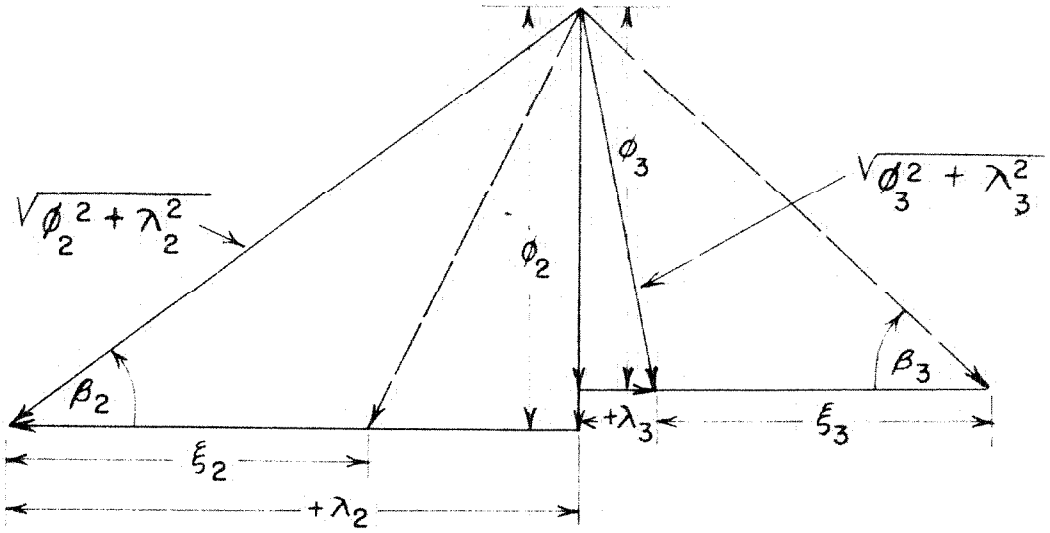

$$\text{Stator: } \cot\beta_2\,(\xi_2) = F(\xi_2) = \frac{\lambda_2}{\phi_2} \qquad \text{Rotor: } \cot\beta_3(\xi_3) = G(\xi_3) = \frac{\xi_3 + \lambda_3}{\phi_3}$$

FIG. 8 — TYPICAL TURBINE VELOCITY DIAGRAM SHOWING SIGN CONVENTION USED IN ALL EXAMPLES

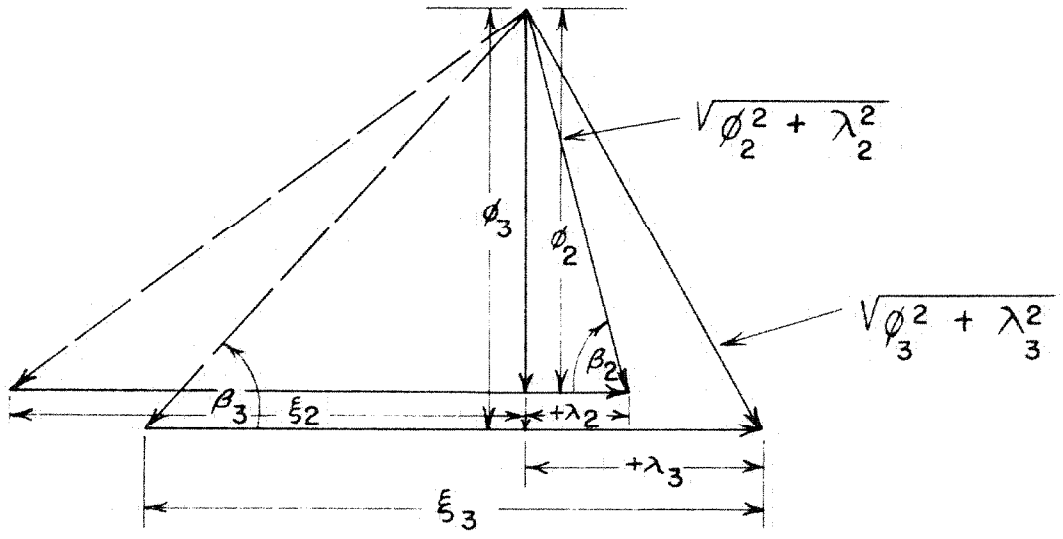

$$\text{Stator: } \cot\beta_2\,(\xi_2) = F(\xi_2) = \frac{\lambda_2}{\phi_2} \qquad \text{Rotor: } \cot\beta_3\,(\xi_3) = G(\xi_3) = \frac{\xi_3 - \lambda_3}{\phi_3}$$

FIG. 9 — TYPICAL COMPRESSOR VELOCITY DIAGRAM SHOWING SIGN CONVENTION